

ADI Ref: 690

①

ADA 025 649

PERFORMANCE EVALUATION
OF NINE CANDIDATE
REMBASS SINGLE-TARGET CLASSIFIERS

Michael F. Whalen
John D. Sanders
Anthony N. Mucciardi, Ph.D.

ADAPTRONICS, INC.
Westgate Research Park
7700 Old Springhouse Road
McLean, Virginia 22101

20 February 1976

DDC
RECEIVED
JUN 17 1976
D

Final Report for Period 1 March 1975 through 31 December 1975

Prepared for
U.S. Army Mobility Equipment Research
and Development Center
Fort Belvoir, Virginia 22060

REPRODUCED BY
NATIONAL TECHNICAL
INFORMATION SERVICE
U. S. DEPARTMENT OF COMMERCE
SPRINGFIELD, VA. 22161

DISTRIBUTION STATEMENT A

Approved for public release;
Distribution Unlimited

REPORT DOCUMENTATION PAGE		READ INSTRUCTIONS BEFORE COMPLETING FORM
1. REPORT NUMBER	2. GOVT ACCESSION NO.	3. RECIPIENT'S CATALOG NUMBER
4. TITLE (and Subtitle) Performance Evaluation of Nine Candidate REMBASS Single-Target Classifiers.		5. TYPE OF REPORT & PERIOD COVERED Final Technical Report 3/1/75 - 12/31/75
7. AUTHOR(s) Michael F. Whalen John D. Sanders Anthony N. Mucciardi, Ph.D.		6. PERFORMING ORG. REPORT NUMBER 690
9. PERFORMING ORGANIZATION NAME AND ADDRESS Adaptronics, Inc. 7700 Old Springhouse Road McLean, Virginia 22101		8. CONTRACT OR GRANT NUMBER(s) DAAK02-74-C-0322.
11. CONTROLLING OFFICE NAME AND ADDRESS U.S. Army Mobility Equipment Research and Development Center Fort Belvoir, Virginia 22060		10. PROGRAM ELEMENT, PROJECT, TASK AREA & WORK UNIT NUMBERS
14. MONITORING AGENCY NAME & ADDRESS (if different from Controlling Office)		12. REPORT DATE 20 February 1976
		13. NUMBER OF PAGES 178
		15. SECURITY CLASS. (of this report) Unclassified.
16. DISTRIBUTION STATEMENT (of this Report)		15a. DECLASSIFICATION/DOWNGRADING SCHEDULE
<div style="border: 1px solid black; padding: 5px; text-align: center;"> DISTRIBUTION STATEMENT A Approved for public release; Distribution Unlimited </div>		
17. DISTRIBUTION STATEMENT (of the abstract entered in Block 20, if different from Report)		
18. SUPPLEMENTARY NOTES		
<p>PRICES SUBJECT TO CHANGE</p>		
19. KEY WORDS (Continue on reverse side if necessary and identify by block number) Seismic classifier, seismic/acoustic classifier, pattern classification, feature extraction, cluster analysis, target discrimination, remote sensor.		
20. ABSTRACT (Continue on reverse side if necessary and identify by block number) The performance evaluation of nine candidate REMBASS Single Target Classifiers is presented. Each classifier is designed to discriminate between six target classes: tracked vehicles, wheeled vehicles, fixed wing aircraft, rotary wing aircraft, personnel, and nuisances. This discrimination is based on features computed from the seismic or seismic and acoustic signatures generated by the target or other disturbance source. Four of the nine classifiers were designed and constructed by Honeywell and Sylvania;		

20. the remaining five were newly synthesized by Adaptronics in the course of this project, using a composite set of 28 seismic and acoustic Honeywell and Sylvania features, plus a 29th: the acoustic to seismic energy ratio. Each of the classifiers was evaluated in simulations using a common field data base, and the performances of these classifiers is compared herein.

Additionally, a cluster analysis of five feature sets was accomplished showing interclass and intraclass cell separability (or lack thereof) and reduced dimensionality plots were prepared showing cell separation between the six classes.

A principal result of this study is that feasibility of designing a seismic/acoustic target classifier, employing 29 features, has been demonstrated. It is shown that an average overall accuracy of 85 percent with good range capability and reasonable site independence is achievable.

FOREWORD

This is the final technical report entitled "Performance Evaluation of Nine Candidate REMBASS Single-Target Classifiers" prepared by Adaptronics, Inc., McLean, Virginia 22101 for the U.S. Army Mobility Equipment Research and Development Center (MERDC) under Contract Number DAAK02-74-C-0322. This report presents the findings of research and development performed by the Contractor during the period 1 March 1975 to 31 December 1975.

The end items of this project, in addition to monthly reports and periodic briefings, include this final technical report, that documents the materials and methods employed, and computer programs that implement the classifiers under study.

Dr. Anthony N. Mucciardi was Project Manager and Principal Investigator for Adaptronics, Inc. The authors thank Dr. Richard K. Young, the MERDC Project Monitor, for his advice, guidance, and enthusiastic encouragement throughout this project. Special thanks are due Mr. Roger L. Barron of Adaptronics for many valuable technical insights and for conducting a number of the briefings. The authors also express their appreciation to Ms. Linda Flickinger, Janice Sennett, and Marilyn Collins of the Adaptronics staff for editorial and typing assistance.

CONTENTS

	<u>Page</u>
1. SUMMARY OF WORK TASKS, RESULTS, AND CONCLUSIONS	1
1.2 Summary of Work Tasks and Results	1
1.2 Summary of Conclusions	11
1.3 Report Organization	11
2. SEISMIC/ACOUSTIC FIELD-RECORD DATA BASE	13
2.1 Introduction	13
2.2 Six Target Classes	13
2.3 Format of Seismic/Acoustic Signatures	19
2.3.1 Geophone and Microphone Specifications	19
2.3.2 Digitization Steps	19
2.4 Target Vehicle Sites	20
3. CLASSIFIER SIMULATIONS	23
3.1 Introduction	23
3.2 Sylvania STC and SATC Simulations	23
2.3.1 Sylvania STC and SATC Feature Extractors	24
2.3.2 Sylvania STC and SATC Classifier Logic	29
3.3 Honeywell STC and SATC Simulations	30
3.4 Sylvania and Honeywell STC and SATC Simulation Results and Summary	36
4. DETERMINATION OF DATA BASE STRUCTURE VIA CLUSTER ANALYSIS	41
4.1 Introduction	41
4.2 Summary Description of the CLUSTER ALGORITHM	42
4.3 Results of Cluster Analyses	43
4.3.1 Cluster Analysis of Honeywell Seismic Features	44
4.3.2 Cluster Analysis of Honeywell Seismic/Acoustic Features	48
4.3.3 Cluster Analysis of Sylvania Seismic Features	51
4.3.4 Cluster Analysis of Sylvania Seismic/Acoustic Features	54
4.3.5 Cluster Analysis of Combined Honeywell and Sylvania Features (28)	56
4.3.5 Summary of Cluster Analysis and Conclusions	59

5.	TABULAR CLUSTER LISTINGS AND REDUCED DIMENSIONALITY PLOTS	63
5.1	Merging of Statistically Similar Cluster Cells	63
5.2	Tabular Cluster Listings for the Five Feature Sets	63
5.3	Correlation and Eigenvector Analysis	67
5.4	Reduced Dimensionality Cluster Plots	71
6.	CLASSIFIER REGENERATION AND SYNTHESSES	77
6.1	Introduction	77
6.2	Linear "One Versus Five" Classifiers	81
6.3	Linear "One Versus One" Classifiers	82
6.4	Nonlinear "One Versus One" Classifiers	102
7.	COMPARISON OF CLASSIFIER RESULTS	107
8.	CONCLUSIONS AND RECOMMENDATIONS	111
8.1	Conclusions	111
8.2	Recommendations	112
9.	REFERENCES	113

APPENDICES

A -	Waveform Identification Log Listing	A-1
B -	Diagrams of Test Sites	B-1
C -	Sylvania Feature Extractor Data	C-1
D -	Adaptive Learning Network Nonlinear Discriminant Function Structures and Eigenvector Weights	D-1

TABLES

<u>Table</u>	<u>Page</u>
1.1 Confusion Matrices for Four Current Classifiers . . .	3
1.2 Simulated Seismic and Seismic/Acoustic Target Classifiers	7
1.3 Performance Rank-Ordering of Nine Classifiers . . .	10
2.1 Six Target Classes	14
2.2 Data Base Composition	16
2.3 Speed Versus Range Distribution for Land Targets. .	17
2.4 Speed Versus Altitude Distribution for Air Targets	18
3.1 Simulated Target Classifiers	23
3.2 Sylvania STC and SATC Features	25
3.3 Sylvania STC and SATC Simulation Classifier Weights	31
3.4 Honeywell STC and SATC Features	33
3.5 Honeywell STC and SATC Weighting Coefficients ($\times 10^{-3}$)	34
3.6 Confusion Matrices for the Sylvania STC Simulation.	37
3.7 Confusion Matrices for the Sylvania SATC Simulation	38
3.8 Confusion Matrices for the Honeywell STC Simulation	39
3.9 Confusion Matrices for the Honeywell SATC Simulation	40
4.1 Honeywell Seismic Features Distribution Per Target Class	45
4.2 Honeywell STC Target Class Separability Analyses. .	47
4.3 Honeywell Seismic/Acoustic Features Distribution Per Target Class	49
4.4 Honeywell SATC Target Class Separability Analyses .	50
4.5 Sylvania Seismic Features Distribution Per Target Class	52
4.6 Sylvania STC Target Class Separability Analyses . .	53
4.7 Sylvania Seismic/Acoustic Features Distribution Per Target Class	55
4.8 Sylvania SATC Target Class Separability Analyses .	57
4.9 Combined Honeywell and Sylvania Features Distribution Per Target Class	58
4.10 Honeywell and Sylvania Combined Feature Target Class Separability Analysis	60

Tables (Continued)

4.11	Populations of Largest Clusters in Each Target Class	62
4.12	Intersections of Most Populated Cells in Honeywell and Sylvania Feature Sets With Most Populated Cells of Combined Feature Set	62
5.1	Number of Cluster Cells Per Class Containing the Largest Number of Points	64
5.2	Example of Tabular Listing for a Cluster Cell . .	65
5.3	Definitions for Tabular Cluster Listing	66
5.4	Correlation Matrix of 28 Honeywell and Sylvania Features	68
5.5	Twenty-Eight Honeywell and Sylvania Combined Features	69
5.6	Explained Variance of the Z-Parameters for the Five Feature Sets	70
6.1	Simulated Seismic and Seismic/Acoustic Target Classifiers	78
6.2	Class Composition of Design and Evaluation Data Bases	79
6.3	Weighting Coefficients for Regenerated Sylvania STC Classifier	83
6.4	Weighting Coefficients for Regenerated Sylvania SATC Classifier	84
6.5	Weighting Coefficients for Regenerated Honeywell STC Classifier	85
6.6	Weighting Coefficients for Regenerated Honeywell SATC Classifier	86
6.7	Weighting Coefficients for Total Feature Set Classifier	87
6.8	Confusion Matrices for the Sylvania STC With Regenerated Weights (Evaluation Set)	88
6.9	Confusion Matrices for the Sylvania SATC With Regenerated Weights (Evaluation Set)	89
6.10	Confusion Matrices for the Honeywell STC With Regenerated Weights (Evaluation Set)	90
6.11	Confusion Matrices for the Honeywell SATC With Regenerated Weights (Evaluation Set)	91
6.12	Confusion Matrices for the Adaptronics SATC #1 (Evaluation Set)	93
6.13	Illustration of Tie-Breaking Strategy	95
6.14	Linear Pairwise Weighting Coefficients for the Combined 29-Feature Set	97

Tables (Continued)

<u>Table</u>		<u>Page</u>
6.15	Confusion Matrices for the Adaptronics SATC #2 (Evaluation Set)	100
6.16	Confusion Matrices for the Adaptronics SATC #4 (Evaluation Set)	101
6.17	Confusion Matrices for Adaptronics SATC #3 (Evaluation Set)	104
6.18	Confusion Matrices for the Adaptronics SATC #5 (Evaluation Set)	105
7.1	Performance Rank-Ordering of Nine Classifiers . .	108

FIGURES

<u>Figure</u>		<u>Page</u>
2.1	Digital Tape Evolution Block Diagram	21
2.2	Digital Tape Format of the Packed 60-Bit Word .	21
5.1	Two-Dimensional Cluster Plots in Z Space for the Sylvania Feature Set	72
5.2	Reduced Dimensionality Cluster Plots Along Three Z Axes for the Honeywell and Sylvania Combined Feature Set	74
6.1	"One-Versus-One" (Pairwise) Classifier Architecture	93
7.1	Class Accuracy of Nine Target Classifiers in Order of Performance	109

Preceding page blank

1. SUMMARY OF WORK TASKS, RESULTS, AND CONCLUSIONS

1.1 SUMMARY OF WORK TASKS AND RESULTS

The main objectives of this project were to:

- Simulate the operation of seismic and seismic/acoustic classifiers developed by Sylvania and Honeywell for the U.S. Army.
- Evaluate the performance (i.e., overall accuracy and site independence) of the simulations using field seismic and acoustic waveforms.
- Determine whether an optimal classifier using a composite set of features could be found to improve the six target-class discrimination accuracies.
- Establish the degree of separability of the six target classes using the composite feature set.
- Investigate alternative means of classification based on the composite feature set.

The simulated Sylvania and Honeywell seismic target classifiers (STC's) and seismic/acoustic target classifiers (SATC's) were extensively tested to ensure that the respective digital simulations mimicked the analog circuitry as closely as possible.

All classifier accuracy comparisons in this report are based on a 10-second epoch. That is, a classification is made for each 10-second signature and it is compared to the correct target class. The overall accuracy for one vehicle run, therefore, would be equal to the number of correctly classified 10-second epochs divided by the total number of epochs for that run.

The six target class (tracked vehicle, wheeled vehicle, fixed-wing aircraft, rotary-wing aircraft, personnel, nuisance) accuracies that resulted when the 671-record digitized field data were classified by the Sylvania and Honeywell STC's and SATC's are given in Table 1.1. It can be seen that low accuracies, severe biases, and considerable site dependencies resulted with all four classifiers. None of the four can be considered to be an acceptable design.

The inherent separability of each of the four feature sets, independent of the classifier weights, was established via a clustering analysis, which is a way to determine regions in the feature space in which the 10-second records from each target class are located when all N features are considered simultaneously.

TABLE 1.1
CONFUSION MATRICES FOR FOUR CURRENT CLASSIFIERS
CONFUSION MATRICES FOR THE SYLVANIA STC SIMULATION

Location	True Class	Decision Class						Class Total	Class Accuracy	Site Accuracy
		1	2	3	4	5	6			
Ft Bragg	1	21	9	8	2	0	0	40	.53	38/171 = .22
	2	21	17	0	1	0	0	39	.44	
	3	6	17	0	0	1	0	54	.00	
	4	0	34	0	0	2	0	36	.00	
	5	0	0	0	0	0	0	0	-	
	6	1	0	1	0	0	0	2	.00	
Grayling	1	32	15	8	0	0	0	55	.58	98/136 = .72
	2	4	66	0	0	0	0	70	.94	
	3	0	0	0	0	0	0	0	-	
	4	0	0	0	0	0	0	0	-	
	5	0	0	0	0	0	0	0	-	
	6	0	11	0	0	0	0	11	.00	
Yuma	1	117	35	50	1	0	40	243	.48	155/364 = .43
	2	43	38	1	0	0	0	82	.46	
	3	0	0	0	0	0	0	0	-	
	4	0	0	0	0	0	0	0	-	
	5	8	26	0	0	0	0	34	.00	
	6	5	0	0	0	0	0	5	.00	

Overall Accuracy: 291/671 = .43

CONFUSION MATRICES FOR THE SYLVANIA SATC SIMULATION

Location	True Class	Decision Class						Class Total	Class Accuracy	Site Accuracy
		1	2	3	4	5	6			
Ft. Bragg	1	4	6	0	25	5	0	40	.10	8/171 = .05
	2	10	4	0	8	17	0	39	.10	
	3	1	8	0	3	42	0	54	.00	
	4	0	21	0	0	15	0	36	.00	
	5	0	0	0	0	0	0	0	-	
	6	0	1	0	1	0	0	2	.00	
Grayling	1	0	10	0	32	13	0	55	.00	18/136 = .13
	2	0	18	0	18	34	0	70	.26	
	3	0	0	0	0	0	0	0	-	
	4	0	0	0	0	0	0	0	-	
	5	0	0	0	0	0	0	0	-	
	6	0	0	0	0	11	0	11	.00	
Yuma	1	7	26	0	202	6	2	243	.03	40/364 = .11
	2	15	1	0	5	47	14	82	.01	
	3	0	0	0	0	0	0	0	-	
	4	0	0	0	0	0	0	0	-	
	5	0	4	0	3	27	0	34	.79	
	6	0	0	0	0	0	5	5	1.00	

Overall Accuracy: 66/671 = .10

Class Number	Nomenclature	Acronym
1	Tracked Vehicle	TV
2	Wheeled Vehicle	WV
3	Fixed-Wing Aircraft	FWA
4	Rotary-Wing Aircraft	RWA
5	Personnel	PER
6	Nuisance	NUS

TABLE 1.1
(Continued)

CONFUSION MATRICES FOR THE HONEYWELL STC SIMULATION

Location	True Class	Decision Class						Class Total	Class Accuracy	Site Accuracy
		1	2	3	4	5	6			
Ft. Bragg	1	2	0	22	8	4	4	40	.05	
	2	0	0	21	10	1	7	39	.00	
	3	0	1	41	1	10	1	54	.76	
	4	3	0	0	28	5	0	36	.78	
	5	0	0	0	0	0	0	0	-	
	6	0	0	2	0	0	0	2	.00	
										71/171 = .42
Grayling	1	0	0	22	3	28	2	55	.00	
	2	0	19	7	1	32	11	70	.27	
	3	0	0	0	0	0	0	0	-	
	4	0	0	0	0	0	0	0	-	
	5	0	0	0	0	0	0	0	-	
	6	0	3	0	0	7	1	11	.09	
										20/136 = .15
Yuma	1	0	2	89	28	90	34	243	.00	
	2	4	7	30	15	3	23	82	.09	
	3	0	0	0	0	0	0	0	-	
	4	0	0	0	0	0	0	0	-	
	5	0	14	0	10	8	2	34	.24	
	6	0	0	0	4	0	1	5	.20	
										16/364 = .04

Overall Accuracy: 107/671 = .16

CONFUSION MATRICES FOR THE HONEYWELL SATC SIMULATION

Location	True Class	Decision						Class Total	Class Accuracy	Site Accuracy
		1	2	3	4	5	6			
Ft. Bragg	1	2	2	0	0	36	0	40	.05	
	2	1	0	0	0	34	0	35	.00	
	3	0	0	0	0	54	0	54	.00	
	4	1	0	0	8	27	0	36	.22	
	5	0	0	0	0	0	0	0	-	
	6	0	0	0	0	2	0	2	.00	
										10/171 = .06
Grayling	1	0	5	0	0	50	0	55	.00	
	2	4	23	0	4	34	0	70	.40	
	3	0	0	0	0	0	0	0	-	
	4	0	0	0	0	0	0	0	-	
	5	0	0	0	0	0	0	0	-	
	6	1	0	0	0	10	0	11	.00	
										28/136 = .21
Yuma	1	3	5	0	0	235	0	243	.01	
	2	1	12	0	1	68	0	82	.15	
	3	0	0	0	0	0	0	0	-	
	4	0	0	0	0	0	0	0	-	
	5	0	28	0	0	6	0	34	.18	
	6	0	0	0	0	5	0	5	.00	
										21/364 = .06

Overall Accuracy: 59/671 = .09

Class Number	Nomenclature	Acronym
1	Tracked Vehicle	TV
2	Wheeled Vehicle	WV
3	Fixed-Wing Aircraft	FWA
4	Rotary-Wing Aircraft	RWA
5	Personnel	PER
6	Nuisance	NUS

After this is performed for each of the six target classes, the degree of separability (indicating potentially accurate discrimination) or overlap (indicating potential misclassifications) can be quantified.

The cluster structures of the feature sets as developed by each of the four simulations did not show promise of good interclass separability. The analysis showed that the Sylvania features (seismic and acoustic) are more appropriate for the separation of tracked vehicles from other types of signatures, while the Honeywell features are more suited for the separation of wheeled vehicles from signatures of other classes.

Although none of the four feature sets was capable of distinguishing unambiguously among all six target classes, the fact that the Sylvania features were good tracked vehicle discriminators and the Honeywell features were good wheeled vehicle discriminators suggested that a combination of all four feature sets could discriminate well among the six classes.

The 19 seismic features from the Honeywell and Sylvania STC's were combined with the nine acoustic features from the Honeywell and Sylvania SATC's to form a composite 28 feature set. The cluster analysis was repeated using this combined feature set and, indeed, a considerable degree of interclass separability was found. In the design of new classifiers, the combined Sylvania and Honeywell feature set was used, plus a 29th, the acoustic-to-seismic energy ratio. It was established that this feature was a key parameter for separating tracked vehicles from all other classes.

In order to prove the superiority of the composite, or "optimized" feature set, classifiers were designed using the original Sylvania and Honeywell features as well as a number of classifiers that used the composite features.

Table 1.2 lists the nine classifiers, labeled A, B, ..., I, along with their pertinent characteristics. It can be seen that the first four classifiers are the Sylvania (A and B) and Honeywell (C and D) classifiers with new weights (based on this three-site data base), while the last five classifiers were newly designed by Adaptronics during this project. Classifier E is identical in its architecture to the Sylvania and Honeywell types except that 29 features are used. Classifiers F and G utilize 15 pairwise-voting, 1 versus 1, discriminant functions with tie-breaking decision logic to render one classification. The difference between F and G is that F employs linear while G uses nonlinear discriminant functions. H and I are similar to F and G except that no tie-breaking logic is used; instead, any target class receiving more than a threshold number of votes is reported.

It is interesting to observe that the linear classifier performed slightly better than nonlinear classifiers. Although not tested specifically in this program, it is our opinion a non-linear classifier would have outperformed a linear classifier if the number of features were reduced drastically, as is desired in operational systems.

Each of the nine classifiers was designed using the same set of signatures -- a subset of 225 from the 671-record field data base. The remaining 446 signatures were used for an independent evaluation. All results are based on the evaluation data subset. Each classifier was designed and evaluated on data from three sites: Ft. Bragg, Grayling, and Yuma. Therefore, three confusion matrices were computed for each classifier.

TABLE 1.2
SIMULATED SEISMIC AND SEISMIC/ACOUSTIC TARGET CLASSIFIERS

Identification	Classifier	Channels	Features	Number of Discriminant Functions	Type of Discriminant Functions	Type of Decision Logic	Outputs or Display	Performance Ranking
A	Sylvania STC	1	7	6	1 vs. 5 Linear	Maximum	Target Class	8th
B	Sylvania SATC	2	7	6	1 vs. 5 Linear	Maximum	Target Class	7th
C	Honeywell STC	1	12	6	1 vs. 5 Linear	Maximum	Target Class	9th
D	Honeywell SATC	2	18	6	1 vs. 5 Linear	Maximum	Target Class	6th
E	Adaptronics SATC #1	2	29	6	1 vs. 5 Linear	Maximum	Target Class	5th
F	Adaptronics SATC #2	2	29	15	1 vs. 1 Linear	Voting with Tie-Breaking	Target Class	4th
G	Adaptronics SATC #3	2	29	15	1 vs. 1 Nonlinear	Voting with Tie-Breaking	Target Class	3rd
H	Adaptronics SATC #4	2	29	15	1 vs. 1 Linear	Voting without Tie-Breaking	All Target Classes Receiving \geq V Votes	1st
I	Adaptronics SATC #5	2	29	15	1 vs. 1 Nonlinear	Voting without Tie-Breaking	All Target Classes Receiving \geq V Votes	2nd

An overall criterion of performance, P, was established for each classifier so that the nine (as well as others not described here) could be rank-ordered on a common scale. The performance measure was a function of three quantities:

1. A - Overall accuracy
2. C - Consistency of overall accuracy
3. S - Site independence

The overall accuracy, A, was defined as the number of correct decisions divided by the total number of decisions for the given classifier. The value of A can range from 0, for total error, to 1, for perfect classification.

Since it is desirable for a classifier to perform equally well for all six target classes, a measure of accuracy consistency, C, was constructed as follows. The average accuracy and its standard deviation, σ , were computed over all six classes, considering all three sites. If the average accuracy was the same for all six classes, σ was zero. Conversely, a large value of σ denoted inconsistent classifications. Therefore, the consistency measure was computed as: $C = 1 - \sigma$. The value of C can range from 0.45, for inconsistent classifications, to 1, for perfectly consistent classifications.

The site independence measure, S, was obtained as follows. The six class accuracies were computed for each of the three sites. The value of S was set equal to the ratio of the lowest site accuracy to the best site accuracy. Thus, if a classifier performed well at one or more sites, but poorly at one of the other sites, S was small. Conversely, S approached 1 as a given classifier produced consistent, i.e., the same, accuracy at all sites.

The overall performance measure was computed as the product of the three criteria of success:

$$P = A \times C \times S$$

Good performance exists when A, C, and S each approach 1, as does P. Therefore, any group of classifiers can be rated on the above performance scale, which ranges from 0 for poor performance to 1 for perfect performance.

Notice that a classifier that had an overall accuracy of 90 percent ($A = 0.9$), with a standard deviation of 10 percent ($C = 1 - 0.1 = 0.9$), and a worst-site-to-best-site accuracy ratio of 90/100 ($S = 0.9/1.0 = 0.9$) -- all very good values -- would achieve a performance value of

$$P = 0.9 \times 0.9 \times 0.9 = 0.729.$$

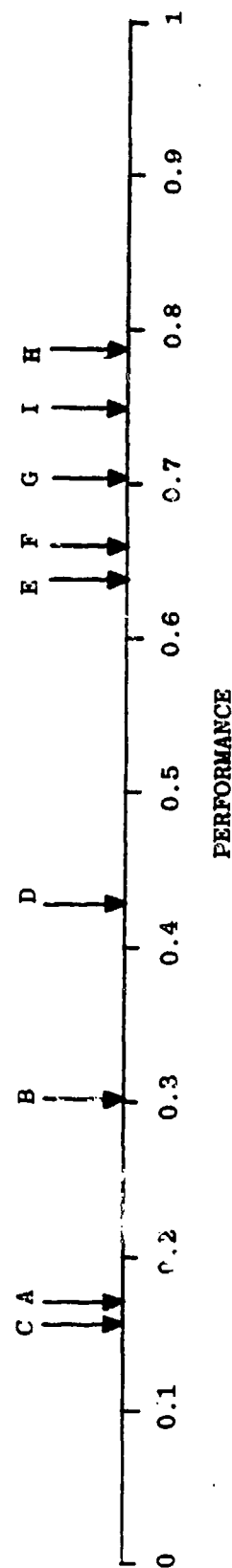
Thus, in practice, a P value greater than about 0.7 can be viewed as signifying excellent performance.

The rank-ordered performance of the nine classifiers is given in Table 1.3. It can be seen that the lowest performers were the two STC's ($P = 0.155$ and 0.169) followed by the two SATC's ($P = 0.303$ and 0.428). Classifier E, the redesigned version of Classifiers A to D using the optimized 29 features, ranked fifth with $P = 0.639$. This verifies the above cluster analysis result that the combined feature set is indeed superior to any of the four feature sets if one uses the same classifier structure.

The best performers were the redesigned classifiers that used the 29th feature and a more sophisticated decision logic for classification; i.e., deciding among pairs of targets rather than one target from all others. The performances of these four classifiers ranged from 0.661 to 0.784.

TABLE 1.3
PERFORMANCE RANK-ORDERING OF NINE CLASSIFIERS

Identification	Overall Accuracy, A		Consistency of Overall Accuracy, C		Site Independence, S	Performance P = AxCxS
H	Adaptronics SATC #4	.895	.935	.937	.784	
I	Adaptronics SATC #5	.874	.940	.908	.751	
G	Adaptronics SATC #3	.845	.958	.870	.704	
F	Adaptronics SATC #2	.854	.886	.874	.661	
E	Adaptronics SATC #1	.859	.930	.800	.639	
D	Honeywell SATC	.596	.854	.840	.428	
B	Sylvania SATC	.675	.867	.518	.303	
A	Sylvania STC	.554	.617	.373	.169	
C	Honeywell STC	.357	.779	.559	.155	



1.2 SUMMARY OF CONCLUSIONS

This study has demonstrated that a seismic/acoustic six-way target classifier can be realized that has the following principal attributes:

- High single epoch classification accuracy of approximately 85 percent.
- Consistent accuracy for different sites, different classes, and different ranges, altitudes, speeds, and headings of targets.
- Signal features taken from prior designs by Sylvania and Honeywell.
- Ability to discriminate tracked vehicles appears to be practical at ranges from up to 900 meters from the sensor.
- Excellent growth potential based on reporting of tied voting classes appears indicated for future multitarget discrimination requirements.

More detailed conclusions and a number of technical recommendations are presented in Section 8.

1.3 REPORT ORGANIZATION

The remainder of this report is divided into the following sections:

- Section 2 - Describes the six-class seismic/acoustic data base and its distribution according to site, target type, target speed, and range from sensor.
- Section 3 - Presents the details of the simulations of the Sylvania and Honeywell classifiers. Results are shown in confusion matrices listed by location.
- Sections 4 and 5 - Give the results of the cluster analysis of the five feature sets and show intra- and inter-class separability. Also, reduced dimensionality plots are presented for visualization purposes.

- Section 6 - Presents results obtained with the four Sylvania and Honeywell classifiers after regeneration of weights in these classifiers. The architecture of five new seismic/acoustic classifiers using a composite feature set is described and comparative results are presented.
- Section 7 - Presents a comparison of the cluster analyses of the various features.
- Section 8 - States the major recommendations of this study.

2. SEISMIC/ACOUSTIC FIELD-RECORD DATA BASE

2.1 INTRODUCTION

The data base used in this study consisted of a total of 671 seismic and acoustic signatures representing six major target categories. Each signature consisted of a data epoch of 10 seconds duration (that is, 10 simultaneous seconds for the seismic and acoustic waveforms).^{1/} The sampling rate was 2,000 Hz for both waveforms. These data were provided by MERDC as a set of four digitized magnetic tape reels compatible with CDC 6000 series computers.

An identification log was created (based on the information provided by MERDC for each of the 671 signatures) so that each waveform could be identified by target class, site, speed, stake number, acoustic and seismic gains, and direction of travel relative to the sensor. A listing of this log appears in Appendix A.

2.2 SIX TARGET CLASSES

The classes for target discrimination are the six shown in Table 2.1. The class number will be used as a convention throughout the remainder of the report, i.e., Class 1 denotes tracked vehicles, Class 2 denotes wheeled vehicles, etc. Each of the signature identities in the data log is tagged with a class number.

Once a data log was created, the data base was interrogated to determine the number of target classes that were represented at each site in order to determine the class composition by target type. Table 2.2 provides this information.

^{1/} The exact signature duration was 10.08 seconds; however the epoch length will be referred to as 10-seconds for reading ease throughout this report.

TABLE 2.1
SIX TARGET CLASSES

<u>Class Number</u>	<u>Type</u>	<u>Abbreviation</u>
1	Tracked Vehicle	TV
2	Wheeled Vehicle	WV
3	Fixed Wing Aircraft	FWA
4	Rotary Wing Aircraft	RWA
5	Personnel	PER
6	Nuisance	NUS

The composition of the data base is shown in Table 2.2. Data were recorded at three sites: Yuma, Grayling, and Ft. Bragg; and signatures from Classes 1, 2, and 6 were available at all three locations. Aircraft data, Classes 3 and 4, were available only at Ft. Bragg, and Class 5 data was available only at Yuma. Historically, the most difficult classes to discriminate have been Classes 1 and 2; the majority of records in the data base were from these two classes; 338 of the 671 signatures (about 50 percent) were Class 1, 28 percent were Class 2 and the remainder of the data were spread among the other four classes. (Seventy-two percent of the Class 1 data were recorded at Yuma).

Class 1 was composed of heavy and light tracked vehicles, i.e., type M48, M60, M107, and M113, in which M48 and M113 signatures were available from all sites. A variety of heavy and light wheeled vehicles were recorded for Class 2, i.e., type M151, M715, M792, T2.5, and T5.0, in which M151 and 2.5-ton truck signatures were available from all sites. The aircraft data were quite limited with respect to type; Class 3 was composed of types OV-10 and TA-4; Class 4 was composed of type UH-1. Three types were observed in Class 5: one man walking (H1), three men walking (H3), and five men walking (H5). Class 6 data were composed of only 18 signatures.

The signatures generated by different targets are a function of many variables. Of primary importance are target speed and distance from sensor (i.e., range). Many combinations of these two conditions were available in the data base. Table 2.3 shows the speed versus range distribution for land targets and Table 2.4 shows the speed versus altitude distribution for air targets.

TABLE 2.2
DATA BASE COMPOSITION

	CLASS					
	1	2	3	4	5	6
YUMA	243	82	0	0	34	5
GRAYLING	55	70	0	0	0	11
FT. BRAGG	40	39	54	36	0	2
	338	191	54	36	34	18

CLASS 1 COMPOSITION

	M48	M60	M107	M113	
YUMA	61	65	47	70	243
GRAYLING	25	0	0	30	55
FT. BRAGG	14	0	0	26	40
	100	65	47	126	

CLASS 2 COMPOSITION

	M151	M715	M792	T2.5	T5.0	
YUMA	16	17	28	21	0	82
GRAYLING	20	0	0	25	25	70
FT. BRAGG	18	0	0	21	0	39
	54	17	28	67	25	

CLASS 3 COMPOSITION

	OV-10	TA-4	
FT. BRAGG	33	21	54
	33	21	

CLASS 4 COMPOSITION

	UH-1	
FT. BRAGG	36	36
	36	

CLASS 5 COMPOSITION

	H1	H3	H5	
YUMA	10	18	6	34
	10	18	6	

CLASS 6 COMPOSITION

	N	
YUMA	5	5
GRAYLING	11	11
FT. BRAGG	2	2
	18	

TABLE 2.3
SPEED VERSUS RANGE DISTRIBUTION FOR LAND TARGETS

Class	Speed (mph)	Range (Meters)										
		<100	100	200	300	400	500	600	700	800	900	Unknown
1	6	7	22	24	9	6	4	2	-	-	-	8
	16	2	32	20	16	17	9	1	1	-	2	2
	20	1	2	5	3	-	2	-	-	-	-	-
	22	4	16	17	10	10	10	1	-	1	-	3
	25	-	3	1	2	2	1	-	-	-	-	-
	28	-	5	1	4	2	2	1	-	-	-	1
	31	1	5	14	3	2	4	7	2	1	-	-
2	6	13	15	8	1	-	-	-	-	-	-	10
	16	6	20	7	5	3	1	-	-	-	-	9
	22	7	17	10	5	2	1	-	-	-	-	8
	31	-	14	14	2	1	5	1	-	-	-	6
5	Walk	34	-	-	-	-	-	-	-	-	-	-

TABLE 2.4
SPEED VERSUS ALTITUDE DISTRIBUTION FOR AIR TARGETS

<u>Class</u>	<u>Speed (Knots)</u>	<u>Altitude (Feet)</u>		
		<u>200</u>	<u>400</u>	<u>600</u>
3	120	4	4	4
	150	4	4	4
	180	3	4	2
	250	2	4	-
	300	4	3	-
	450	4	4	-
4	60		5	5
	80	5	4	4
	100	4	4	5

2.3 FORMAT OF SEISMIC/ACOUSTIC SIGNATURES

2.3.1 Geophone and Microphone Specifications

The geophone used to record the seismic data was the HS-1, with a sensitivity of 0.3 V/in/sec, a resonant frequency of 7 Hz, and a 70 percent damping ratio. The microphone was a B and K Model 4133 (1/2-inch). A B and K Model 4135 (1/4-inch) microphone was used for two of the runs. Both microphones have a sensitivity of 1.25 mv/ μ bar and a flat response from 39 Hz to 40 kHz. The acoustic pre-amp was the B and K Model 2619. Rockland filters, used on the acoustic recordings, had passbands of 5 to 5,000 Hz at Grayling and 5 to 500 Hz at Yuma and Ft. Bragg.

2.3.2 Digitization Steps

The signals produced by the geophone and microphone were amplified and recorded on a seven channel analog recorder at 15 inches per second. (The amplification factors are listed in the data log shown in Appendix A.) Most of the seismic signatures were recorded at 70 db gain, whereas the acoustic gains varied from 16 db to 70 db. A low gain seismic channel and an additional microphone channel were also recorded but not used in the present study.

Both seismic and acoustic signatures were digitized at a rate of 2,000 Hz by a 16-bit Sigma minicomputer and written in multiplexed form on magnetic tape. It was determined from the calibration signals that there was a -4.44 db attenuating factor to the seismic channel and a 2.0 gain factor to the acoustic channel in the data acquisition system.

The magnetic tapes produced by the Sigma minicomputer were made compatible with a CDC Cyber 70 system having a 60-bit word length. The least significant bit was dropped and four multiplexed 15-bit words were packed into each 60-bit word in order to conserve tape footage.

The digitization and packing of the 60-bit word tapes were performed by USAMERDC. A diagram of the digital tape evolution is shown in Figure 2.1 and the format of the packed word is shown in Figure 2.2.

2.4 TARGET VEHICLE SITES

The data base was recorded at the Ft. Bragg, Grayling, and Yuma test sites. Sketches of the instrumentation configuration at each of these sites are shown in Appendix B. The acoustic recordings used in this study were those taken from the microphone nearest to the road. The distance between transducers was 20 meters at each site.

Range stakes were used to indicate the approximate distances of land vehicles from the sensors. These stakes were placed at increments of 100 meters along the road, as indicated on each of the site diagrams (Appendix B). The stake numbers were recorded for each signature and entered into the data log (Appendix A). These stake numbers were converted to approximate range in meters.

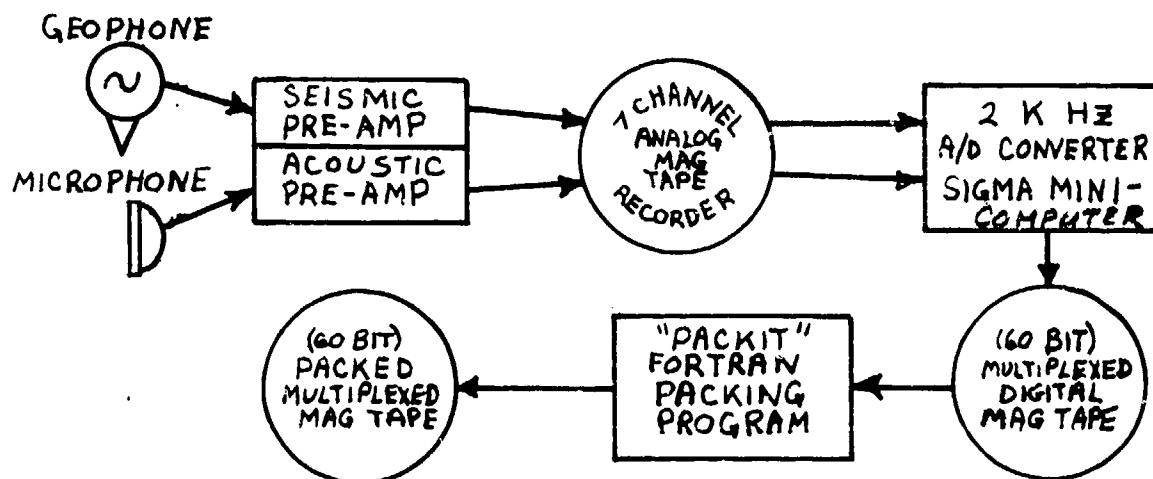


FIGURE 2.1: DIGITAL TAPE EVOLUTION BLOCK DIAGRAM

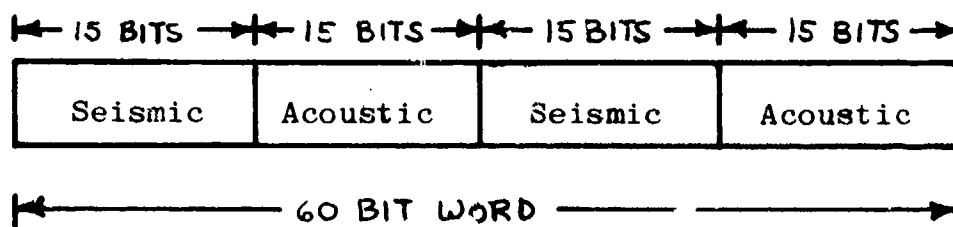


FIGURE 2.2: DIGITAL TAPE FORMAT OF THE PACKED 60-BIT WORD

3. CLASSIFIER SIMULATIONS

3.1 INTRODUCTION

Digital simulations were created for the prototype hardware devices listed in Table 3.1. The intent of the simulation was to mimic the analog circuitry as close as possible (using the classifier weights listed in the respective manufacturer's final technical reports) to evaluate the performance of each classifier on an independent set of field data.

The simulations were written in FORTRAN source code and were performed on a CDC Cyber 70 computer. Listings and card decks have been given to Dr. Richard K. Young, UASMERDC, Ft. Belvoir, Virginia.

3.2 SYLVANIA STC AND SATC SIMULATIONS

Available information used in performing simulations of the Sylvania classifiers was obtained from References 3 and 11. Information was also gathered via telephone conversations with Mr. M. D. Layman, Technical Director of the Sylvania STC and SATC projects. Additionally, the schematic diagrams for the SATC were provided by Dr. Richard K. Young of MERDC.

TABLE 3.1
SIMULATED TARGET CLASSIFIERS

<u>Contractor</u>	<u>Type</u>	<u>Seismic Features</u>	<u>Acoustic Features</u>	<u>Total Features</u>
Sylvania	STC <u>1/</u>	7	0	7
Sylvania	SATC <u>2/</u>	4	3	7
Honeywell	STC	12	0	12
Honeywell	SATC	12	6	18

1/ Seismic Target Classifier.

2/ Seismic/Acoustic Target Classifier. Sylvania has redesigned this SATC using a feature computed from the automatic gain controls circuits. This AGC feature was not used in our simulations.

3.2.1 Sylvania STC and SATC Feature Extractors

The Sylvania STC and SATC both extracted seven features from the input signatures. These features are listed in Table 3.2. It can be seen that there are four seismic features common to both classifiers.

The feature extractor block diagrams for the Sylvania STC and SATC are shown in Figures 3.1 and 3.2, respectively. The feature extractors are composed of automatic gain control (AGC) circuitry, full- and half-wave rectifiers squaring functions, and high and low pass filters.

Both the rectifier and squaring functions are easy to implement in a digital computer. The AGC was simulated by analyzing the schematic diagram of the SATC. Its action is to maintain the amplifier output constant at 3 volts peak. The filters were simulated by first writing the transfer functions for each and then deriving the appropriate difference equations. Appendix C presents these difference equations plus a flow chart for the feature extractor simulation illustrating the filter transfer equations.

Both of the Sylvania classifiers use manual gain settings which may be present at each target site. These were maintained constant while processing the 671 signatures. The seismic and acoustic gain settings were fixed at 98 db and 66 db, respectively. Each signature tape was "de-gained" so that the seismic and acoustic signal voltages would match those produced by the field transducers. Extensive testing was performed to ensure that the digital programs properly mimicked the operation of the analog feature extractors. An eight-channel Brush chart recorder was used to monitor the response of different test signals at various probe points in the simulated network.

TABLE 3.2
SYLVANIA STC AND SATC FEATURES

<u>Classifier</u>	<u>Feature Definition</u>	<u>Range (Volts)</u>
STC	1. Low Band Envelope	0-6
	2. Low Band Envelope Variance	0-6
	3. Wide Band Envelope	0-6
	4. Wide Band Envelope Variance	0-6
	5. Frequency	0-6
	6. Frequency Variance	0-6
	7. Variance of Frequency Variance	0-6
SATC	1. Seismic Low Band Envelope	0-6
	2. Seismic Low Band Envelope Variance	0-6
	3. Acoustic High Band Envelope	0-6
	4. Acoustic Wide Band Envelope	0-6
	5. Seismic Frequency	0-6
	6. Seismic Frequency Variance	0-6
	7. Acoustic Low Band Envelope	0-6

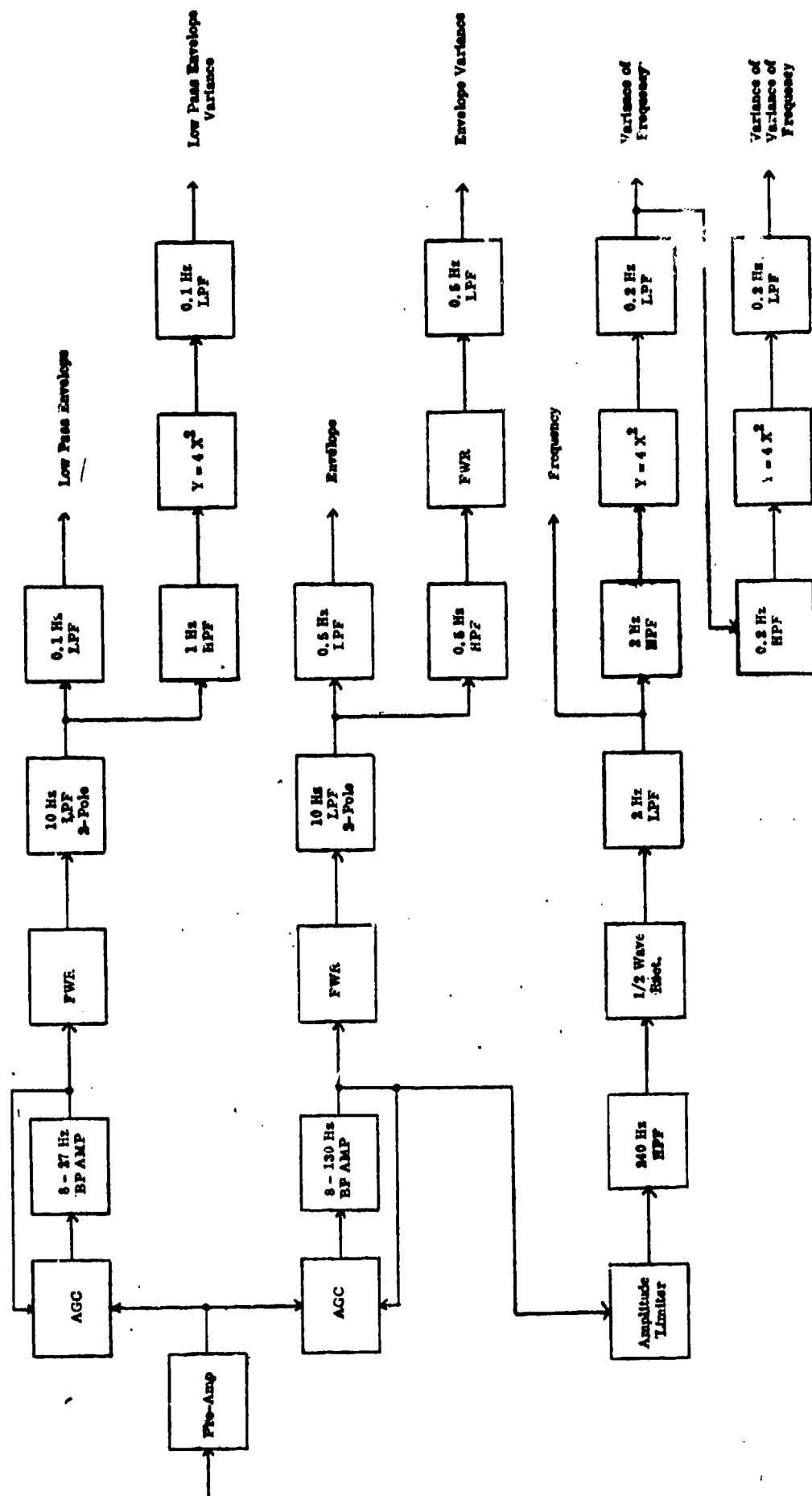


Figure 3.1: Sylvania Seismic Target Classifier Feature Extractor

(Reprinted from Sylvania STC Final Technical Report - Ref. 11.)

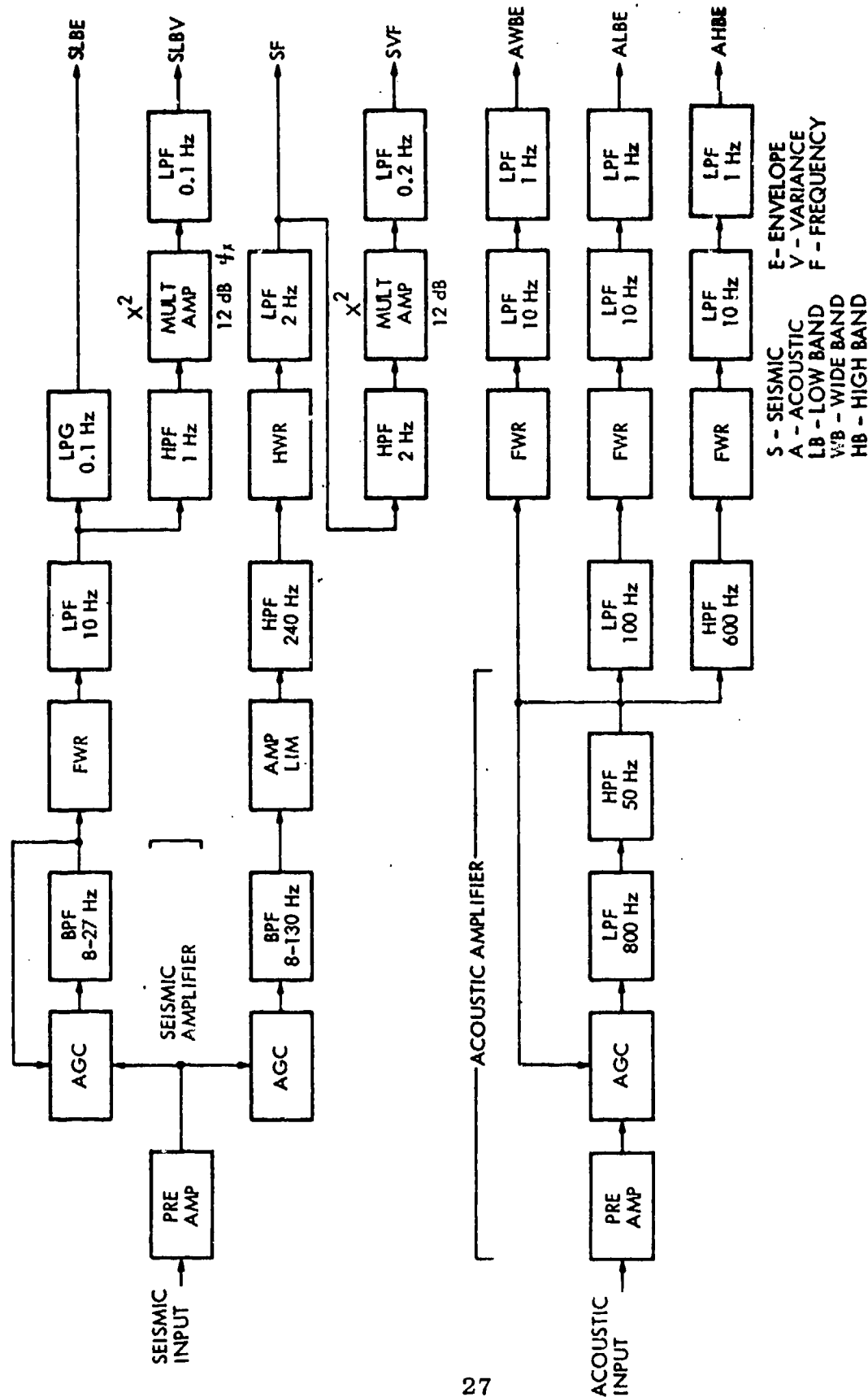


Figure 3.2: Sylvania Seismic Acoustic Target Classifier Feature Extractor

(Reprinted from Sylvania SATC Final Technical Report - Ref. 3.)

Some examples are shown in Appendix C. Also, each filter was tested at its cutoff frequency with a sine wave input for the -3 db point. The higher frequency filters tended to give a slightly attenuated response because the shape of the sine wave became slightly distorted as the test signal frequency approached the sampling rate. However, this result is to be expected in a digital simulation and is not considered to be a serious deficiency.

The AGC was tested by observing the response of the low and wide band outputs to different amplitude sine waves at various frequencies. It was found that the AGC response was acceptable in the frequency range of interest.

The final tests were made by checking the response of each feature to a sinusoid, after amplification, and comparing the results with those specified in the manufacturer's report. Close agreement was found.

At the beginning of each 10-second target observation, all filters in the simulation were initialized to zero. During each 10-second epoch, each feature value was continually developed and these values were tabulated every 0.72 second. Three sets of features were computed for each signature for two cases: each feature was weighted and summed over the 14 0.72-second time increments, then normalized by the sum of the weights. The j th feature is thus given by:

$$f_j = \frac{\sum_{i=1}^{14} w_i f_{ji}}{\sum_{i=1}^{14} w_i}$$

In one case the weighting vector (w) was equal to time, t, in seconds, over the 10-second epoch. In the other case, w was equal to the value of the wide band envelope. The third set of features was equal to the feature values that were fully developed at the end of the 10-second epoch. All three sets were tested with the classifier weights. It was found that the third set yielded the best results in the Sylvania simulation, so it was used for the remainder of the study.

The sampling rates for the acoustic and seismic channels were 2,000 Hz and 500 Hz, respectively, for the simulated Sylvania feature extractor. Therefore, every acoustic and every fourth seismic data points were chosen from the input tapes.

After the simulations were performed, it was noted that some feature values (mostly low band envelope and variance) associated with the heavy tracked- and wheeled-vehicle targets assumed values larger than the 6-volt capacity for their envelope and variance features. This happened when the AGC was unable to attenuate large signal amplitude bursts within the epoch at a sufficiently rapid rate. These features were clipped at the 6-volt level. This occurred for a number of Class 4 data at Ft. Bragg and for 5-ton trucks and M48's at Grayling.

The overall effect of this clipping is not known; however, it is possible that it might have resulted in a change in the feature space. This should be investigated in future analyses.

3.2.2 Sylvania STC and SATC Classifier Logic

As described, the feature values at the end of the 10-second epoch were used in conjunction with the classifier weights supplied in Sylvania's Final Technical Reports, to implement the linear equations

$$d_i = a_{i0} + a_{i1}x_1 + a_{i2}x_2 \dots a_{in}x_n$$

where d_i is the decision logic for Class i ($i = 1, \dots, 6$); a_{i0}, \dots, a_{in} are the classifier weights; and x_1, \dots, x_n are the computed feature values.

The STC and SATC weights are given in Table 3.3. The constants for the SATC were not given in Ref. 3. These were obtained from Mr. Marv Layman of Sylvania via telephone conversation.

The Sylvania and Honeywell classifiers each use a two-stage classification procedure. A "target/no target" decision is made in the first stage -- the "no target" decision signifying Class 6 (NUS). A five-way discrimination is then made in the second stage if a "target present" decision is reached in the first stage. The first-stage decision is "target" if the output of the first-stage classifier is positive and "no target" if this output is negative. In the second stage, the maximum of five individual subclassifier outputs is selected as being the best indicator of the target class.

3.3 HONEYWELL STC AND SATC SIMULATIONS

The material available to Adaptronics, Inc. for simulation of the Honeywell STC and SATC was contained in Refs. 9 and 11. In addition to these publications, the Honeywell seismic and seismic/acoustic feature extractor and classification programs were supplied by USAMERDC. The feature extractor programs and the classification programs were written in SDS 9300 FORTRAN. Telephone conversations were held with Mr. R. R. Roth of Honeywell concerning: (1) data preprocessing procedures needed for the simulation, (2) the weights to be used in the classifiers, and (3) certain aspects of the simulation programs written by Honeywell.

TABLE 3.3
SYLVANIA STC AND SATC SIMULATION CLASSIFIER WEIGHTS (Refs. 9 and 10)

Type	Class Number	Features							
		SLBE	SLBV	SWBE	SWBV	SF	SFV	SVFV	Constant
STC	1	18.730	-15.077	14.284	19.430	2.915	56.621	71.715	-27.601
	2	15.175	-11.882	11.282	25.144	3.282	53.107	75.843	-23.030
	3	12.369	-14.958	14.478	17.855	4.674	60.194	65.323	-27.202
	4	28.010	-22.915	9.378	26.022	5.325	65.474	87.855	-36.907
	5	10.031	-13.407	6.407	34.491	3.121	60.795	67.104	-18.959
	6	3.280	-.029	-.029	5.600	.574	2.920	5.100	-4.390
SATC	1	1.866	-.065	AHBE 4.310	AWBE -3.922	.787	3.571	ALBE 5.233	-2.693
	2	1.025	.280	5.917	-5.495	.549	6.061	7.874	-3.029
	3	.667	.191	1.468	-.261	1.333	2.262	.633	-2.747
	4	1.399	-.133	6.667	-6.993	1.366	2.315	9.346	-3.616
	5	.039	2.004	1.399	-2.874	1.366	4.016	4.425	-3.729
	6	1.049	.826	5.495	-2.315	.952	1.241	3.236	-3.800

The Honeywell simulation was made compatible with the CDC 6000 series computers. The primary task was the conversion of the seismic/acoustic feature extraction program to CDC FORTRAN. The contents of the Honeywell reports indicated that their SATC design resulted from the addition of six acoustic features to the 12 STC features. Table 3.4 shows the features employed by the Honeywell STC and SATC, and the weights employed in the classifiers are shown in Table 3.5.

Next, computation steps for obtaining the feature values were compared with the hardware block diagrams, as well as the feature extractor simulation program, to verify that the sequences of filtering, rectification, and amplification of the signals were properly cascaded. The forms of the difference equations used in the feature extractor program were re-derived and compared with the program listings to ensure correct coding. After verifying that the listings compared well with the hardware feature extraction processes, conversion of the Honeywell seismic/acoustic feature extractor program to CDC FORTRAN was done.

Tests were made on the converted program by using input signals of known form and by printing output values from various points in the simulation program which represented feature values. The feature extractor program included a provision for utilizing data recorded with high or low gains. However, since the field data were recorded at a single gain, this portion of the program was not exercised.

The Honeywell classifiers used "on-off" and "adaptive threshold" criteria to limit the operation of the feature extractor in order to increase battery life. The setting of the threshold values depended on the long-term average signal level. Since

TABLE 3.4
HONEYWELL STC AND SATC FEATURES

<u>Type</u>	<u>Feature Definition</u>	<u>Range</u>
STC	1. Zero Crossing 1	0-1,240
	2. Zero Crossing 2	0-220
	3. Zero Crossing 3	0-49
	4. Zero Crossing 4	0-105
	5. Time Between Events 1	0-45
	6. Time Between Events 2	0-10
	7. Time Between Events 3	0-14
	8. Time Between Events 4	0-21
	9. Smoothness	0-46
	10. Duty Cycle Consistency	0-397
	11. High Frequency Energy	0-30
	12. Low Frequency Energy	0-40
SATC	1. Zero Crossing 1	0-1,240
	2. Zero Crossing 2	0-220
	3. Zero Crossing 3	0-49
	4. Zero Crossing 4	0-105
	5. Time Between Events 1	0-45
	6. Time Between Events 2	0-40
	7. Time Between Events 3	0-14
	8. Time Between Events 4	0-21
	9. Smoothness	0-46
	10. Duty Cycle Consistency	0-397
	11. High Frequency Energy	0-30
	12. Low Frequency Energy	0-40
	13. Zero Crossing 1	0-2,518
	14. Zero Crossing 2	0-944
	15. Zero Crossing 3	0-516
	16. Zero Crossing 4	0-328
	17. Duty Cycle Consistency	0-466
	18. Roughness Count	0-467

TABLE 3.5
HONEYWELL STC AND SATC WEIGHTING COEFFICIENTS ($\times 10^{-3}$)

Type	1 vs. All	1 vs. All	3 vs. All	4 vs. All	5 vs. All	6 vs. All
STC						
	1.422	1.043	2.140	1.311	2.069	0.000
	5.660	2.017	4.118	2.618	4.728	0.000
	8.587	1.436	4.261	3.623	6.252	0.000
	6.049	2.979	3.701	0.171	2.318	0.000
	25.110	27.089	18.276	20.393	0.000	22.607
	21.972	23.520	9.849	31.670	0.000	17.624
	19.006	24.149	16.965	19.252	0.000	32.451
	14.786	23.005	6.392	0.000	14.424	30.379
	0.000	11.176	11.812	10.893	28.523	6.292
	1.104	1.028	2.027	0.413	0.000	0.469
	9.211	10.867	0.000	24.661	20.394	30.416
	15.068	30.040	25.729	26.846	43.268	0.000
Constant	-1119.090	-1012.750	-1094.580	-1205.900	-1417.270	0.000
SATC						
	0.399	0.972	0.764	0.000	0.836	0.164
	2.214	3.035	1.792	0.000	2.439	0.515
	3.650	1.805	2.001	0.000	3.273	0.176
	4.062	2.310	3.072	0.000	4.796	0.000
	5.663	1.959	1.733	5.145	0.000	2.287
	3.466	3.706	2.202	11.165	0.000	4.232
	0.000	10.365	3.366	3.539	11.663	7.363
	7.891	3.207	3.034	6.886	21.480	0.000
	0.000	3.090	2.561	2.765	9.275	2.465
	2.034	0.187	2.469	2.024	14.390	2.401
	7.610	3.116	1.235	7.006	1.160	0.000
	2.194	21.217	6.672	7.874	0.000	11.442
	0.226	0.218	0.291	0.323	0.794	0.211
	0.360	0.766	0.390	0.663	0.000	0.392
	0.310	1.607	0.352	1.536	0.000	0.389
	0.525	0.697	0.632	2.395	0.000	0.605
	0.000	1.125	1.223	0.765	0.000	0.830
	1.455	0.000	0.331	1.148	0.000	0.800
Constant	-538.690	-1000.000	-867.240	-832.880	-735.410	-440.410

the data represented discontinuous 10-second epochs, one-third of the data was often required to establish the threshold values. This limited the actual interval for feature extraction to times of much less than 10 seconds. For this reason, the simulation of the on-off criterion was not performed, thus enabling full 10-second feature extraction.

Prior to the decision to not model the "on-off" and "adaptive threshold" criteria, tests were performed using signals of the same frequency but of different amplitude, to determine how feature development was affected by the on-off criterion. These tests showed that feature development exhibited a nearly linear relationship to the length of time the features were extracted. This indicated that the Honeywell features were dependent on the signal frequency and independent of the signal amplitude.

The effect of sampling frequency on the feature values was examined by using sampling frequencies of 2,000 Hz and 1,000 Hz for the acoustic and seismic channels, respectively, as well as 1,000 Hz and 500 Hz, respectively. It was found that the feature values, computed for a limited number of test records, varied by five percent or less. Therefore the simulations were performed using the lower frequencies of 1,000 Hz and 500 Hz for the acoustic and seismic channels.

The Honeywell classifier was designed to perform successive classifications on a continuous segment of data lasting significantly more than 10 seconds, using certain "game rules" to select a class for transmission. The data used for simulation normally consisted of isolated intervals of 10 seconds, making it impracticable to employ these game rules in the simulations. Thus, the features extracted at the end of each 10-second epoch formed the basis for classification in the simulations.

3.4 SYLVANIA AND HONEYWELL STC AND SATC SIMULATION RESULTS AND SUMMARY

The complete file of 671 field data records was used to obtain the classifications made by the Sylvania and Honeywell STC and SATC simulation programs. Confusion matrices were generated for each of the four classifiers. These matrices are presented, by site, in Tables 3.6 through 3.9. The diagonal elements of each matrix are the numbers of correct decisions. The class total is the row sum (i.e., the sum of the targets in the true class). Individual target class accuracy represents the number of correct decisions for a given class divided by the total number of records for which a target in that class existed. The site accuracy is the sum of the diagonal elements divided by total number of elements in the confusion matrix for a given site. The overall accuracy, listed at the bottom of the page, is the ratio of the total number of correct decisions to the total number of decisions.

It can be seen that the simulation accuracies are quite poor and do not correspond to the accuracies given in the manufacturer's technical reports. Each classifier exhibits considerable site dependency. The Sylvania STC decisions are heavily biased toward wheeled vehicles, and the Honeywell SATC decisions are heavily biased toward personnel. The Sylvania STC had the best overall accuracy of the four, i.e., 43 percent. (This may be due to the fact that this classifier was synthesized using data that was recorded at 23 different locations.)

The results given in Tables 3.6 through 3.9 show that low accuracies, severe biases, and considerable site dependencies are associated with all four classifiers.

TABLE 3.6
CONFUSION MATRICES FOR THE SYLVANIA STC SIMULATION

<u>Location</u>	<u>True Class</u>	<u>Decision Class</u>						<u>Class Total</u>	<u>Class Accuracy</u>	<u>Site Accuracy</u>
		<u>1</u>	<u>2</u>	<u>3</u>	<u>4</u>	<u>5</u>	<u>6</u>			
Ft. Bragg	1	21	9	8	2	0	0	40	.53	38/171 = .22
	2	21	17	0	1	0	0	39	.44	
	3	6	47	0	0	1	0	54	.00	
	4	0	34	0	0	2	0	36	.00	
	5	0	0	0	0	0	0	0	-	
	6	1	0	1	0	0	0	2	.00	
Grayling	1	32	15	8	0	0	0	55	.58	98/136 = .72
	2	4	66	0	0	0	0	70	.94	
	3	0	0	0	0	0	0	0	-	
	4	0	0	0	0	0	0	0	-	
	5	0	0	0	0	0	0	0	-	
	6	0	11	0	0	0	0	11	.00	
Yuma	1	117	35	50	1	0	40	243	.48	155/364 = .43
	2	43	38	1	0	0	0	82	.46	
	3	0	0	0	0	0	0	0	-	
	4	0	0	0	0	0	0	0	-	
	5	8	26	0	0	0	0	34	.00	
	6	5	0	0	0	0	0	5	.00	

Overall Accuracy: 291/671 = .43

TABLE 3.7
CONFUSION MATRICES FOR THE SYLVANIA SATC SIMULATION

<u>Location</u>	<u>True Class</u>	<u>Decision Class</u>						<u>Class Total</u>	<u>Class Accuracy</u>	<u>Site Accuracy</u>
		<u>1</u>	<u>2</u>	<u>3</u>	<u>4</u>	<u>5</u>	<u>6</u>			
Ft. Bragg	1	4	6	0	25	5	0	40	.10	8/171 = .05
	2	10	4	0	8	17	0	39	.10	
	3	1	8	0	3	42	0	54	.00	
	4	0	21	0	0	15	0	36	.00	
	5	0	0	0	0	0	0	0	-	
	6	0	1	0	1	0	0	2	.00	
Grayling	1	0	10	0	32	13	0	55	.00	18/136 = .13
	2	0	18	0	18	34	0	70	.26	
	3	0	0	0	0	0	0	0	-	
	4	0	0	0	0	0	0	0	-	
	5	0	0	0	0	0	0	0	-	
	6	0	0	0	0	11	0	11	.00	
Yuma	1	7	26	0	202	6	2	243	.03	40/364 = .11
	2	15	1	0	5	47	14	82	.01	
	3	0	0	0	0	0	0	0	-	
	4	0	0	0	0	0	0	0	-	
	5	0	4	0	3	27	0	34	.79	
	6	0	0	0	0	0	5	5	1.00	

Overall Accuracy: 66/671 = .10

TABLE 3.8
CONFUSION MATRICES FOR THE HONEYWELL STC SIMULATION

Location	True Class	Decision Class						Class Total	Class Accuracy	Site Accuracy
		1	2	3	4	5	6			
Ft. Bragg	1	2	0	22	8	4	4	40	.05	71/171 = .42
	2	0	0	21	10	1	7	39	.00	
	3	0	1	41	1	10	1	54	.76	
	4	3	0	0	28	5	0	36	.78	
	5	0	0	0	0	0	0	0	-	
	6	0	0	2	0	0	0	2	.00	
Grayling	1	0	0	22	3	28	2	55	.00	20/136 = .15
	2	0	19	7	1	32	11	70	.27	
	3	0	0	0	0	0	0	0	-	
	4	0	0	0	0	0	0	0	-	
	5	0	0	0	0	0	0	0	-	
	6	0	3	0	0	7	1	11	.09	
Yuma	1	0	2	89	28	90	34	243	.00	16/364 = .04
	2	4	7	30	15	3	23	82	.09	
	3	0	0	0	0	0	0	0	-	
	4	0	0	0	0	0	0	0	-	
	5	0	14	0	10	8	2	34	.24	
	6	0	0	0	4	0	1	5	.20	

Overall Accuracy: 107/671 = .16

TABLE 3.9
CONFUSION MATRICES FOR THE HONEYWELL SATC SIMULATION

<u>Location</u>	<u>True Class</u>	<u>Decision</u>						<u>Class Total</u>	<u>Class Accuracy</u>	<u>Site Accuracy</u>
		<u>1</u>	<u>2</u>	<u>3</u>	<u>4</u>	<u>5</u>	<u>6</u>			
Ft. Bragg	1	2	2	0	0	36	0	40	.05	10/171 = .06
	2	1	0	0	0	38	0	39	.00	
	3	0	0	0	0	54	0	54	.00	
	4	1	0	0	8	27	0	36	.22	
	5	0	0	0	0	0	0	0	-	
	6	0	0	0	0	2	0	2	.00	
Grayling	1	0	5	0	0	50	0	55	.00	28/136 = .21
	2	4	28	0	4	34	0	70	.40	
	3	0	0	0	0	0	0	0	-	
	4	0	0	0	0	0	0	0	-	
	5	0	0	0	0	0	0	0	-	
	6	1	0	0	0	10	0	11	.00	
Yuma	1	3	5	0	0	235	0	243	.01	21/364 = .06
	2	1	12	0	1	68	0	82	.15	
	3	0	0	0	0	0	0	0	-	
	4	0	0	0	0	0	0	0	-	
	5	0	28	0	0	6	0	34	.18	
	6	0	0	0	0	5	0	5	.00	

Overall Accuracy: 59/671 = .09

4. DETERMINATION OF DATA BASE STRUCTURE VIA CLUSTER ANALYSIS

4.1 INTRODUCTION

Cluster analysis encompasses many diverse techniques for discovering structure within complex bodies of data. In a typical example, one has a sample of data units (subjects, persons, cases) each described by scores on selected variables (attributes, characteristics, measurements). The objective is to group either the data units or the variables into clusters such that the elements within a cluster have a high degree of "natural association" among themselves while the clusters are "relatively distinct" from one another. The approach to the problem and the results achieved depend principally on how the investigator chooses to give operational meaning to the phrases "natural association" and "relatively distinct".

In cluster analysis, little or nothing is known about the category structure -- that is, the natural groupings or classes of the data. The objective is to discover a class structure that fits the observations. The essence of cluster analysis might be viewed as assigning appropriate meaning to the terms "natural groups" and "natural association".

A cluster algorithm can assemble observations into groups which prior misconception and lack of understanding would otherwise preclude. A cluster algorithm can also apply a principle of grouping more consistently in a large problem than can a human. A series of interconnected hypothesis may suggest models for the mechanism generating the observed data. Cluster analysis may, therefore, be used to reveal structure and relationships in the data -- it is a tool of discovery.

This is the spirit of its use in this study. The objective was to determine the extent of homogeneity within each of the six target classes. If the multivariate data for a given class yield one cluster containing most of the observations, the hypothesis of homogeneity is confirmed. If two or more clusters are found that contain an appreciable fraction of the data, the hypothesis is rejected. In the latter case, the conclusion that two or more prototype waveform signatures exist within the given target class is justified.

4.2 SUMMARY DESCRIPTION OF THE CLUSTER ALGORITHM

The algorithm for determining the data clusters can be summarized as follows. The first data sample is introduced and the first cell is centered at this point. The cells are hyperellipsoids, and their initial radii (principal axes) are preselected. The birth of each cell defines a new cluster in the space. The next sample is presented and it either falls within the boundary of the existing cell, within a "guard zone" surrounding the cell, or outside of the guard zone so that a second cell is generated and centered at this point. Similarly, all succeeding points either fall within one of the cells in existence at that time, within their guard zones, or determine the generation of new cells. When a point falls within a cell, the cell's location (its mean) and radii are changed to accommodate this new point. The cells thus locate themselves at the dense regions (modes) of the data and assume a shape which conforms to the spread of data about these modes.

The algorithm therefore examines the geometric interrelationships of the multivariate data, and finds clusters of data which are very close to one another, and hence very similar. Five results are reported:

1. The number of cells
2. Their (N-dimensional) location
3. Their (N-dimensional) shape
4. The identity of the data points in each cell
5. The amount of overlap existing (if any) between cells

These results yield the following information about the data space:

- The structure of the space
- The presence of noisy data
- The number and type of operating regions of the process which generated the data
- The presence of non-stationary (time-varying) conditions

CLUSTR is a one-pass, non-iterative algorithm; hence, convergence to the final result is rapid. The control constants which govern the birth rate, growth rate, and shape of the clusters are computed from the data.

The CLUSTR algorithm was used five times in this study to assess the degree of similarity between classes, using data bases consisting of features from each of the four prior-existing classifiers and using the combined Sylvania and Honeywell seismic/acoustic features.

4.3 RESULTS OF CLUSTER ANALYSES

The cluster algorithm was used to group the data into cells for each of the six target classes and to determine the amount of overlap between the cells.

Clustering of the data by classes was accomplished by organizing the data according to classes and then allowing the cluster algorithm to form cells from one class data independently of cells formed from other class data. Thus, the cells formed never contained

points from more than single target class. This approach, rather than the approach of clustering of all data as a single class, was taken because it was capable of providing more information on the similarity or dissimilarity of data within a single class. The overlap analysis portion of each cluster run resulted in a statistical measurement of the degree of overlap or separation between cells formed in the particular cluster run.^{1/} All cells, regardless of the class to which they belonged and as long as they met minimum size criteria, were compared with other cells to determine the degree of statistical overlap or separability.

In the analyses, many cells were formed that contained only a few points; such cells were not taken into consideration in the results to be described nor were they included in the accompanying figure or tables. No attempt was made to correlate these points with any of the signal identification parameters.

4.3.1 Cluster Analysis of Honeywell Seismic Features

The 12 Honeywell seismic features (Table 3.4) were used to cluster the data base of 671 records. A total of 156 cells was formed with 72.6 percent (487) of the data contained in the 25 largest cells shown in Table 4.1. The other 184 points were distributed among the remaining 131 cells, giving an average point density of 1.40. (Point density is defined as the number of points per cell.) Table 4.1 identifies the number of cells containing a large number of points in each class along with the number of points contained within each cell.

^{1/} A multivariate F-test was used to assess the probability of two cells being dissimilar at the 0.05 level of significance.

TABLE 4.1
HONEYWELL SEISMIC FEATURES
DISTRIBUTION PER TARGET CLASS

Target Class	Number of 10-Second Epochs Per Cell (Cell Identification No.)										Sum	Percent of Total in Class
	70(79)	11(81)	20(83)	14(86)	38(87)	14(101)	51(107)	18(121)				
1	70(79)	11(81)	20(83)	14(86)	38(87)	14(101)	51(107)	18(121)			236	70
2	55(32)	58(33)	7(35)	8(60)	6(68)						134	70
3	38(20)	3(25)	3(31)								44	81
4	27(10)	4(17)	4(18)								35	97
5	14(11)	4(12)	5(15)								23	68
6	8(1)	3(2)	4(4)								15	83
Overall Total:											487	73

The largest Class 1 cells did not exhibit strong grouping tendencies either by vehicle type or by site. However, in the large cells containing the Class 2 data, several cells were composed predominantly of either 5-ton trucks or M151 vehicles from the Grayling site. One cell in each Class 3 and one in Class 4 contained a large majority of the fixed-wing and rotary-wing data, respectively. (Recall that Class 3 and Class 4 data have no site variability because all records for these classes were obtained at a single site.) Two of the three major cells in Class 5 (Cells 12 and 15) were composed solely of 1- and 5-human records, respectively. The most populated Class 5 cell was composed of nearly all 3-human records. The cells in Class 6 grouped nuisance records by site.

The results of the overlap analysis portion of the cluster algorithm are shown in Table 4.2. Whenever two cells have been computed to be statistically separable at the 95 percent confidence level (via a multivariate F-test), an asterisk has been placed in the appropriate location in the table. Results of the overlap analysis show that the two most populated Class 2 cells are not separable from each other and that neither of these cells is easily separated from Class 1 cells. However, both cells are separable from the most populated Class 1 cell. This means that the 12 Honeywell seismic features are not, in general, good tracked versus wheeled vehicle discriminators. Only the major cell from Class 4 shows good separation from the populous cells of other classes. This means that rotary-winged aircraft can be well separated using these features.

These conclusions are supported by the confusion matrices in Table 3.8; only 1 percent and 14 percent of the tracked and wheeled vehicles were correctly classified, respectively, while the aircraft classifications were 76 and 78 percent correct, respectively.

TABLE 4.2
HONEYWELL STC TARGET CLASS SEPARABILITY ANALYSES

CLASS	6	5	4	3	2	1
Cell No. 1	1	11	16	20	32	81
2	2	12	17	25	35	86
3	3	13	18	31	60	101
4	4	14	19	33	68	107
5	5	15	21	35	81	121
6	6	16	22	36	83	
7	7	17	23	37	86	
8	8	18	24	38	87	
9	9	19	25	39	88	
10	10	20	26	40	89	
11	11	21	27	41	90	
12	12	22	28	42	91	
13	13	23	29	43	92	
14	14	24	30	44	93	
15	15	25	31	45	94	
16	16	26	32	46	95	
17	17	27	33	47	96	
18	18	28	34	48	97	
19	19	29	35	49	98	
20	20	30	36	50	99	
21	21	31	37	51	100	
22	22	32	38	52	101	
23	23	33	39	53	102	
24	24	34	40	54	103	
25	25	35	41	55	104	
26	26	36	42	56	105	
27	27	37	43	57	106	
28	28	38	44	58	107	
29	29	39	45	59	108	
30	30	40	46	60	109	
31	31	41	47	61	110	
32	32	42	48	62	111	
33	33	43	49	63	112	
34	34	44	50	64	113	
35	35	45	51	65	114	
36	36	46	52	66	115	
37	37	47	53	67	116	
38	38	48	54	68	117	
39	39	49	55	69	118	
40	40	50	56	70	119	
41	41	51	57	71	120	
42	42	52	58	72	121	
43	43	53	59	73		
44	44	54	60	74		
45	45	55	61	75		
46	46	56	62	76		
47	47	57	63	77		
48	48	58	64	78		
49	49	59	65	79		
50	50	60	66	80		
51	51	61	67	81		
52	52	62	68	82		
53	53	63	69	83		
54	54	64	70	84		
55	55	65	71	85		
56	56	66	72	86		
57	57	67	73	87		
58	58	68	74	88		
59	59	69	75	89		
60	60	70	76	90		
61	61	71	77	91		
62	62	72	78	92		
63	63	73	79	93		
64	64	74	80	94		
65	65	75	81	95		
66	66	76	82	96		
67	67	77	83	97		
68	68	78	84	98		
69	69	79	85	99		
70	70	80	86	100		
71	71	81	87	101		
72	72	82	88	102		
73	73	83	89	103		
74	74	84	90	104		
75	75	85	91	105		
76	76	86	92	106		
77	77	87	93	107		
78	78	88	94	108		
79	79	89	95	109		
80	80	90	96	110		
81	81	91	97	111		
82	82	92	98	112		
83	83	93	99	113		
84	84	94	100	114		
85	85	95	101	115		
86	86	96	102	116		
87	87	97	103	117		
88	88	98	104	118		
89	89	99	105	119		
90	90	100	106	120		
91	91	101	107	121		
92	92	102	108			
93	93	103	109			
94	94	104	110			
95	95	105	111			
96	96	106	112			
97	97	107	113			
98	98	108	114			
99	99	109	115			
100	100	110	116			
101	101	111	117			
102	102	112	118			
103	103	113	119			
104	104	114	120			
105	105	115	121			
106	106	116				
107	107	117				
108	108	118				
109	109	119				
110	110	120				
111	111					
112	112					
113	113					
114	114					
115	115					
116	116					
117	117					
118	118					
119	119					
120	120					
121	121					



Cells not compared.

* Indicates cell separability.

4.3.2 Cluster Analysis of Honeywell Seismic/Acoustic Features

The 671 records containing the 18 Honeywell seismic/acoustic features clustered into 123 cells. The 17 largest cells, included in Table 4.3, contain 73.3 percent (492) of the 671 records. The remaining 179 points are distributed among 106 cells for an average point density of 1.69.

The second largest tracked vehicle cluster, Cell 69, has 93.4 percent of its points from Yuma. Eighty percent of the points in this cell are those arising from M113 records, and the records not from Yuma were also M113 records. Seventy-one percent of the data in the cell were M113 records from Yuma.

Cell 70 has 75 percent of its points from Yuma. Cell 106 is composed of M48 records from Grayling.

The largest of the Class 2 cells contains 71 points, with 20, 32, 13, and 6 points representing, respectively, the following vehicle types: M141, 2½-ton truck, M792, and M15. Cluster Cells 63 and 64 are composed of 5-ton truck signature features and cluster Cell 59 is composed of 2½-ton truck records from the Ft. Bragg and Grayling sites.

The largest cells for Class 3 and Class 4 data contain about three-quarters of the data in the respective classes. The Class 6 data are grouped into three distinct cells -- one cell for nuisance records from each of the three sites.

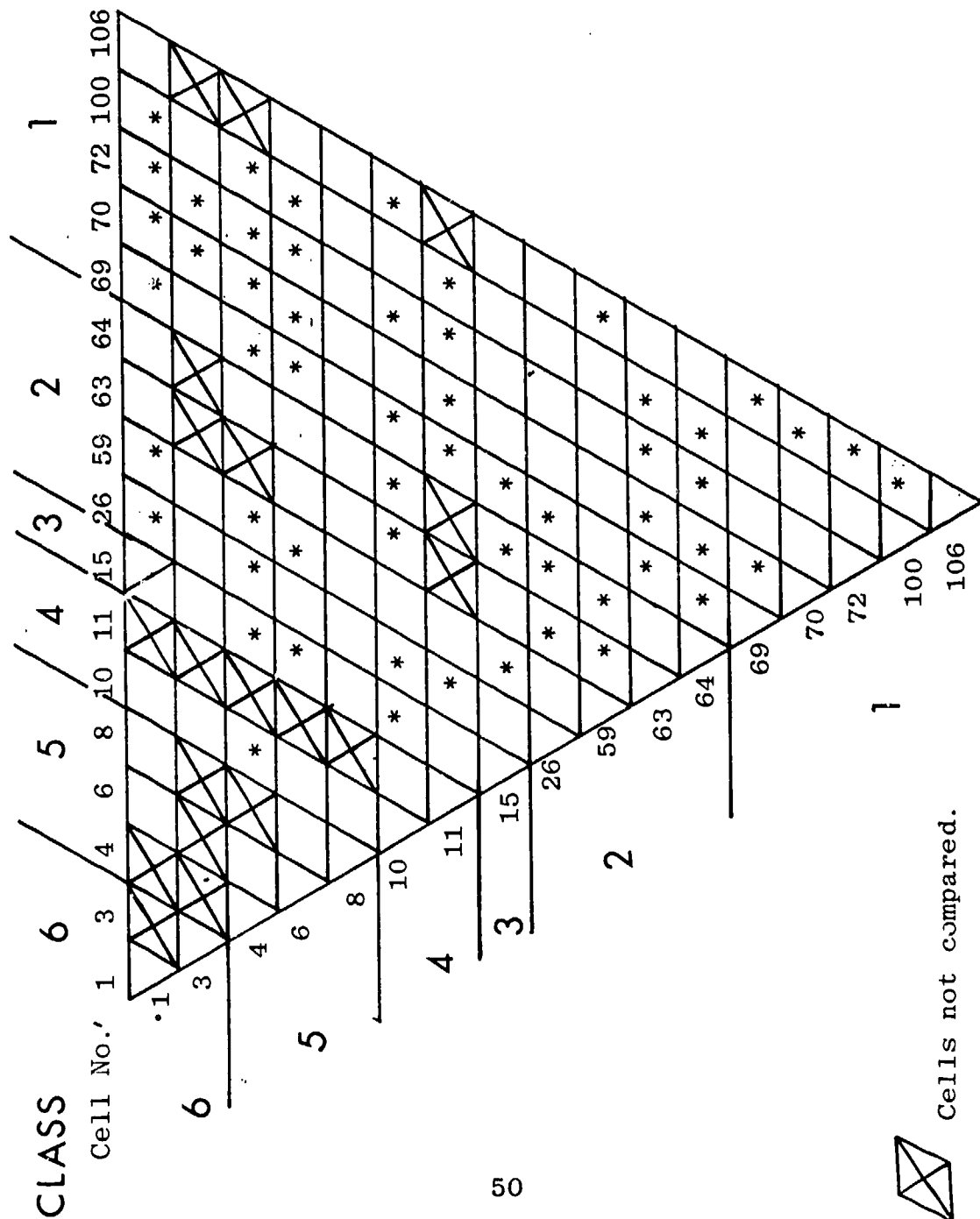
Examination of Table 4.4 indicates that the largest cells of Class 4 are separable from most major cells of all the remaining classes. None of the remaining major cells shows such a marked degree of separability from other cells. The confusion matrices in Table 3.9 support this data structure analysis -- the 27 Class 4 records are correctly classified, while almost all other targets are misclassified. These features were the worst performers (only 9 percent overall accuracy).

TABLE 4.3
HONEYWELL SEISMIC/ACOUSTIC FEATURES
DISTRIBUTION PER TARGET CLASS

Target Class	Number of 10-Second Epochs Per Cell (Cell Identification No.)						Sum	Percent of Total in Class
	91(69)	96(70)	35(72)	27(100)	10(106)			
1	91(69)	96(70)	35(72)	27(100)	10(106)		259	77
2	71(26)	18(59)	11(63)	12(64)			112	59
3	41(15)						41	76
4	27(10)	7(11)					34	94
5	8(40)	12(6)	10(8)				30	88
6	11(1)	5(3)					16	89
Overall Total:							492	73

TABLE 4.4

HONEYWELL SATC TARGET CLASS SEPARABILITY ANALYSES



Cells not compared.

* Indicates cell separability.

4.3.3 Cluster Analysis of Sylvania Seismic Features

Table 4.5 shows the 18 largest cluster cells formed for the six target classes using the Sylvania seismic features. These cells contain 427 or 63.6 percent of the entire data base. The remaining 244 points are distributed into 143 cells for an average point density of 1.71.

Fifty-two percent of the Class 1 data are contained within the most populated cell, Cell 87. Approximately 70 percent of the M60's and M113's, and 31 percent and 47 percent of the M48 and M107 data, respectively, are contained in this cell. Eighty-three percent of the records in this cell were obtained at the Yuma site, as compared to the 72 percent representation of Yuma data in the entire data base. The second largest cell, Cell 88, consists primarily of M48 and M113 Ft. Bragg records.

In general, the compositions of Class 2 cells fail to show any large incongruities between the distribution of the Class 2 data base and cell structures. However, 76 percent of the 5-ton truck data from the Grayling site, the only site from which 5-ton data were available, are clustered together.

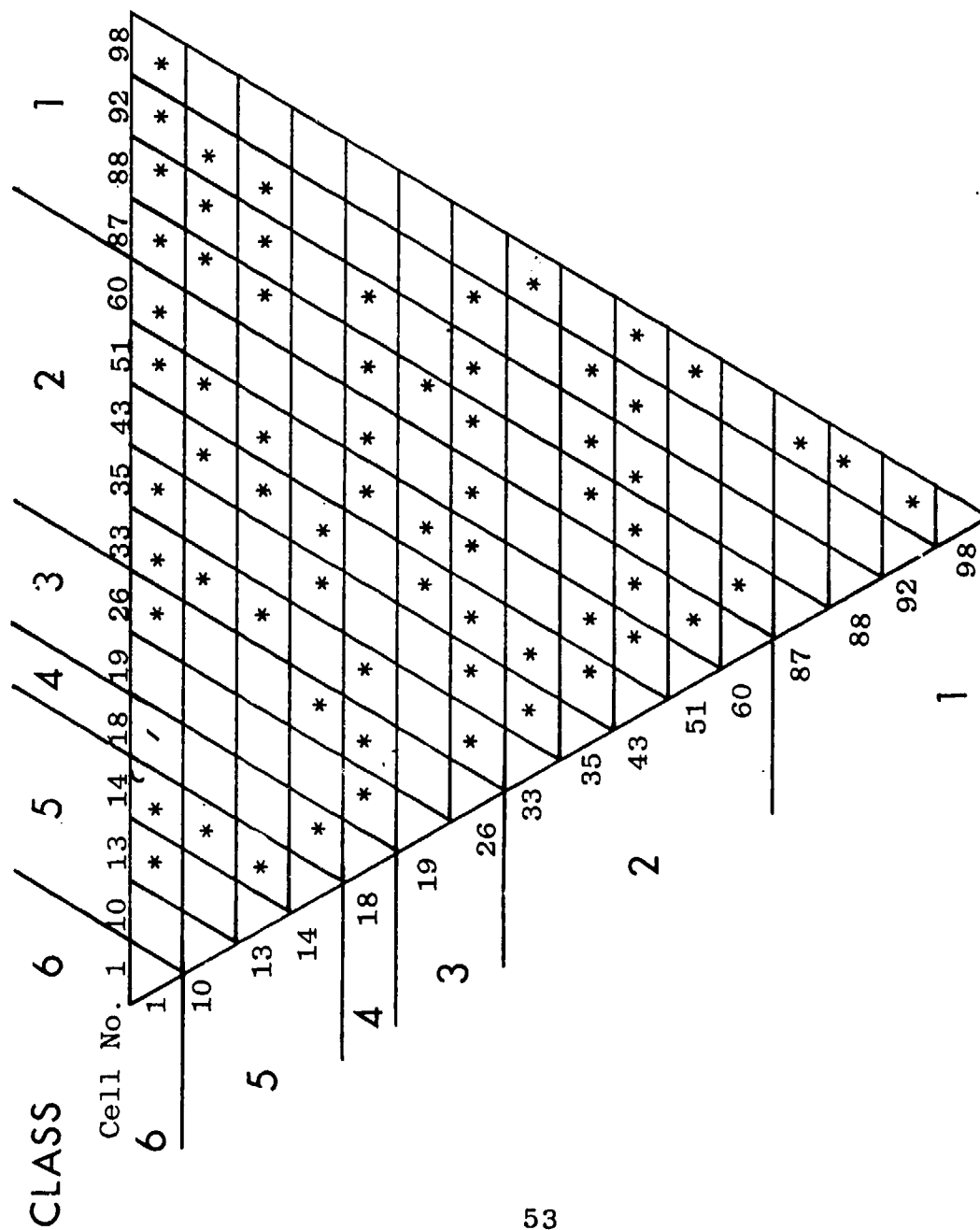
Class 3 and Class 4 data clustered tightly, with all the points in the latter clustered into a single cell. The clustering of Class 5 and Class 6 data did not show any strong grouping tendencies.

Table 4.6 presents the separability of the cells in Table 4.5. It shows that the large cell of Class 1, Cell 87, is separable from most other large cells, and that Class 3 and Class 4 data are separable from each other. These results are confirmed by the confusion matrix of Table 3.6 which shows that 117 of the tracked vehicles were correctly classified.

TABLE 4.5
 SYLVANIA SEISMIC FEATURES
 DISTRIBUTION PER TARGET CLASS

Target Class	Number of 10-Second Epochs Per Cell (Cell Identification No.)						Sum	Percent of Total in Class
	186(87)	18(88)	19(92)	7(98)	21(51)	16(60)		
1	186(87)	18(88)	19(92)	7(98)			230	68
2	16(33)	11(35)	23(43)	21(51)		16(60)	87	46
3	29(19)	8(26)					37	69
4	36(18)						36	100
5	4(8)	5(10)	7(13)	10(14)			26	76
6	7(1)	4(6)					11	61
Overall Total							427	64

TABLE 4.6
 SYLVANIA STC TARGET CLASS SEPARABILITY ANALYSES



* Indicates cell separability.

4.3.4 Cluster Analysis of Sylvania Seismic/Acoustic Features

Table 4.7 shows the 22 largest cluster cells formed for the six classes of data using the 7 Sylvania seismic/acoustic features. These cells contain 432 points, 64.4 percent, of the entire data base. The remaining 239 points are distributed among 134 cells, for an average point density of 1.78.

The largest Class 1 cell, Cell 70, contains 88 points (26 percent) of the 338 Class 1 points in the data base. Approximately 91 percent of the points in the cell are from the Yuma site. Cluster Cell 111 is also predominantly composed of M113 records from the Yuma site: 17 of the 18 records (approximately 94 percent) are from the Yuma site. Cell 72 is also made up predominantly of records from the Yuma site (approximately 83 percent), or 14 of the 17 records in this cell. The points in Cell 72 are not predominantly for one type of vehicle.

The most populated Class 2 cell, Cell 21, consists primarily of M792 records from the Yuma site and M151 records from the Ft. Bragg site. Seventy-five percent of the M792 records, and 77.8 percent of the M151 records are included in this cell. The points contained in Cells 23, 25, and 29 are composed, with the exception of a single record, entirely of M151 and 2½-ton truck records. The proportion of M151 records to 2½-ton truck records for the three cells are: 1,20, 0.20, and 4.0, respectively.

Data for the 5-ton trucks from the Grayling site form separate cells, but are not included in the table of major cells nor in the separability figure.

Class 3 and Class 4 data form tightly grouped cells; however, none of the cells contains a disproportionate number of points from a particular type of aircraft, if more than a single type was present in the class. The cells of Classes 5 and 6 show little grouping tendency, except that some three-personnel points are separated. The nuisance points from Ft. Bragg also form a distinct cell.

TABLE 4.7
 SYLVANIA SEISMIC/ACOUSTIC FEATURES
 DISTRIBUTION PER TARGET CLASS

Target Class	Number of 10-Second Epochs Per Cell (Cell Identification No.)						Sum	Percent of Total in Class
1	26(27)	19(69)	88(70)	17(72)	10(99)	29(100)	207	61
2	10(19)	48(21)	12(23)	10(25)	15(29)		95	50
3	26(9)	14(11)	5(12)				45	83
4	36(8)						36	100
5	16(3)	7(4)	4(6)	4(7)			31	91
6	16(1)	2(2)					18	100
Overall Total:							432	64

Table 4.8 shows the separability of the large cells. Table 4.8 shows the cells of Class 1 are statistically separable from the large cells of all other classes, while the major cells of the remaining classes do not show as much separability among each other.

4.3.5 Cluster Analysis of Combined Honeywell and Sylvania Features (28)

Table 4.9 shows the 20 largest cells formed for the six class cluster analysis using the 28 unique seismic and acoustic features from the Honeywell and Sylvania simulations. These 20 cells contain 560 (approximately 83 percent) of the 671 points in the data base. The remaining 111 points are distributed among 91 cells, for an average point density of 1.22.

The most populated cell in Class 1, cluster Cell 57, contains 214 points (approximately 63 percent) of all Class 1 data, with 170 (approximately 79 percent) of the 214 points from the Yuma site. Approximately 82 percent (103 of 126) of the M113 records are contained in this cell. There is not a predominant vehicle type in Cell 4; however, approximately 82 percent (27 of 33 points) in Cell 4 represent data from the Yuma site. Cells 5 and 6 consist entirely of M48 points from the Grayling site, while Cell 1 is composed entirely of M107 records from the Yuma site. Cell 2 has neither a predominant number of records from a particular site nor from a particular type of vehicle.

Approximately one-half of the points (31 of 63) in the most populated cell of Class 2 are from 2½-ton truck records. The 31 points are distributed nearly evenly by site and by the fraction of total 2½-ton truck records. The fifth Class 2 cell, Cell 44, has 11 of its 12 points representing 2½-ton trucks, while cells 6 and 7 (Cluster Cells 48 and 49) consist entirely of 5-ton truck records from the Grayling test site.

TABLE 4.8
 SYLVANIA SATC TARGET CLASS SEPARABILITY ANALYSES

CLASS	6	5	4	3	2	1
Cell No.	1 3 4 8 9	11 12 19	21 23 25 29	67 69 70 72	99 100 111	
6	1 *	*	*	*	*	*
5	3 *	*	*	*	*	*
4	4	*	*	*	*	*
3	9	*	*	*	*	*
2	11	*	*	*	*	*
1	12	*	*	*	*	*
	19	*	*	*	*	*
	21	*	*	*	*	*
	23	*	*	*	*	*
	25	*	*	*	*	*
	29	*	*	*	*	*
	67	*	*	*	*	*
	69	*	*	*	*	*
	70	*	*	*	*	*
	72	*	*	*	*	*
	99	*	*	*	*	*
	100	*	*	*	*	*
	111	*	*	*	*	*

* Indicates cell separability.

TABLE 4.9
COMBINED HONEYWELL AND SYLVANIA FEATURES
DISTRIBUTION PER TARGET CLASS

Target Class	Number of 10-Second Epochs Per Cell (Cell Identification No.)										Sum	Percent of Total in Class
	6(55)	11(56)	214(57)	33(58)	10(90)	6(95)						
1											280	83
2	7(19)	25(20)	63(21)	23(23)	12(44)	10(48)	13(49)				153	80
33	45(12)										45	83
44	36(11)										36	100
55	9(3)	10(6)	9(8)								28	82
66	16(1)	2(2)									18	100
Overall Total:											560	83

Class 3 data are found in one cell, as is all Class 4 data. The latter result was also found in the clustering of Sylvania Class 4 data. Class 5 and Class 6 data do not show noteworthy grouping tendencies.

Table 4.10 shows that the most populated cells of Classes 1, 2, 3, and 4 data are not statistically separable from each other.

4.3.6 Summary of Cluster Analysis and Conclusions

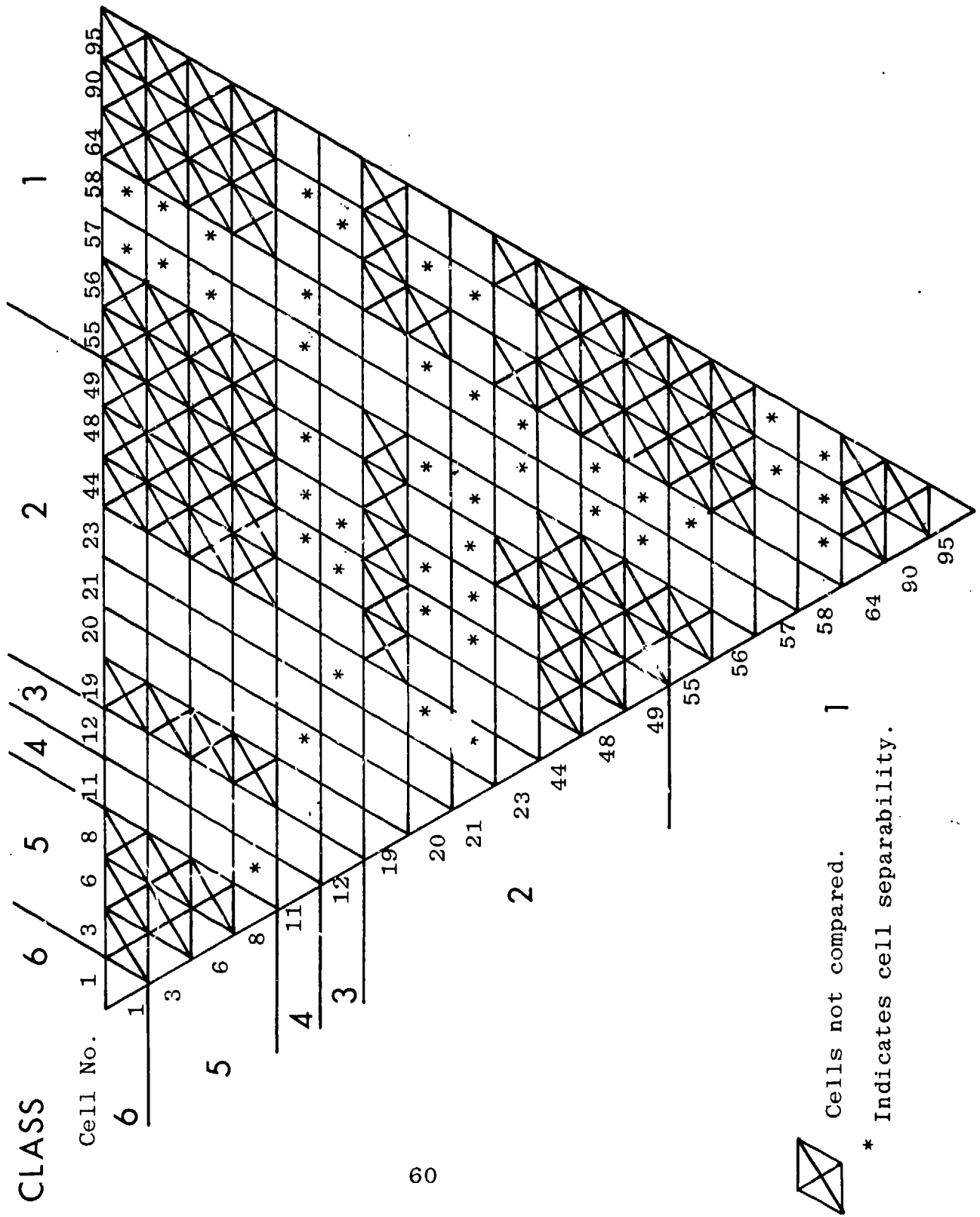
The objective of the cluster analysis was to determine the extent of homogeneity/heterogeneity of each of the five feature sets within each of the six target classes. The most favorable finding of the cluster analysis for the six-class discrimination problem would be (independently of site):

- Intra-class homogeneity of features
- Inter-class heterogeneity of features

Of course, these represent idealized situations in which all points within a class group in a single cell and the cell for each class is distinct from all other cells. Such situations rarely occur with field data.

The results of the cluster analysis exhibit some of the ideal characteristics, but not to a sufficient degree to render the six-class discrimination task easily manageable. A method of evaluating the above two characteristics would be to consider the size of the most populated cell within each class and the separability of such cells. Therefore, the more points from a given class contained in the most populated cell, and the more distinct the cell is from the others, the more easily one class is distinguished from the other.

TABLE 4.10
HONEYWELL AND SYLVANIA COMBINED FEATURE TARGET CLASS SEPARABILITY ANALYSES




 Cells not compared.
* Indicates cell separability.

Table 4.11 shows the population of the largest cells for each of the six classes based on the five cluster studies. Classes 3 through 6 have been included in the table for completeness but were not analyzed due to the small amount of data in both quantity and variety.

Comparison of the most populated cells in Classes 1 and 2 of the two Sylvania feature sets against the two Honeywell features sets shows that the Sylvania cells for Class 1 contain more points than the Honeywell cells, while for Class 2 the opposite is the case. The numbers of points in the most populated cells for the combined features resemble those in the four original feature sets.

The term "variety within a class" is used in the sense of different types and motions of signature sources, different sites and different climatic conditions for targets within a given class.

Table 4.12 was obtained by examining the most populated cells in each of the four original feature sets and tabulating the numbers of points in common between these cells and those of the combined (28) feature set. As indicated by the table, the cells formed by the Sylvania feature sets have significantly more points in common with the combined feature cells in the tracked vehicle classes than do the Honeywell cells, while the converse occurs in the comparison of wheeled cells of the four feature sets with the combined feature cells.

In conclusion, the Sylvania features show strong potential for separating tracked vehicles (Class 1), while the Honeywell features show strong potential for separating wheeled vehicles (Class 2). Furthermore, the cluster analysis shows the Honeywell features to be capable of finer discrimination on an intra-class basis, as evidenced by cells with high degrees of homogeneity within a class it also shows the Sylvania features to be capable of finer discrimination on an inter-class basis. This latter conclusion is supported by the large, but distinguishable, cells found for the tracked vehicle class.

TABLE 4.11
POPULATIONS OF LARGEST CLUSTERS IN EACH TARGET CLASS

<u>Feature Set</u>	<u>Class</u>					
	<u>1</u>	<u>2</u>	<u>3</u>	<u>4</u>	<u>5</u>	<u>6</u>
Honeywell STC	70	58	38	27	14	8
Honeywell SATC	96	71	41	27	12	11
Sylvania STC	186	23	29	36	10	7
Sylvania SATC	88	48	26	36	16	16
Combined Features	214	63	45	36	10	16

TABLE 4.12
INTERSECTIONS OF MOST POPULATED CELLS IN HONEYWELL AND SYLVANIA
FEATURE SETS WITH MOST POPULATED CELLS OF COMBINED FEATURE SET

<u>Feature Set</u>	<u>Class 1</u>	<u>Class 2</u>
Honeywell STC	65/70 = .93	47/71 = .66
Honeywell SATC	38/96 = .96	38/58 = .66
Sylvania STC	175/186 = .94	None
Sylvania SATC	73/88 = .83	17/48 = .35

5. TABULAR CLUSTER LISTINGS AND REDUCED DIMENSIONALITY PLOTS

5.1 MERGING OF STATISTICALLY SIMILAR CLUSTER CELLS

Part of the cluster analysis was to determine the statistical similarity among the cells containing the largest number of points (Section 4.3). Those cells in the same target class that are statistically similar (based on a multivariate F-test) have been merged to form larger cells. New mean (\bar{X}) and standard deviation (Σ) vectors were recomputed for the merged cells. Table 5.1 shows, for the five feature sets, the number of merged cluster cells per class. The numbers in parentheses indicate the fraction of data in the merged cluster cells relative to the total amount of data in the class.

5.2 TABULAR CLUSTER LISTINGS FOR THE FIVE FEATURE SETS

A tabular listing was generated for the five feature sets to identify the content of the cluster cells by target type, site, speed, range, acoustic and seismic gains, and target direction of motion. In addition, the \bar{X} and Σ vectors were printed showing their positions in N-dimensional space. (Due to the length of these listings, they do not appear in this report. However, copies have been provided to Dr. Richard K. Young, USAMERDC, Ft. Belvoir, Virginia; and Dr. Ted Gifford, REMBASS PM, Ft. Monmouth, New Jersey.) An example for a typical cluster cell is shown in Table 5.2. Definitions for the various fields are given in Table 5.3. (The merged cluster cells have been used for these listings.)

TABLE 5.1
NUMBER OF CLUSTER CELLS PER CLASS CONTAINING THE LARGEST NUMBER OF POINTS
(Fraction of Total in Class)

Class	Feature Sets				
	Sylvania		Honeywell		
	Seismic (7) *	Seismic/Acoustic (7)	Seismic (12)	Seismic/Acoustic (18)	Combined (28)
1	2 (.77)	4 (.70)	7 (.67)	4 (.83)	4 (.83)
2	4 (.57)	7 (.68)	6 (.75)	4 (.73)	2 (.80)
3	1 (.69)	2 (.83)	1 (.70)	1 (.76)	1 (.83)
4	1 (1.0)	1 (1.0)	1 (.75)	1 (.94)	1 (1.0)
5	2 (.65)	2 (.68)	1 (.56)	2 (.88)	3 (.82)
6	1 (.39)	1 (.89)	1 (.44)	2 (.89)	1 (.89)

* Denotes number of features.

TABLE 5.2
EXAMPLE OF TABULAR LISTING FOR A CLUSTER CELL
(See Table 5.3 for Field Definitions)

CLUSTER_ANALYSIS_EOR_12 SEISMIC_FEATURES (PONEYWELL.SIG) 1

2	3	4	5	6	7	8	9	10	11	12	13
CELL= 121	HYSE= 14										
1	121	1	M113	YUMA	6	200	30	70	E-M	1	
2	147	1	M113	YUMA	16	-100	26	70	W-F	1	
3	150	1	M113	YUMA	16	200	26	70	E-M	1	
4	167	1	M113	YUMA	22	-100	26	70	W-F	1	
5	211	1	M4A	YUMA	6	300	26	70	E-M	1	
6	219	1	M4A	YUMA	14	-300	20	70	E-M	1	
7	272	1	M4A	GRAVING	6	200	20	40	S-M	1	
8	273	1	M4A	GRAVING	6	100	20	40	S-M	1	
9	274	1	M4A	GRAVING	6	-20	20	40	S-M	1	
10	296	1	M113	GRAVING	6	-0	36	70	S-M	1	
11	307	1	M113	GRAVING	6	-0	36	70	S-M	1	
12	314	1	M113	GRAVING	14	-100	36	70	S-M	1	
13	332	1	M113	FT. DRAGG	6	200	40	70	N-S	1	
14	335	1	M113	FT. DRAGG	6	-200	40	70	N-S	1	
15	339	1	M113	FT. DRAGG	14	400	40	70	N-S	1	
16	354	1	M113	FT. DRAGG	25	-100	40	70	S-M	1	
17	364	1	M4A	FT. DRAGG	6	400	30	70	N-S	1	
18	369	1	M4A	FT. DRAGG	20	-200	30	70	S-M	1	
14	YUMA	6									
	GRAVING	-6									
	FT. DRAGG	6									
15	1	14									
	2	0									
	3	0									
	4	0									
	5	0									
	6	0									
16	M4A	0									
	M113	0									
	M113	11									
	M113	0									
	T2+5	0									
	T5+0	0									
	M715	0									
	M702	0									
	CV-10	0									
	T0-4	0									
	UH-1	0									
	H1	0									
	M3	0									
	M5	0									
	N	0									
17											
	X VECTOR										
	.83223E+03	.18555E+02	.83333E+00	.50000E+00	.33222E+02	.74444E+01	.90444E+00				
	.13388E+01	.19888E+01	.05777E+02	.50000E+02	.12999E+02						
18											
	SIG VECTOR										
	.561259E+02	.111103E+02	.204319E+01	.923548E+00	.277713E+01	.185416E+01	.105564E+01				
	.697401E+00	.140058E+01	.13584E+02	.257610E-11	.194447E+01						

TABLE 5.3
DEFINITIONS FOR TABULAR CLUSTER LISTING

<u>Identification Number</u>	<u>Definition</u>
1	Title
2	Cluster Cell Number. (Cells with less than 5 hits have been excluded from this printout.)
3	Hits: Number of Signatures in Cluster
4	MERDC ID Number
5	Class Number (a) 1 TV (b) 2 WV (c) 3 FWA (d) 4 RWA (e) 5 PER (H1, H3, H5) (f) 6 NUS
6	Vehicle Type
7	Target Site
8	Target Speed. (mph for land vehicles and personnel, knots for aircraft.)
9	Range (meters) or Altitude (feet). For personnel, range is given as stake numbers.
10	Acoustic Gain (db)
11	Seismic Gain (db)
12	Target Direction
13	File Section. (Files longer than 10 seconds were divided into 10 second epochs.)
14	Number of Signatures From Each Site
15	Number of Signatures From Each Target Class. (In this study each class was clustered separately.)
16	Number of Vehicles From Each Target Type
17	X Vector: Indicates the mean value for each feature, or center of mass of the cluster.
18	Signature Vector: Standard deviation associated with the X vector.

5.3 CORRELATION AND EIGENVECTOR ANALYSIS

As explained in Section 4.1, a cluster analysis is a valuable tool for finding the structure of a multivariate data base. However, it is difficult to visualize a group of data clusters in N-dimensions when N is larger than three. Accordingly, the dimensionality of the cluster space has been reduced via an Eigenvector transformation, for the purposes of visualization. Such a task is feasible when the features exhibit high mutual correlations, in which case the redundancy can be removed.

A correlation and Eigenvector analysis of the 671-record data base was performed and high correlations between many of the parameters were observed. Table 5.4 shows the correlation matrix of the unique 28 Honeywell and Sylvania features which are identified in Table 5.5. A separate Eigenvalue analysis was performed for each of the five data sets. Table 5.6 shows the amount of explained variance for each of these sets for each eigenvariable ("z") parameter). Each eigenvariable is a linear weighted combination of the original 28 features; the weights for z_k are the components of the k^{th} Eigenvector.

Over 94 percent of the variance is represented with two z features for the Sylvania feature sets (Table 5.6). Therefore, the Sylvania cluster can be reduced to two or three dimensions with small distortion of interpoint distances. The Honeywell features were less mutually correlated, so that z_1 and z_2 do not account for as much variance as is the case for the Sylvania features. However, over 70 percent of the variance is accounted for by z_1 and z_2 for the Honeywell features.

TABLE 5.4

CORRELATION MATRIX OF 28 HONEYWELL AND SYLVANIA FEATURES

Feature	1	2	3	4	5	6	7	8	9	10	11	12	13	14	15
1.	1.000														
2.	-.709	1.000													
3.	-.823	.664	1.000												
4.	-.850	.390	.749	1.000											
5.	.194	-.254	-.145	-.052	1.000										
6.	-.148	.422	.224	.075	-.411	1.000									
7.	.134	.153	.153	.090	-.533	.279	1.000								
8.	.018	-.007	-.042	-.094	-.751	-.106	.420	1.000							
9.	-.738	.304	.636	.904	.111	.024	.013	-.174	1.000						
10.	.867	-.627	-.646	-.642	.212	-.201	-.153	-.044	-.075	1.000					
11.	-.852	-.416	-.740	-.979	.048	-.072	-.089	.075	1.000	.642	1.000				
12.	-.865	.594	.807	.855	-.264	.171	.216	.075	.756	-.716	-.824	1.000			
13.	-.226	.206	.197	.252	-.243	.010	.090	.143	.141	-.194	-.241	.292	1.000		
14.	.162	-.109	-.158	-.178	-.042	.039	.047	.102	.150	.107	.168	-.164	-.164	1.000	
15.	-.147	.093	.064	.044	-.054	.047	.032	.051	.061	-.145	-.056	.062	-.258	-.150	1.000
16.	.119	-.128	-.070	-.091	.206	.084	-.121	-.131	-.076	.132	.097	-.156	-.600	-.568	-.317
17.	-.103	.054	.099	.130	-.186	-.071	.014	.114	.072	-.073	-.152	.193	.852	.128	-.137
18.	-.102	.128	.051	.044	-.201	.211	.116	.086	-.060	-.152	-.055	.060	.424	.271	-.156
19.	-.680	.476	.660	.671	.039	.194	-.052	-.242	.637	-.463	-.645	.621	.159	-.126	-.002
20.	-.570	.418	.582	.558	.140	.125	-.138	.305	.563	-.363	-.525	.546	.140	-.140	-.032
21.	-.530	.359	.527	.535	.214	.246	-.149	-.414	.546	-.335	-.526	.359	.070	-.115	.068
22.	-.615	.420	.563	.584	-.080	.334	.020	-.142	.595	-.427	-.584	.511	.073	-.117	-.113
23.	.789	-.596	-.656	-.648	.155	-.239	-.074	.037	-.579	.682	.640	-.696	-.211	.117	-.148
24.	.041	.063	.073	-.004	.141	-.081	-.143	-.135	.068	.112	.056	.163	.130	-.048	-.172
25.	.129	-.103	-.042	.026	.158	.125	-.131	-.121	.040	.242	.044	-.033	.081	.034	-.194
26.	.227	-.281	-.188	-.125	-.047	-.028	.024	.059	-.123	.220	.143	-.149	-.451	-.062	-.201
27.	.238	-.292	-.199	-.131	-.055	-.027	.022	.067	-.140	.231	.148	-.157	-.443	-.049	-.185
28.	.214	-.274	-.182	-.116	-.030	-.054	.022	.045	-.117	.205	.132	-.141	-.479	-.121	

16.	1.000														
17.	-.555	1.000													
18.	-.439	.312	1.000												
19.	.093	.091	-.039	1.000											
20.	-.038	.096	-.110	.685	1.000										
21.	.050	.001	-.019	.819	.696	1.000									
22.	.037	-.036	.017	.827	.665	.875	1.000								
23.	.148	-.093	-.031	-.612	-.525	-.571	-.616	1.000							
24.	-.062	.123	-.160	.239	.394	.213	.204	-.160	1.000						
25.	-.054	.150	-.161	.214	.296	.164	.165	.019	.571	1.000					
26.	.505	-.285	-.151	-.112	-.177	-.071	-.055	.271	-.098	.017	1.000				
27.	.498	-.267	-.140	-.123	-.186	-.086	-.073	.234	-.190	.022	.992	1.000			
28.	.562	-.326	-.184	-.111	-.176	-.070	-.057	.255	-.099	.004	.989	.988	1.000		

TABLE 5.5

TWENTY-EIGHT HONEYWELL AND SYLVANIA COMBINED FEATURES

Feature	Feature Definition	Counts/ Epoch
Honeywell Seismic	1. Zero Crossing 1	0-1,240
	2. Zero Crossing 2	0-220
	3. Zero Crossing 3	0-49
	4. Zero Crossing 4	0-105
	5. Time Between Events 1	0-45
	6. Time Between Events 2	0-40
	7. Time Between Events 3	0-14
	8. Time Between Events 4	0-21
	9. Smoothness	0-46
	10. Duty Cycle Consistency	0-397
	11. High Frequency Energy	0-30
	12. Low Frequency Energy	0-40
Honeywell Acoustic	13. Zero Crossing 1	0-2,518
	14. Zero Crossing 2	0-944
	15. Zero Crossing 3	0-516
	16. Zero Crossing 4	0-328
	17. Duty Cycle Consistency	0-466
	18. Roughness Count	0-467
Sylvania Seismic	19. Low Frequency Energy	<u>Volts</u> 0-6
	20. Low Band Envelope Variance	0-6
	21. Wide Band Envelope	0-6
	22. Wide Band Envelope Variance	0-6
	23. Frequency	0-6
	24. Frequency Variance	0-6
	25. Variance of Frequency Variance	0-6
Sylvania Acoustic	26. High Frequency Energy	0-6
	27. Wide Band Envelope	0-6
	28. Low Band Envelope	0-6

I/ Note that certain features identified by separate contractors are conceptually the same; however, their methods of extraction were different and therefore all the features were included for completeness. The similar features are:

Honeywell Seismic Zero Crossings	-	Sylvania Seismic Frequency
Honeywell Seismic Smoothness	-	Sylvania Seismic Wide Band Frequency
Honeywell Seismic Duty Cycle Consistency	-	Sylvania Seismic Frequency Variance
Honeywell Seismic High and Low Frequency Energy	-	Sylvania Seismic Wide Band Envelope

TABLE 5.6
EXPLAINED VARIANCE OF THE Z-PARAMETERS
FOR THE FIVE FEATURE SETS

<u>Feature Set</u>	<u>Z Parameter</u>	<u>Explained Variance</u>
Sylvania Seismic	1	.836551
	2	.945533
	3	.965647
	4	.983249
	5	.999441
	6	.999991
	7	1.000000
Sylvania Seismic/Acoustic	1	.630282
	2	.945747
	3	.981310
	4	.997267
	5	.998974
	6	.999512
	7	1.000000
Honeywell Seismic	1	.538796
	2	.791986
	3	.865301
	4	.905383
	5	.934377
	6	.954164
	7	.970069
	8	.981889
	9	.989737
	10	.995673
	11	.998574
	12	1.000000
Honeywell Seismic/Acoustic	1	.393631
	2	.595473
	3	.722784
	4	.782288
	5	.835100
	6	.874335
	7	.932060
	8	.928955
	9	.948531
	10	.961205
	11	.972340
	12	.981633
	13	.986961
	14	.991925
	15	.995971
	16	.997947
	17	.999049
	18	1.000000
Honeywell/Sylvania Combined	1	.414540
	2	.564610
	3	.682408
	4	.747074
	5	.794903
	6	.835086
	7	.865469
	8	.890200
	9	.907269
	10	.923146
	11	.938231
	12	.949391
	13	.959661
	14	.967579
	15	.973191
	16	.978376
	17	.982428
	18	.985824
	19	.988871
	20	.991538
	21	.994072
	22	.996058
	23	.995711
	24	.998452
	25	.999016
	26	.999517
	27	.999823
	28	1.000000

5.4 REDUCED DIMENSIONALITY CLUSTER PLOTS

Each cluster cell in the original feature space may be transformed to the (rotated and orthogonal) Eigenvariable z-space by the operation:

$$z_{k_{\max}} = \sum_{i=1}^N u_{ki} [(X_i + \Sigma_i) - \bar{X}_i]$$
$$z_{k_{\min}} = \sum_{i=1}^N u_{ki} [(X_i - \Sigma_i) - \bar{X}_i]$$

where $z_{k_{\max}}$ and $z_{k_{\min}}$ are the maximum and minimum boundaries, respectively, of the cell on the kth z axis ($k=1,2,3$), and

u_{ki} is the ith Eigenvector weight for the kth Eigenvector,
 X_i is the ith mean value of the cell in the X-space,
 Σ_i is the ith standard deviation of the cell in the X-space,
 \bar{X}_i is the mean value of the ith feature,
 N is the number of original features.

Figure 5.1 shows the cluster cells from the Sylvania seismic feature sets plotted in two-dimensional Z space for every pair of target classes. Notice that some classes are clearly separable from other classes, for instance, Class 4 is distinct from Class 1 and Class 3. Other classes are very close together but not overlapping (at the one-sigma level). Thus, Classes 1, 3, and 5 are sufficiently separated to permit accurate discrimination. However, some of the classes overlap one another extensively; e.g., Classes 2 and 4, 2 and 5, etc.

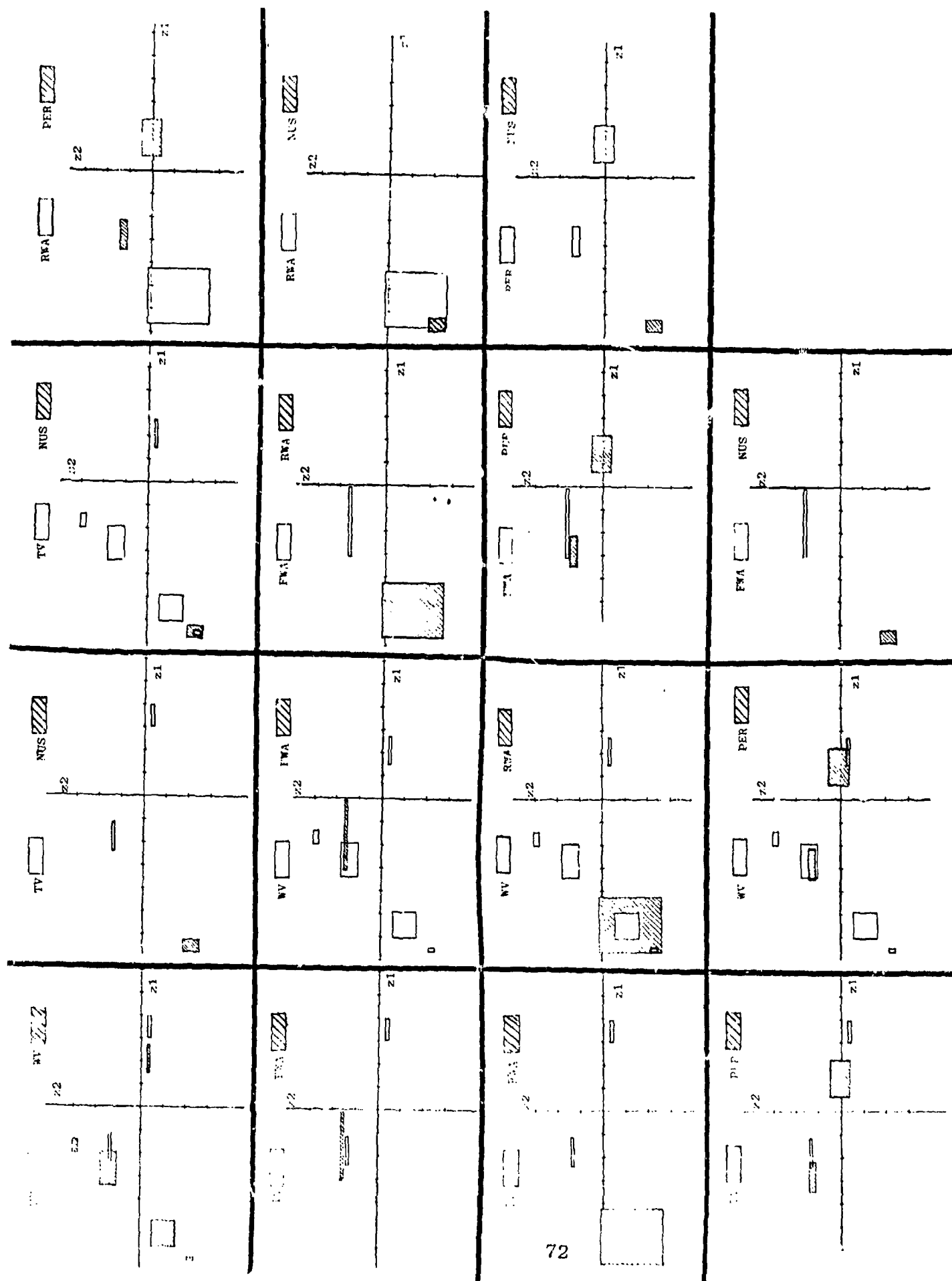


FIGURE 5.1: TWO-DIMENSIONAL CLUSTER PLOTS IN Z SPACE FOR THE SYLVANIA FEATURE SET

The clusters shown in Figure 5.1 represent the major groups of data for each target class (Table 5.1). The results of the reduced-dimensionality cluster analysis agree well with the confusion matrices found below for the Sylvania STC using regenerated weights (Table 6.8). For example, consider the Class 2 cluster in the center of Class 4. It can be seen from Table 6.8 that 19 of 43 Class 2 at Grayling are misclassified as Class 4 targets. Similarly 10 of 36 Class 3 targets at Ft. Bragg are misclassified as Class 2. Thus, the confusion matrix results are supported by the high degree of overlap as shown in Figure 5.1. Also, those classes appearing clearly separable in Figure 5.1 are rarely misclassified (Table 6.8).

A cluster plot was prepared for the combined Honeywell and Sylvania feature set showing cell boundaries along the first three Z axes. This plot is presented in Figure 5.2. The vertical axis denotes the number of members in a given cell. A logarithm scale was chosen for plotting ease. The three Z axes represent approximately 68 percent of the variance of the feature set. The twelve rectangles shown correspond to the merged cluster cells. (Note: on the z2 axis, the three PER clusters were so close together they are shown as one rectangle.) Although most clusters on a single axis seem to overlap with those of another class, there is actually a good degree of separability when all three axes are considered. A necessary and sufficient condition for two cells to be separable in N dimensions is that they are separable on any one of the N axes. For example, notice that Cell 1 (NUS) overlaps with Cell 6 (FWA) and Cell 8 (WV) on z1, but on z2 it is separated from these cells. Since the nuisance class only contains only this one cell, this class is separable from both WV and RWA.

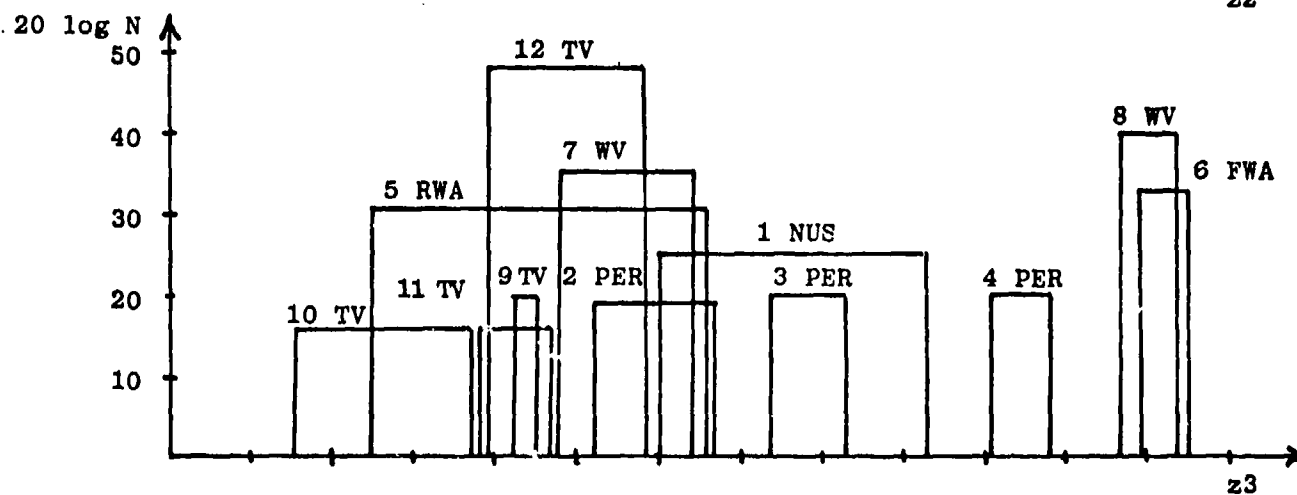
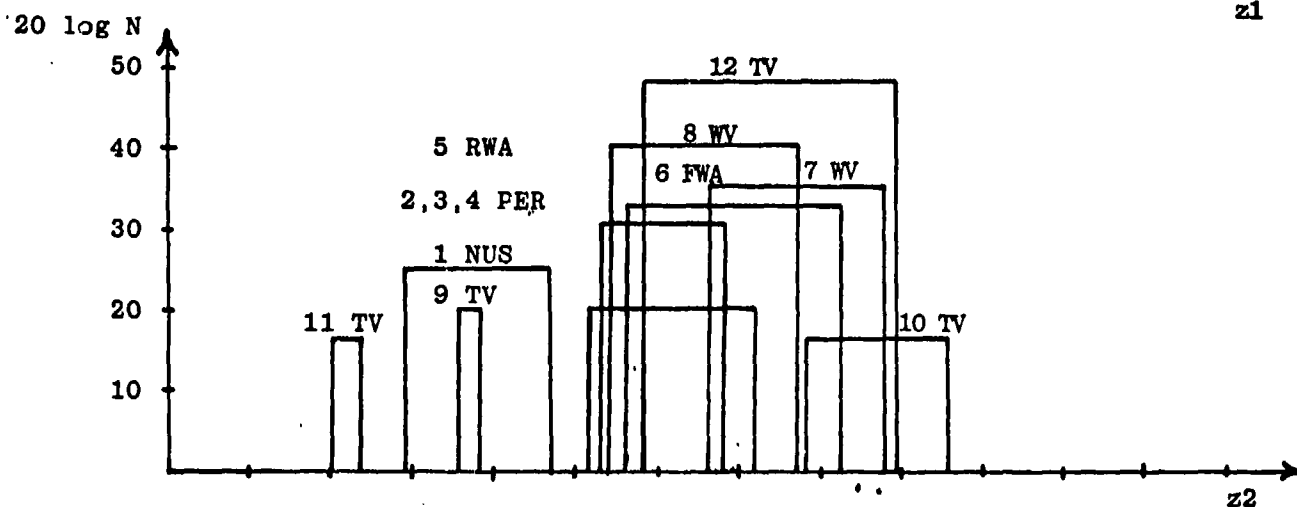
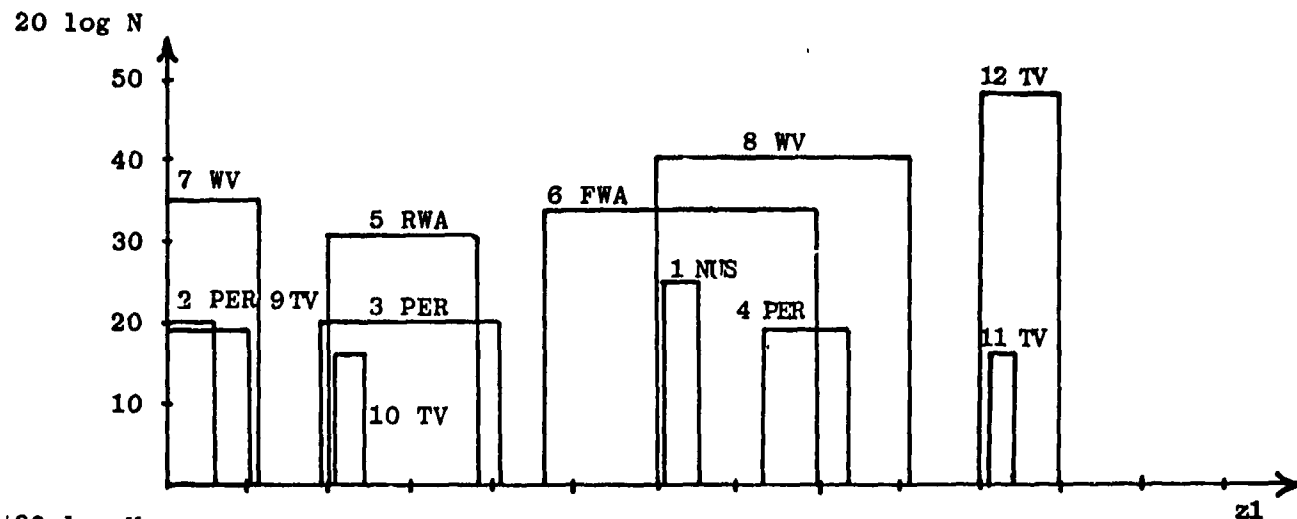


FIGURE 5.2: REDUCED DIMENSIONALITY CLUSTER PLOTS ALONG THREE Z AXES FOR THE HONEYWELL AND SYLVANIA COMBINED FEATURE SET

It can be seen from Figure 5.1 that a linear classifier could be implemented for pairwise separation between the following classes using the Sylvania STC features:

TV, RWA
TV, NUS
FWA, RWA
FWA, NUS
RWA, PER
PER, NUS

Thus, a linear classifier could be used for separating Class 1 from Class 3 and Class 3 from Class 5. However, these clusters are very close together, and slight changes in the circuit parameter of analog circuits could cause misclassifications. The following remaining target classes can only be separated nonlinearly:

TV, WV
TV, PER
WV, FWA
WV, RWA
WV, PER
WV, NUS
RWA, NUS

6. CLASSIFIER REGENERATION AND SYNTHESSES

6.1 INTRODUCTION

The Honeywell and Sylvania STC and SATC classifiers have been regenerated, i.e., optimized vis-a-vis the present field data, and five new classifiers have been synthesized by Adaptronics, Inc. The number of sensor channels, signal features, and discriminant functions; and the type of discriminant function, decision logic, and display for each classifier, are summarized in Table 6.1. The weights for all nine classifiers were computed from an identical design data base of 225 records and evaluated on the remaining 446 records. This provided a common design and evaluation data base for comparing the performance characteristics of the nine classifiers. The numbers of records included in each class in the data bases are given in Table 6.2. The records in the design set were selected at random, and represent about one-third of the data from each class.

Classifiers A, B, C, and D correspond to the classifiers simulated in the work described in Section 3 of the report; however, new weighting coefficients were computed from the design data base. A single set of coefficients was obtained for classifiers F and H since these classifiers differed only in the decision logic and display method. A single set of nonlinear, adaptive learning networks (ALN) was generated for classifiers G and I, since these two differed in the same way as classifiers F and H.

A composite feature set for each record was produced by combining: (1) 28 selected Sylvania and Honeywell seismic and acoustic signature features, and (2) the acoustic-to-seismic energy ratio. The last parameter was suggested by Dr. Richard K. Young, USAMERDC Project Monitor. Dr. Young had observed in the data collection and digitization process that the ratio of acoustic-to-seismic energy showed promising potential as a class discrimination parameter.

TABLE 6.1
SIMULATED SEISMIC AND SEISMIC/ACOUSTIC TARGET CLASSIFIERS

Identification	Classifier	Channels	Features	Number of Discriminant Functions	Type of Discriminant Functions	Type of Decision Logic	Outputs or Display	Performance Ranking
A	Sylvania STC	1	7	6	1 vs. 5 Linear	Maximum	Target Class	8th
B	Sylvania SATC	2	7	6	1 vs. 5 Linear	Maximum	Target Class	7th
C	Honeywell STC	1	12	6	1 vs. 5 Linear	Maximum	Target Class	9th
D	Honeywell SATC	2	18	6	1 vs. 5 Linear	Maximum	Target Class	6th
E	Adaptronics SATC #1	2	29	6	1 vs. 5 Linear	Maximum	Target Class	5th
F	Adaptronics SATC #2	2	29	15	1 vs. 1 Linear	Voting with Tie-Breaking	Target Class	4th
G	Adaptronics SATC #3	2	29	15	1 vs. 1 Nonlinear	Voting with Tie-Breaking	Target Class	3rd
H	Adaptronics SATC #4	2	29	15	1 vs. 1 Linear	Voting without Tie-Breaking	All Target Classes Receiving \geq V Votes	1st
I	Adaptronics SATC #5	2	29	15	1 vs. 1 Nonlinear	Voting without Tie-Breaking	All Target Classes Receiving \geq V Votes	2nd

TABLE 6.2
CLASS COMPOSITION OF DESIGN
AND EVALUATION DATA BASES

<u>Class</u>	<u>Design</u>	<u>Evaluation</u>
1	113	225
2	64	127
3	18	36
4	12	24
5	12	22
6	<u>6</u>	<u>12</u>
TOTAL	<u>225</u>	<u>446</u>

Root mean square (RMS) values were obtained for the two transducer channels during the simulation phase of the project, and these were used to derive the 29th parameter value for each record. The input RMS values were reduced to transducer output RMS values, and the logarithm of the ratio of acoustic-to-seismic energy transducer output values was used as the value of the 29th parameter.

Classifiers E, F, and H employed linear functions of the 29 parameters in their discriminant functions, while Classifiers G and I employed nonlinear combinations of the 29 parameters for their discriminant functions. The values from the nine Eigenvector transformations associated with the largest Eigenvalues and the acoustic-to-seismic ratio described above were used to generate the nonlinear discriminant functions. (The Eigenvector analysis of the Sylvania and Honeywell features was described in Section 5.1.) Thus, the 10 independent variables used for the nonlinear discriminant functions of Classifiers G and I were:

$$x'_1 = \sum_{i=1}^{28} u_{1i} x_i$$

.

.

.

$$x'_9 = \sum_{i=1}^{28} u_{9i} x_i$$

$$x'_{10} = x_{29}$$

where the x_i are the 29 features while the x'_i represent the transformed inputs used to synthesize the nonlinear ALN discriminant functions.

6.2 LINEAR "ONE VERSUS FIVE" CLASSIFIERS

Classifiers A, B, C, D, and E are all linear "one versus five" classifiers; that is, they used six discriminant functions with 7, 7, 12, 18, and 29 features, respectively. The discriminant functions are of the form:

$$d_i = \sum_{j=1}^N w_{ij}x_j + w_{i0} \quad (i = 1, 2, \dots, 6)$$

where N is the number of features in the discriminant function. The weights in each function were computed by using the design data as input to a linear regression program. This program computed the regression equations in a stepwise (i.e., one variable at-a-time) manner. At each step an additional variable was added to the regression equation. The variable added was the one which resulted in the greatest reduction in the error sum of squares. The added variable had the highest partial correlation with the dependent variable partialled on the previously added variables. The dependent variable in all cases was assigned a value of +1.0 for the category of interest.

In a "one versus five" type discriminant function, the data for category one, +1.0 dependent variable value, were all from the same class; data for category two, -1.0 dependent variable value, were records from the remaining five classes. (In a "one versus one" function, data in the second category would be selected from only one other class.)

For example, to derive d_2 , the function to discriminate Class 2 targets from targets of the other classes (one versus five), a dependent variable, y , was added to each design data record. For Class 2 data, y was assigned a +1.0 value, while for all other classes a -1.0 was assigned. The numerical imbalance between the number of Class 2 data and the data of all other classes was

corrected by duplicating the Class 2 records until a numerical balance was attained between the two categories. (The five "one versus five" discriminant functions were obtained via the same technique.) The weighting coefficients obtained for classifiers A, B, C, D, and E are shown in Tables 6.3 to 6.7 for the respective classifiers.

The six "one versus five" discriminant functions gave each target class one opportunity of being selected. A positive discriminant function output was related to a single class, while a negative output indicated the possibility of any one of the other five classes as the source. The target class whose associated discriminant function output value was the maximum of the six discriminant function outputs was selected as the classified target. Tables 6.8 to 6.12 are the confusion matrices obtained by applications of the five classification procedures A, B, C, D, and E to the evaluation data base (446 signatures). Comparing these results with Tables 3.6 to 3.9 show a considerable classification accuracy increase.

6.3 LINEAR "ONE VERSUS ONE" CLASSIFIERS

The linear "one versus one" (pairwise) discriminant functions were derived using the same techniques as were used to derive the linear "one versus five" discriminant functions. However, in the design data, only two classes were represented at a time rather than the six classes. Since there were six classes of interest, $K = 6$ and all possible non-repetitive pairs of classes were to be discriminated, the number of discriminant functions was:

$$\frac{K(K-1)}{2} = \frac{6(5)}{2} = 15$$

The classifier architecture is shown in Figure 6.1.

TABLE 6.3

WEIGHTING COEFFICIENTS FOR REGENERATED SYLVANIA STC CLASSIFIER

Feature	1 VS ALL	2 VS ALL	3 VS ALL	4 VS ALL	5 VS ALL	6 VS ALL
1	.00073	-.03980	-.15655	.26356	-.08142	-.15196
2	-.10855	.10195	.21637	.01319	.04882	.04439
3	-.33510	.47601	.13422	.17938	.11485	-.33516
4	.04751	-.23715	-.01194	0.00000	-.16050	.31178
5	.00176	-.14234	.48984	-.01539	-.95941	-.47143
6	.48530	-.52893	1.66315	-1.40894	-1.32045	1.11421
7	1.68101	-4.10440	4.58118	-8.50164	.73846	-7.70700
Constant	1.08154	-1.00895	-2.20551	-1.49930	1.35644	1.38106

TABLE 6.4

WEIGHTING COEFFICIENTS FOR REGENERATED SYLVANIA SATC CLASSIFIER

Feature	1 VS ALL	2 VS ALL	3 VS ALL	4 VS ALL	5 VS ALL	6 VS ALL
1	-.20147	.17774	-.04255	.36422	-.17376	.14196
2	-.07649	0.00000	.15243	-.00758	.05427	-.08217
3	-2.01174	.07175	.77934	-.44126	1.84470	.89836
4	1.48494	-2.17881	.15986	.70556	-.71942	-1.72949
5	-.16381	.10180	.43453	-.19585	-.75679	.05879
6	.42176	-.02008	1.84092	-2.09662	-1.04829	.47778
7	-.03201	1.46687	-.87197	-.43423	-.51854	.91173
Constant	.15744	.16777	-1.46259	-.94075	1.71429	.24011

TABLE 6.5

WEIGHTING COEFFICIENTS FOR REGENERATED HONEYWELL STC CLASSIFIER

Feature	1 VS ALL	2 VS ALL	3 VS ALL	4 VS ALL	5 VS ALL	6 VS ALL
1	.00174	-.00086	.00070	-.00042	-.00166	-.00096
2	-.00862	.00144	.00422	.01086	-.00302	.00573
3	.02481	-.02937	-.01433	.00297	.00632	-.03453
4	-.00434	-.00230	-.02417	.03887	-.03962	-.03450
5	.01851	-.02891	-.05161	-.02291	-.04182	-.05302
6	.02883	-.00446	-.06290	.00256	-.05692	-.07019
7	-.00347	.00000	.03555	0.00000	-.02388	.04542
8	.12801	.16240	.18139	.08071	.00082	.19349
9	-.06216	.03448	.05934	-.04950	.02167	.01622
10	-.00043	-.00442	.00423	.00351	-.00192	.00125
11	-.10220	.05751	-.05320	.08679	-.02357	-.09693
12	.02640	-.01083	0.00000	-.02499	.04285	.02375
Constant	.77528	1.16791	2.19911	-2.45689	3.42573	4.93537

TABLE 6.6

WEIGHTING COEFFICIENTS FOR REGENERATED HONEYWELL SATC CLASSIFIER

Feature	1 VS ALL	2 VS ALL	3 VS ALL	4 VS ALL	5 VS ALL	6 VS ALL
1	.00199	-.00125	.00033	-.00022	.00009	-.00129
2	-.00557	-.00147	-.00057	.01136	.00220	.00217
3	.01012	-.02192	-.00522	.00180	-.00959	-.02291
4	-.01747	.00320	-.00414	.04031	-.00585	-.03153
5	0.00060	-.01858	-.02852	-.02389	-.00924	-.03220
6	.00722	-.05115	-.03355	.00155	-.01428	-.04958
7	-.00601	-.02449	.03706	-.00488	-.01643	.03012
8	.09539	.14663	.11521	.07751	.08057	.13193
9	-.03589	.06310	.01448	-.04927	-.02107	.02634
10	-.00084	-.00291	.00218	.00322	-.00151	.00185
11	-.11091	.09673	-.01452	.08387	-.03248	-.04904
12	.04403	-.01870	-.00540	-.02382	.02791	.02013
13	-.00083	.00152	.00085	.00032	-.00056	.00070
14	.00017	.00081	.00109	.00117	.00025	.00039
15	-.00014	.00154	-.00156	.00036	.00333	.00026
16	.00439	.00145	-.00137	.00104	-.00211	.00163
17	.00468	-.00819	-.00215	-.00257	.00331	-.00141
18	.00341	.00031	-.00507	-.00108	-.00232	.00181
Constant	.30696	-.70839	1.53036	-2.71230	.74939	2.03707

TABLE 6.7

WEIGHTING COEFFICIENTS FOR TOTAL FEATURE SET CLASSIFIER

Feature	1 VS ALL	2 VS ALL	3 VS ALL	4 VS ALL	5 VS ALL	6 VS ALL
1	.00101	-.00067	-.00023	.00048	-.00109	-.00149
2	-.00228	-.00430	.00154	.00780	0.00000	.00616
3	.01210	-.00132	-.00306	.00806	-.00501	-.01260
4	-.00767	0.00000	.03922	.02963	.00593	-.02102
5	-.00518	.02602	-.00522	.00930	.01308	-.01759
6	-.03228	-.00181	-.00987	.03012	.01752	0.00000
7	-.00088	-.003804	.05290	-.01745	-.00708	-.00268
8	-.00813	.02756	-.01255	.05982	-.01964	.00935
9	-.01004	.04411	-.01006	-.06702	-.03479	.01451
10	.00065	-.00250	.00048	.00067	.00068	.00285
11	-.06636	.07514	.00509	.06154	-.04589	-.03230
12	.02074	.00614	-.04350	-.00841	.00734	.03178
13	-.00020	.00089	.00101	.00036	-.00098	.00048
14	.00041	.00047	.00042	.00095	-.00030	.00018
15	.00088	-.00039	-.00295	.00048	.00207	0.00000
16	.00242	.00230	-.00370	.00186	-.00304	.00208
17	.00220	-.00015	-.00093	-.00154	.00285	.00140
18	.00065	.00146	-.00584	-.00137	-.00322	.00326
19	0.00000	.04775	-.03201	.16374	-.05645	-.32397
20	-.00558	-.00943	.10251	.02329	-.05328	.07728
21	-.07407	.00256	.14202	.15377	-.13970	-.08981
22	-.06030	-.02657	-.08359	-.01656	-.01910	.25691
23	-.12206	-.04367	.17856	.04902	-.12678	.37476
24	.46675	-1.18501	.84028	-.62326	1.01020	-.48291
25	1.51986	.08331	-2.77286	-.33084	-.53908	1.91027
26	-1.07110	.44517	.33252	.54653	.88456	-.36743
27	.76657	-.68173	-.08785	0.00000	-.10589	-.39528
28	.34707	.33677	-.16474	-.36259	-.42193	.63703
29	.21175	-.22015	.16564	.03168	-.07968	-.05283
Constant	.05605	-1.68010	-2.03392	-4.92647	2.82591	-1.12174

TABLE 6.8
CONFUSION MATRICES FOR THE SYLVANIA STC WITH REGENERATED WEIGHTS (EVALUATION SET)

Location	True Class	Decision						Class Total	Class Accuracy	Site Accuracy
		1	2	3	4	5	6			
Ft. Bragg	1	25	2	1	0	1	0	29	.86	
	2	7	9	5	2	2	1	26	.35	
	3	3	10	15	2	2	4	36	.42	
	4	0	6	0	15	0	3	24	.63	
	5	0	0	0	0	0	0	0	-	
	6	2	0	0	0	0	0	2	.00	
64/117 = .55										
Grayling	1	15	10	4	4	7	0	40	.38	
	2	1	7	3	19	2	8	43	.16	
	3	0	0	0	0	0	0	0	-	
	4	0	0	0	0	0	0	0	-	
	5	0	0	0	0	0	0	0	-	
	6	0	0	0	5	1	1	7	.14	
23/90 = .26										
Yuma	1	129	7	9	3	6	2	156	.83	
	2	23	22	4	5	3	1	58	.38	
	3	0	0	0	0	0	0	0	-	
	4	0	0	0	0	0	0	0	-	
	5	4	4	0	1	9	4	22	.41	
	6	3	0	0	0	0	0	3	.00	
160/239 = .67										

Overall Accuracy: 247/446 = .55

TABLE 6.9

CONFUSION MATRICES FOR THE SYLVANIA SATC WITE REGENERATED WEIGHTS (EVALUATION SET)

<u>Location</u>	<u>True Class</u>	<u>Decision</u>						<u>Class Total</u>	<u>Class Accuracy</u>	<u>Site Accuracy</u>
		<u>1</u>	<u>2</u>	<u>3</u>	<u>4</u>	<u>5</u>	<u>6</u>			
Ft. Bragg	1	21	6	2	0	0	0	29	.72	75/117 = .64
	2	1	17	2	2	2	2	26	.65	
	3	4	6	18	4	4	0	36	.50	
	4	0	4	1	19	0	0	24	.79	
	5	0	0	0	0	0	0	0	-	
	6	2	0	0	0	0	0	2	.00	
Grayling	1	19	1	2	17	1	0	40	.48	37/90 = .41
	2	2	18	5	15	3	0	43	.42	
	3	0	0	0	0	0	0	0	-	
	4	0	0	0	0	0	0	0	-	
	5	0	0	0	0	0	0	0	-	
	6	0	6	0	0	1	0	7	.00	
Yuma	1	134	8	3	4	7	0	186	.86	189/239 = .79
	2	1	41	4	2	3	7	58	.71	
	3	0	0	0	0	0	0	0	-	
	4	0	0	0	0	0	0	0	-	
	5	0	8	1	1	12	0	22	.55	
	6	0	0	0	0	1	2	3	.67	

Overall Accuracy: 301/446 = 67

TABLE 6.10

CONFUSION MATRICES FOR THE HONEYWELL STC WITH REGENERATED WEIGHTS (EVALUATION SET)

<u>Location</u>	<u>True Class</u>	<u>Decision</u>						<u>Class Total</u>	<u>Class Accuracy</u>	<u>Site Accuracy</u>
		<u>1</u>	<u>2</u>	<u>3</u>	<u>4</u>	<u>5</u>	<u>6</u>			
Ft. Bragg	1	8	14	3	0	4	0	29	.28	
	2	3	20	1	0	2	0	26	.77	
	3	3	9	16	0	8	0	36	.44	
	4	0	0	0	17	6	1	24	.71	
	5	0	0	0	0	0	0	0	-	
	6	2	0	0	0	0	0	2	.00	
61/117 = .52										
Grayling	1	8	4	3	0	20	5	40	.20	
	2	1	20	0	0	21	1	43	.47	
	3	0	0	0	0	0	0	0	-	
	4	0	0	0	0	0	0	0	-	
	5	0	0	0	0	0	0	0	-	
	6	0	1	0	0	5	1	7	.14	
29/90 = .32										
Yuma	1	26	32	17	1	40	40	156	.17	
	2	12	27	1	0	14	4	58	.47	
	3	0	0	0	0	0	0	0	-	
	4	0	0	0	0	0	0	0	-	
	5	0	6	0	0	16	0	22	.73	
	6	0	1	0	1	1	0	3	.00	
69/239 = .29										

Overall Accuracy: 159/446 = .36

TABLE 6.11
CONFUSION MATRICES FOR THE HONEYWELL SATC WITH REGENERATED WEIGHTS (EVALUATION SET)

<u>Location</u>	<u>True Class</u>	<u>Decision</u>						<u>Class Total</u>	<u>Class Accuracy</u>	<u>Site Accuracy</u>
		<u>1</u>	<u>2</u>	<u>3</u>	<u>4</u>	<u>5</u>	<u>6</u>			
Ft. Bragg	1	12	11	3	0	2	1	29	.41	75/117 = .64
	2	4	22	0	0	0	0	26	.85	
	3	0	9	23	0	0	4	36	.64	
	4	2	2	0	18	0	2	24	.75	
	5	0	0	0	0	0	0	0	-	
	6	2	0	0	0	0	0	2	.00	
75/117 = .64										
Grayling	1	20	6	1	3	1	9	40	.50	59/90 = .66
	2	4	38	0	1	0	0	43	.88	
	3	0	0	0	0	0	0	0	-	
	4	0	0	0	0	0	0	0	-	
	5	0	0	0	0	0	0	0	-	
	6	0	6	0	0	0	1	7	.14	
59/90 = .66										
Yuma	1	69	62	3	2	2	18	156	.44	132/239 = .55
	2	4	43	2	1	6	2	58	.74	
	3	0	0	0	0	0	0	0	-	
	4	0	0	0	0	0	0	0	-	
	5	0	4	1	0	17	0	22	.77	
	6	0	0	0	0	0	3	3	1.00	
132/239 = .55										

Overall Accuracy: 266/446 = .60

TABLE 6.12
CONFUSION MATRICES FOR THE ADAPTRONICS SATC. #1 (EVALUATION SET)

Location	True Class	Decision						Class Total	Class Accuracy	Site Accuracy
		1	2	3	4	5	6			
Ft. Bragg	1	22	2	2	1	1	1	29	.75	
	2	0	24	1	0	1	0	26	.92	
	3	2	1	32	0	0	1	36	.89	
	4	0	1	0	23	0	0	24	.95	
	5	0	0	0	0	0	0	0	-	
	6	2	0	0	0	0	0	2	.00	
101/117 = .86										
Grayling	1	26	1	10	1	1	1	40	.65	
	2	4	37	1	0	1	0	43	.86	
	3	0	0	0	0	0	0	0	-	
	4	0	0	0	0	0	0	0	-	
	5	0	0	0	0	0	0	0	-	
	6	0	6	0	1	0	0	7	.00	
63/90 = .70										
Yuma	1	154	0	1	1	0	0	156	.98	
	2	3	45	1	0	5	4	58	.77	
	3	0	0	0	0	0	0	0	-	
	4	0	0	0	0	0	0	0	-	
	5	0	3	0	1	17	1	22	.77	
	6	0	0	0	0	0	3	3	1.00	
219/239 = .92										

Overall Accuracy: 383/446 = .86

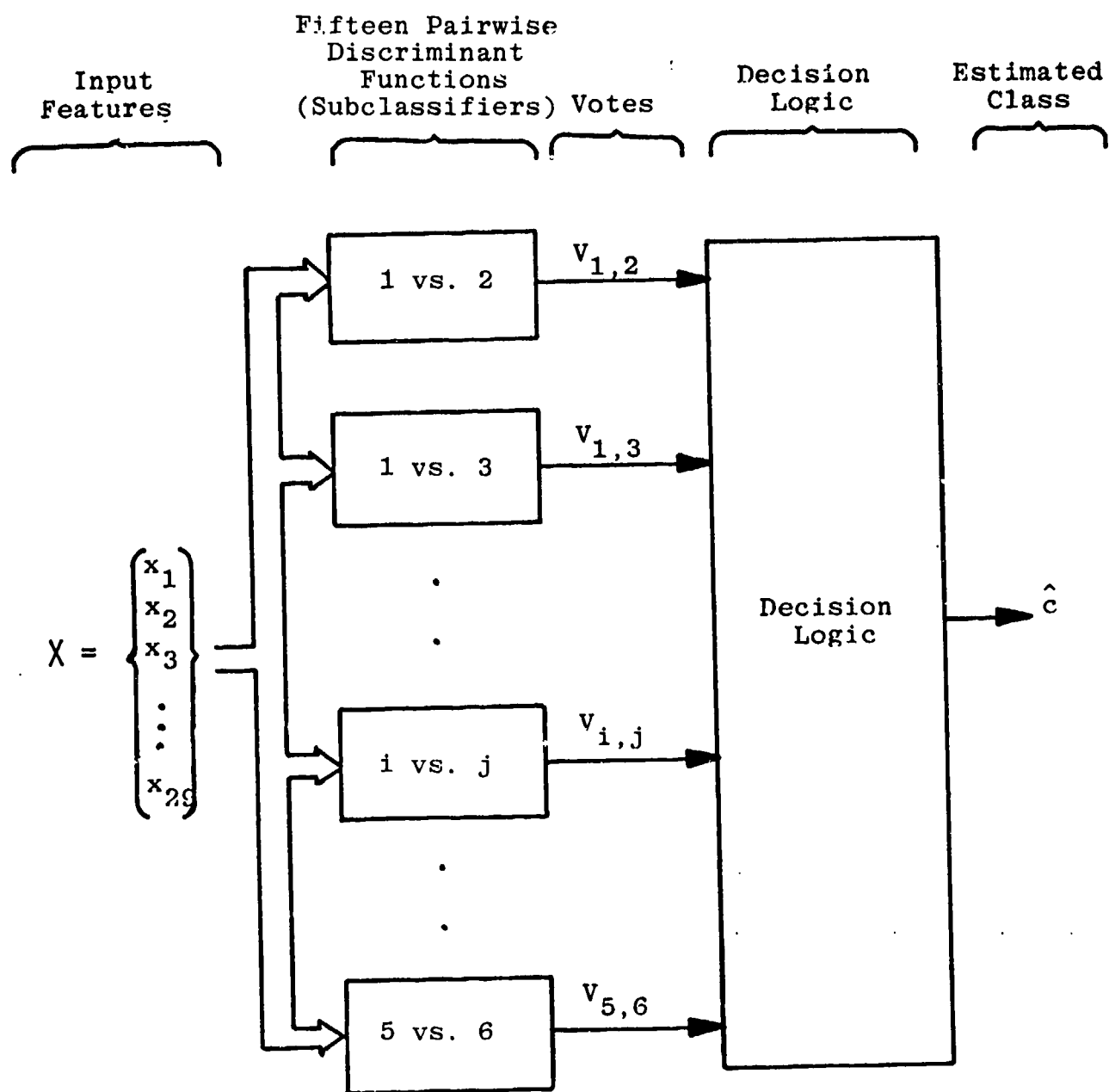


FIGURE 6.1: "ONE-VERSUS-ONE" (PAIRWISE) CLASSIFIER ARCHITECTURE

The decision surface of each pairwise subclassifier is such that one target class tends to be mapped into a fixed value below its threshold and the other target class into a fixed value above. The usual convention is that a pairwise discriminant function attempts to map all class i members onto the number $+1.0$ and all class j members onto the number -1.0 , with the discrimination threshold set midway between these two values, i.e., set equal to zero.

In a pairwise test, the proximity of the computed discriminant function output to one of the number $+1$ and -1 (i.e., the expected outputs) governs the decision -- the threshold represents the point of uncertainty. The closer the output is to either $+1$ or -1 (using a suitable metric such as squared normalized difference), the greater the confidence that can be placed in the consequent decision. A tie-breaking strategy that exploits this confidence information is illustrated by means of the following example.

Table 6.13 contains the hypothetical outputs of the 15 pairwise tests for one 10-second record. It can be seen that with a threshold equal to zero, a positive output renders a unit "vote" for Class i and vice versa for a negative output. (The value " i " is always less than " j "). In this illustrative example, Classes 1 and 2 are tied with four votes each. Classes 3, 4, 5, and 6 are eliminated from further consideration.

TABLE 6.13
ILLUSTRATION OF TIE-BREAKING STRATEGY

<u>ALN No.</u>	<u>Class i Versus Class j</u>	<u>Output</u>	<u>Winning Class</u>
1	1 vs. 2	+1.01	1
2	1 vs. 3	+0.91	1
3	1 vs. 4	-0.13	4
4	1 vs. 5	+0.85	1
5	1 vs. 6	+1.15	1
6	2 vs. 3	+0.69	2
7	2 vs. 4	+0.71	2
8	2 vs. 5	+.87	2
9	2 vs. 6	-0.85	2
10	3 vs. 4	-0.88	4
11	3 vs. 5	+0.92	3
12	3 vs. 6	+1.00	3
13	4 vs. 5	-0.78	5
14	4 vs. 6	+0.91	4
15	5 vs. 6	+0.93	5

<u>Voting Logic</u>	
<u>Target Class</u>	<u>No. Votes</u>
1	4
2	4
3	2
4	3
5	2
6	0

The following measure of confidence may be used in the case of ties:

$$M_k = \sum_{m=1}^{K(K-1)/2} V_m \left| 1 - |k_A| \right|$$

where:

K = Number of classes

K_A = Actual output for Class K

V_m = "Selection operation" $V_m = 0$ if Class k is not involved in the m th test or if k is involved but loses; $V_m = 1$ if Class k is involved in m th test and wins.

M_k is equal to zero if the actual outputs, k_A , always equal unity. Larger values of M_k usually denote weaker decisions. Therefore, a tie-breaking strategy is to evaluate M_k for those classes k in contention and to choose that class for which the M_k value is smallest.

Continuing, for the example given in Table 6.13, the associated M_1 and M_2 values for the tied Classes 1 and 2 are:

$$M_1 = |1-1.01| + |1-0.91| + |1-0.85| + |1-1.15| = 0.40$$

$$M_2 = |1-0.69| + |1-0.71| + |1-0.87| + |1-0.85| = 0.88$$

Therefore, Class 1 is the classified target due to its obtaining the larger degree of confidence.

The coefficients of the 15 linear discriminant functions are shown in Table 6.14.

TABLE 6.14
LINEAR PAIRWISE WEIGHTING COEFFICIENTS FOR THE COMBINED 29-FEATURE SET

Feature	1 VS 2	1 VS 3	1 VS 4	1 VS 5	1 VS 6	2 VS 3	2 VS 4	2 VS 5
1	.00117	.00151	.00014	.00050	.00051	-.00083	-.00076	.00246
2	.00408	-.00389	-.00964	-.01016	-.01581	.00178	-.00851	.00118
3	.02913	.00182	-.00833	.01957	.03699	-.02022	-.01558	-.00525
4	-.00279	-.02261	-.02637	.00223	.01312	-.02451	-.02604	-.01681
5	-.03515	-.00331	-.01131	-.02477	-.01342	-.01116	-.01564	.03968
6	0.00000	.01403	-.01835	-.01326	-.00586	-.00812	-.05093	.01415
7	-.00772	-.04375	.02502	-.00531	.01919	-.05517	-.03439	.05252
8	-.02336	.00172	-.03886	-.01321	-.00570	-.0214	-.03293	.21270
9	-.01194	-.01644	.08342	0.00100	-.05593	.02694	.04045	.02844
10	.00022	-.00021	-.00138	.00050	-.00035	.00126	-.00085	-.01078
11	-.02974	-.00899	-.03889	.06063	.02823	-.01330	-.06922	-.00957
12	-.01514	.06093	.02283	.01629	.00092	.03746	.01359	.00494
13	-.00047	-.00062	-.00025	.00096	-.00002	-.00159	-.00056	.00208
14	0.00000	.00070	-.00051	.00060	.00008	-.00203	-.00198	.00269
15	.00148	.00379	.00041	-.00076	.00045	-.00084	-.00351	.00120
16	.00064	.00596	.00011	.00335	.00036	-.00104	-.00518	.01079
17	.00694	.00332	.00227	-.00095	-.00070	-.00250	-.000568	-.00320
18	.00113	.00388	.00150	.00171	-.00049	.00696	.00017	.00390
19	.04273	.09292	-.04932	.09837	.19949	-.06605	-.06375	0.00000
20	-.00931	-.12278	.00889	-.04335	.00426	-.03815	-.06581	.12754
21	0.00000	-.20803	-.04924	.04984	-.05581	.05147	-.15393	.40587
22	-.08488	.07515	-.07203	.05144	-.10179	0.00000	.11245	-.01987
23	-.12732	-.26296	-.08639	.03601	-.36571	.04082	.14333	.23141
24	.49371	-.49524	.20309	-.11295	-.31032	-.37910	.62033	-.126862
25	.73113	1.86812	3.68124	.80736	-.43355	3.06819	2.57165	-3.06349
26	-.04714	0.00000	-.67819	-.58730	.17458	-.37635	1.03669	-.54017
27	.52797	-.07410	.17055	.03792	.15120	-.14843	-.43188	0.00000
28	.11705	.14921	.26102	.33762	-.24023	.44567	-.18212	.19944
29	.30644	0.00000	.04551	.24881	.18726	-.21022	-.18825	.11870
Constant	-.73475	.78124	2.32828	-3.24419	.13030	2.85912	7.63217	-7.08980

(Continued)

TABLE 6.14
(Continued)

Feature	2 VS 6	3 VS 4	3 VS 5	3 VS 6	4 VS 5	4 VS 6	5 VS 6
1	-.00027	.00124	.00110	0.00000	.00159	0.00000	0.00000
2	.00141	.01578	-.00676	-.04524	0.00000	0.00000	0.00000
3	.02015	-.00451	.10202	.12450	.00282	.00939	0.00000
4	.02561	0.00000	.02570	.01526	.01534	0.00000	.02696
5	-.04684	.06141	.08620	-.03728	0.00000	-.00239	0.00000
6	.00718	-.02156	.21981	0.00100	.03075	.01691	.21748
7	-.10449	.15820	-.19255	-.47287	-.02349	-.03036	0.00000
8	-.14423	-.03813	.63225	-.11348	.01262	0.00000	.34817
9	.05194	.05995	-.16295	-.15223	-.06260	0.00000	-.01634
10	.00467	.00273	-.00356	-.00230	0.00000	0.00000	0.00000
11	.10764	.04762	-.21257	-.09798	-.02108	0.00000	.29453
12	-.08377	.01751	-.13622	.03789	-.03794	0.00000	0.00000
13	-.00071	.00471	-.00135	0.00000	0.00000	0.00000	-.00389
14	-.00183	.00770	-.00515	0.00000	0.00000	.00395	.01225
15	.00029	.02551	-.00795	0.00000	-.00218	0.00000	.01592
16	-.00850	.00341	-.01675	0.00000	.00154	.00978	0.00000
17	-.00582	.00219	.00187	.00306	0.00000	.00119	.00296
18	-.00301	-.00836	-.00193	-.00534	-.00486	-.00272	.01799
19	.00867	-.03863	-.28578	.14544	.26409	.08612	-2.99797
20	-.12008	-.19437	.20031	0.00000	.23999	0.00000	.70541
21	-.41548	-.04058	-.77545	-.45426	0.00000	0.00000	.22407
22	-.04855	.17512	.76497	.16686	.04959	0.00000	2.14023
23	-.55944	-.68569	.58992	0.00000	.24603	.09672	0.00000
24	.45571	-1.14923	.18867	.53128	0.00000	-1.20971	0.00000
25	8.32266	-12.26537	17.94618	4.04592	-18.73417	22.95428	0.00000
26	.64316	0.00000	.16561	0.00000	0.00000	0.00000	0.00000
27	.73809	1.25131	0.00000	-1.01230	-.95938	0.00000	-1.75156
28	-1.16508	-1.22013	-.37700	1.45780	.95432	.15127	0.00000
29	.17922	-.07364	.50160	.17437	.29234	0.00000	0.00000
Constant	4.66708	-10.01749	6.92690	7.36496	-1.65026	-1.78764	-14.75704

Table 6.15 presents results obtained with Classifier F for the data in the evaluation subset. This classifier employs the "one versus one" architecture with the above tie-breaking procedure. The discriminant functions are linear.

As an alternative to tie-breaking, it may be desirable to report all classes receiving at least V votes. Table 6.16 presents the results for Classifier H, which also uses "one versus one" architecture and linear discriminant functions. The classifier is regarded as having produced a correct response whenever it generated at least four votes ($V = 4$) for the true class. With this classifier, the following vote tallies are obtained:

- 4 correct votes reported 55 times out of 446 cells (12.3 percent)
- 5 correct votes reported 344 times out of 446 cells (77.1 percent)

Thus, at least four votes were received for the correct class on 399 records out of 446 in the evaluation data subset, or on 89.5 percent of the evaluation records.

It is also noteworthy that when it reported five votes for a single class, Classifier H was correct on 344 out of 380 records or 90.5 percent of the time.

TABLE 6.15
CONFUSION MATRICES FOR THE ADAPTRONICS SATC #2 (EVALUATION SET)

Location	True Class	Decision						Class Total	Class Accuracy	Site Accuracy
		1	2	3	4	5	6			
Ft. Bragg	1	19	7	2	0	1	0	29	.66	
	2	0	22	0	0	2	2	26	.85	
	3	4	4	27	0	0	1	36	.75	
	4	0	0	0	24	0	0	24	1.00	
	5	0	0	0	0	0	0	0	-	
	6	2	0	0	0	0	0	2	.00	
92/117 = .79										
Grayling	1	35	1	2	1	1	0	40	.88	
	2	2	36	2	0	1	2	43	.84	
	3	00	0	0	0	0	0	0	-	
	4	0	0	0	0	0	0	0	-	
	5	0	0	0	0	0	0	0	-	
	6	0	3	0	0	1	3	7	.43	
74/90 = .82										
Yuma	1	151	0	2	3	0	0	156	.97	
	2	3	45	1	0	9	0	58	.78	
	3	0	0	0	0	0	0	0	-	
	4	0	0	0	0	0	0	0	-	
	5	0	5	1	0	16	0	22	.73	
	6	0	0	0	0	0	3	3	1.00	
215/239 = .90										

Overall Accuracy: 381/446 = .85

TABLE 6.16
CONFUSION MATRICES FOR THE ADAPTRONICS SATC #4 (EVALUATION SET)

<u>Location</u>	<u>True Class</u>	<u>Decision</u>						<u>Class Total</u>	<u>Class Accuracy</u>	<u>Site Accuracy</u>
		<u>1</u>	<u>2</u>	<u>3</u>	<u>4</u>	<u>5</u>	<u>6</u>			
Ft. Bragg	1	21	5	2	0	1	0	29	.72	102/117 = .87
	2	0	23	0	0	1	2	26	.88	
	3	0	2	34	0	0	0	36	.94	
	4	0	0	0	24	0	0	24	1.00	
	5	0	0	0	0	0	0	0	-	
	6	2	0	0	0	0	0	2	.00	
Grayling	1	36	0	2	1	1	0	40	.90	78/90 = .87
	2	2	38	0	0	1	2	43	.88	
	3	0	0	0	0	0	0	0	-	
	4	0	0	0	0	0	0	0	-	
	5	0	0	0	0	0	0	0	-	
	6	0	2	0	0	1	4	7	.57	
Yuma	1	153	0	2	1	0	0	156	.98	221/239 = .92
	2	3	46	1	0	8	0	58	.79	
	3	0	0	0	0	0	0	0	-	
	4	0	0	0	0	0	0	0	-	
	5	0	2	1	0	19	0	22	.86	
	6	0	0	0	0	0	3	3	1.00	

Overall Accuracy: 399/446 = .89

6.4 NONLINEAR "ONE VERSUS ONE" CLASSIFIERS

Nonlinear pairwise ("one versus one") discriminant functions have been synthesized by combining pairs of inputs, x_i and x_j , into building-block polynomial elements according to the equation

$$y = w_0 + w_1x_i + w_2x_j + w_3x_ix_j + w_4x_i^2 + w_5x_j^2$$

A nonlinear discriminant function may consist of layers of such elements combined to model a given dependent variable. Each layer may consist of as many elements as the number of pairwise combinations of the input parameters processed by that layer, but only the most discriminating elements need be retained. These elements may then, in turn, be used as inputs to the next layer of the network. Reference 2 gives a concise explanation of learning network theory and applications.

The Eigenvalue Analyses (Section 5.3) showed that a large percentage of the data variance for the combined feature set could be explained or represented with a reduced number of new orthogonal "Z" variables. Taking advantage of this fact, only ten features were used to train the 15 nonlinear discriminant functions. The first nine Z variables (of the 28 combined features), representing 90 percent of the data variance, plus the acoustic to seismic energy ratio (mentioned above) as the tenth feature. In effect, all 28 Honeywell and Sylvania features are represented in the nonlinear classifiers. The i th Z variables are given by:

$$Z_i = \sum_{j=1}^{28} u_{ij}x_j$$

where the u_{ij} are the 28 Eigenvector weights for the i th z variable and the x_j are the 28 Honeywell and Sylvania features.

Appendix D gives the Eigenvector weighting coefficients for the first nine Z variables, and the structures of the 15 nonlinear discriminant functions which have been synthesized. The weighting coefficients are shown for each pairwise discriminator.

Two sets of confusion matrices have been generated for the nonlinear "one versus one" classifier. The first set, shown in Table 6.17, was obtained by application of the tie-breaking decision logic; and the second set, shown in Table 6.18, was obtained by the vote-reporting technique, as described above.

The misclassifications have been tabulated for the nonlinear classifier using the tie-breaking decision logic (G) and are shown in Table D.2 of Appendix D. The letters "D" and "E" in this table, which appear under header word "SET," indicate which signatures were used for "Design" or "Evaluation" of the classifier. Range is given in meters for tracked and wheeled vehicles.

Figure D.16 indicates how the nonlinear classifier performed as a function of range for tracked and wheeled vehicles. In the figure, the blank bars show the distribution of signatures for the two classes as a function of range from the sensor. Superimposed on each blank bar is the number of misclassifications made for the appropriate class. It can be seen from this diagram that the relative number of misclassifications is reasonably independent of the range between target and sensor. Although only a few signatures were available at high ranges, no misclassifications were made for tracked vehicles beyond 600 meters.

TABLE 6.17
CONFUSION MATRICES FOR ADAPTRONICS SATC #3 (EVALUATION SET)

Location	True Class	Decision						Class Total	Class Accuracy	Site Accuracy
		1	2	3	4	5	6			
Ft. Bragg	1	19	8	2	0	0	0	29	.66	
	2	0	21	4	0	1	0	26	.81	
	3	3	2	29	0	0	2	36	.81	
	4	0	2	0	22	0	0	24	.92	
	5	0	0	0	0	0	0	0	-	
	6	2	0	0	0	0	0	2	.00	
91/117 = .78										
Grayling	1	29	8	2	0	0	1	40	.73	
	2	2	40	1	0	0	0	43	.93	
	3	0	0	0	0	0	0	0	-	
	4	0	0	0	0	0	0	0	-	
	5	0	0	0	0	0	0	0	-	
	6	0	2	1	0	0	4	7	.57	
73/90 = .81										
Yuma	1	148	5	2	1	0	0	156	.95	
	2	2	45	4	0	7	0	58	.78	
	3	0	0	0	0	0	0	0	-	
	4	0	0	0	0	0	0	0	-	
	5	0	3	0	0	19	0	22	.86	
	6	2	0	0	0	0	1	3	.33	
213/239 = .89										

Overall Accuracy: 377/446 = .85

TABLE 6.18
CONFUSION MATRICES FOR THE ADAPTRONICS SATC #5 (EVALUATION SET)

<u>Location</u>	<u>True Class</u>	<u>Decision</u>						<u>Class Total</u>	<u>Class Accuracy</u>	<u>Site Accuracy</u>
		<u>1</u>	<u>2</u>	<u>3</u>	<u>4</u>	<u>5</u>	<u>6</u>			
Ft. Bragg	1	20	7	2	0	0	0	29	.69	96/117 = .82
	2	0	21	4	0	1	0	26	.81	
	3	3	1	30	0	0	2	36	.83	
	4	0	1	0	23	0	0	24	.96	
	5	0	0	0	0	0	0	0	-	
	6	2	0	0	0	0	0	2	.00	
Grayling	1	32	6	1	0	0	1	40	.80	.78/90 = .87
	2	2	40	1	0	0	0	43	.93	
	3	0	0	0	0	0	0	0	-	
	4	0	0	0	0	0	0	0	-	
	5	0	0	0	0	0	0	0	-	
	6	0	0	1	0	0	6	7	.86	
Yuma	1	150	3	2	.1	0	0	156	.96	216/239 = .90
	2	2	45	4	0	7	0	58	.78	
	3	0	0	0	0	0	0	0	-	
	4	0	0	0	0	0	0	0	-	
	5	0	3	0	0	19	0	22	.86	
	6	1	0	0	0	0	2	3	.67	

Overall Accuracy: 390/446 = .87

7. COMPARISON OF CLASSIFIER RESULTS

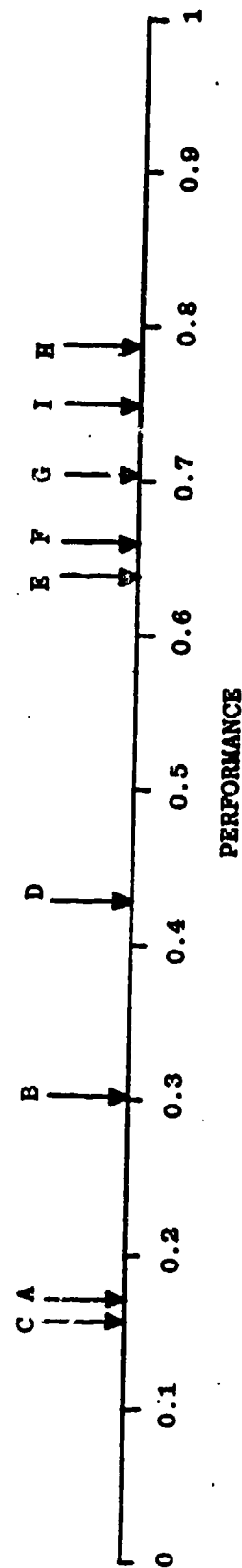
In evaluating the performance of a classifier, three criteria should be taken into consideration. These criteria reflect the ability of a classifier to perform both accurately and consistently. Thus the performance of the classifier is herein defined as the product of three metrics: the classifier accuracy (A), the consistency of the classifier accuracy (C), and the degree of site independence of the classifier (S). These quantities were explained in Section 1. The performance of the nine classifiers were computed from the confusion matrices of Section 6. The results are shown in Table 7.1. In addition, the class accuracies of all nine classifiers have been plotted in Figure 7.1. (The abscissa of this plot is non-Euclidian.)

The performance of the nine classifiers demonstrates that a significant increase occurs when the combined set of 29 parameters is utilized. (It was observed in the discrimination function generation procedure that the acoustic-to-seismic energy ratio was one of the first parameters to be selected in the linear discriminant functions, and it was selected as a key parameter in 10 of the 15 nonlinear ALN discriminant functions.) Classifiers using all 29 parameters, whether in "one versus five" or "one versus one" discriminant functions, all achieve accuracies in the 85 percent range. A further increase in classifier performance is obtained when the alternative method of reporting ties is used.

The consistency factor, C, improved with the addition of the acoustic parameters to the Sylvania and Honeywell seismic parameters, and improved again as the classifiers using the combined 29 features were evaluated. The additional of the acoustic parameters also resulted in a decrease of the site dependency.

TABLE 7.1
PERFORMANCE RANK-ORDERING OF NINE CLASSIFIERS

<u>Identification</u>	<u>Overall Accuracy, A</u>	<u>Consistency of Overall Accuracy, C</u>	<u>Site Independence, S</u>	<u>Performance P = AxCxS</u>
H	.895	.935	.937	.784
I	.874	.946	.908	.751
G	.845	.958	.870	.704
F	.854	.886	.874	.661
E	.859	.930	.800	.639
D	.596	.854	.840	.428
B	.675	.867	.518	.303
A	.554	.817	.373	.169
C	.357	.779	.559	.155



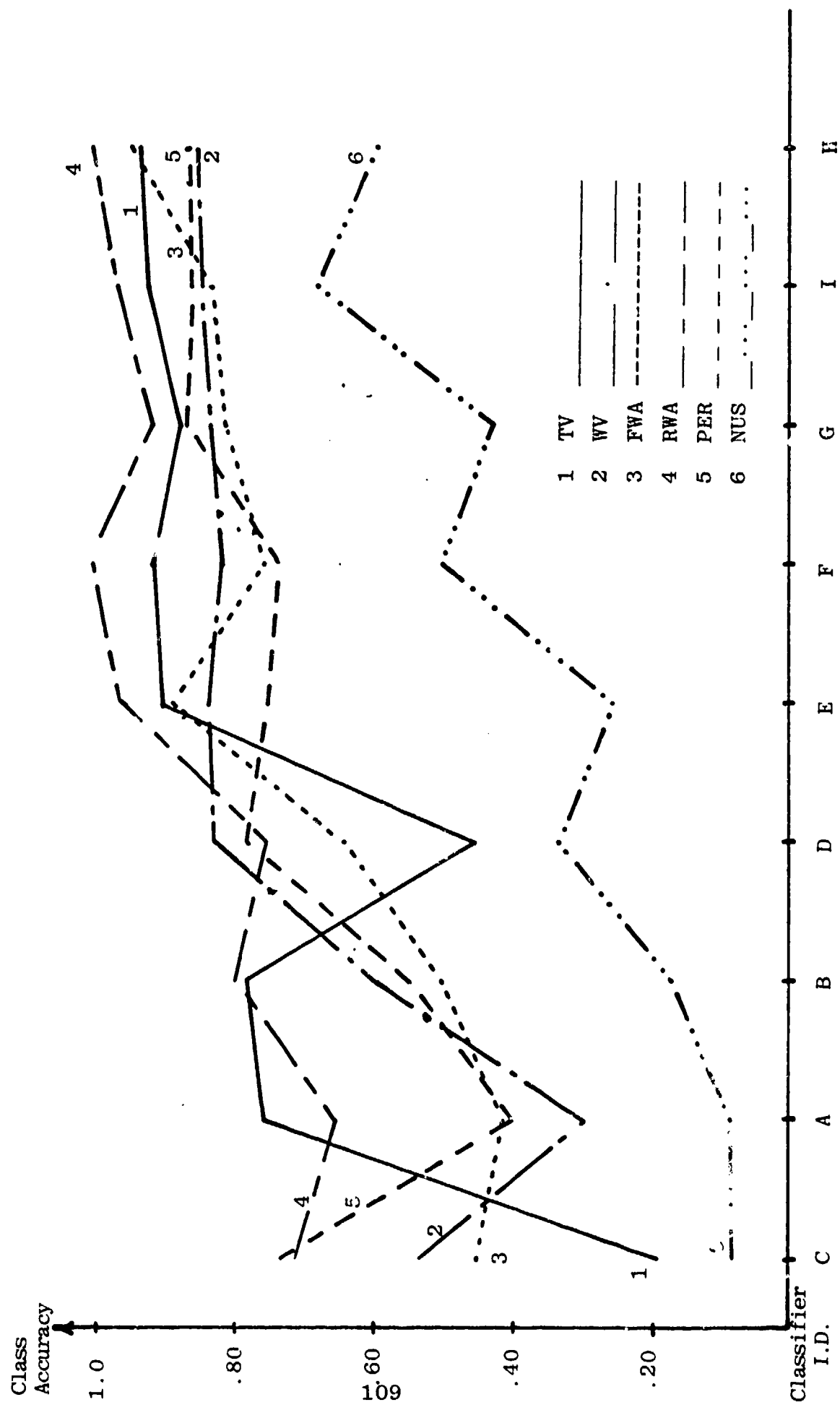


FIGURE 7.1: CLASS ACCURACY OF NINE TARGET CLASSIFIERS IN ORDER OF PERFORMANCE

As indicated in Table 7.1, the highest accuracy and highest performance attained were produced by classifier H utilizing all 29 features in "one versus one" linear discrimination functions -- reporting all classes receiving at least four votes. The accuracy of this classifier is approximately 90 percent and its performance is approximately 0.8.

8. CONCLUSIONS AND RECOMMENDATIONS

8.1. CONCLUSIONS

A detailed study has been performed of the REMBASS six-class seismic/acoustic target classification problem. It has been demonstrated that a six-way classifier can be realized that, in simulations, exhibits improved overall accuracy, improved site independence and improved class invariance, and improved range invariance. The specific conclusions reached in the course of this study are:

1. An average single epoch classification accuracy of 85 percent can be realized with a practicable design.
2. The above accuracy is achieved with high consistency at different sites and for the different target classes, and the classifier is relatively insensitive to target range (out to the periphery of the target detection zone) and the speed, altitude (where applicable), and heading of the target.
3. If the combined set of 28 features from prior Honeywell and Sylvania designs is used with an additional acoustic/seismic energy ratio feature, the different classes of targets are separable using linear discriminant functions. Nonlinear discriminant functions offer possibilities for using reduced feature sets.
4. By utilizing a pairwise voting logic structure, the classifier circuitry is potentially less prone to manufacturing tolerance errors and to parameter drift.
5. Using vote reporting in lieu of class reporting, the voting structure is also suitable for multi-target classifications. Furthermore, the likelihood of intentional or unintentional jamming of the sensor is reduced, and the user has greater opportunity to exercise judgment concerning the tactical situation.
6. Further work is needed to develop the most cost-effective classifier design. As a foundation for this work, additional field and/or synthetic data should be obtained so as to represent more fully the wide variety of targets and terrain conditions that could be encountered by an operational system.

8.2 RECOMMENDATIONS

It is recommended that the following further investigations be performed:

1. Detail the range capabilities of any newly designed classifiers, by computing different confusion matrices as a function of target range.
2. Estimate the expected accuracy and performance of each classifier on the basis of multi-epoch averaging, i.e., calculate expected performance versus number of epochs averaged. This will evaluate each classifier on a target run rather than a target partial run basis.
3. Compare the cluster structures of seismic/acoustic signatures obtained from foreign and domestic vehicles. If there is a pronounced difference, incorporate the foreign vehicle data into the data base and retrain/re-evaluate the classifiers.
4. Compare cluster structures of synthetically-generated seismic/acoustic signatures (based upon assumed terrain conditions) with known clusters in the existing field data records. If agreement is satisfactory, incorporate synthetic data for sites not represented by field records into the data base and retrain/re-evaluate the classifiers.
5. Identify optimal number and type of features; determine if fewer than 29 features can be used without sacrificing classifier performance. Investigate trade-off between numbers of features required and degrees of nonlinearity of the classifier discriminant functions. (Fewer features are needed when using nonlinear discriminant functions within a given classifier architecture.)
6. Investigate the relative merits of "one versus five" maximum selection, "one versus one" voting, and possible "one versus five" voting. The last would probably be competitive in accuracy and consistency with "one versus one" voting, and would require less circuitry, but these circuits could be more prone to instability than those for "one versus one" voting.
7. Investigate use of confidence-weighted voting wherein a subclassifier producing an output that is numerically close to the expected output for a given class votes more strongly for that class than when its output is far from the expected output.
8. Investigate multi-target classifications using the vote reporting concept.

9. REFERENCES

1. Angelo, E. J., Electronics: BJT's, FET's and Microcircuits, pp. 149-171, McGraw-Hill, 1969.
2. Barron, R. L., "Learning Networks Improve Computer-Aided Prediction and Control," August 1975, Computer Design.
3. Hunt, S. P., M. D. Layman, and D. L. Wilson, Seismic Acoustic Target Classifier, GTE Sylvania, Inc. FTR to USA MERDC, Contract DAAK02-72-C-0546, June 1974.
4. Miller, K. H., Field Deployable Breadboard Classifier, Scope Electronics, Inc., IR to USA MERDC, Contract DAAK02-73-C-0121, September 1973.
5. Miller, K. H., Power Spectrum Classifier, Scope Electronics, Inc., FTR to USA MERDC, Contract DAAK02-73-C-0121, December 1974.
6. Mucciardi, A. N. and E. E. Gose, "An Automatic Clustering Algorithm and Its Properties in High-Dimensional Spaces," IEEE Trans. Computers, Vol. SMC-2, No. 2, April 1972, pp. 247-254.
7. Mucciardi, A. N., "Elements of Learning Control Systems With Applications to Industrial Processes," Proc. 1972 IEEE Conference on Decision and Control, New Orleans, La. December 13-15, 1972, pp. 320-325.
8. Ogota, K., Modern Control Engineering, pp. 216-252, Prentice-Hall, Inc. 1970.
9. Roth, R. R., Design and Development of the Seismic Target Classifier, Honeywell, Inc. FTR to USA MERDC, Contract DAAK02-72-C-0547, July 1973.
10. Roth, R. R., Seismic Acoustic Target Classifier, Honeywell, Inc. FTR to USA MERDC, Contract DAAK02-72-C-0547.
11. Scott, R. W. and M. D. Laymon, Seismic Target Classifier, GTE Sylvania, Inc. FTR to USA MERDC, Contract DAAK02-72-C-0546, December 1973.
12. Scott, J. A., Automatic Vehicle Classification System, Ensco, Inc. FTR to USA MERDC, Rept. No. P-I-241, June 1974.
13. Shankar, R., A. N. Mucciardi and E. E. Gose, "Classification into K-Categories Via Discrimination Between Pairs of Categories," 1975 Proc. Milwaukee Symposium on Automatic Computation and Control, Milwaukee, Wisconsin, April 17-19, 1975.

14. Southworth, R. W. and S. L. Deleeuw, Digital Computation and Numerical Methods, pp. 350-377, McGraw-Hill, 1965.
15. Whalen, M. F. and A. N. Mucciardi, Synthesis of Nonlinear Adaptive Learning Network Seismic Target Classifier, Adaptronics, Inc. Interim Report to USA MERDC, Contract DAAK02-74-C-0322, March 1975.

APPENDIX A

WAVEFORM IDENTIFICATION LOG LISTING

NUM	MERDCID	CLASS	TYPE	SITE	SPEED	STAKE	A/S	GAIN	DIRECTION
1	469	6	N	GRAYLING	-0	-0	50	70	
2	469	6	N	GRAYLING	-0	-0	50	70	
3	470	6	N	GRAYLING	-0	-0	50	70	
4	471	6	N	GRAYLING	-0	-0	50	70	
5	472	6	N	GRAYLING	-0	-0	50	70	
6	473	6	N	GRAYLING	-0	-0	50	70	
7	474	6	N	GRAYLING	-0	-0	50	70	
8	495	6	N	GRAYLING	-0	-0	60	70	
9	496	6	N	GRAYLING	-0	-0	60	70	
10	497	6	N	GRAYLING	-0	-0	60	70	
11	498	6	N	GRAYLING	-0	-0	60	70	
12	553	6	N	FT. BRAGG	-0	-0	30	70	N-S
13	554	6	N	FT. BRAGG	-0	-0	30	70	N-S
14	535	6	N	YUMA	-0	-0	50	70	
15	586	6	N	YUMA	-0	-0	50	70	
16	587	6	N	YUMA	-0	-0	50	70	
17	588	6	N	YUMA	-0	-0	50	70	
18	589	6	N	YUMA	-0	-0	50	70	
19	602	5	H1	YUMA	3	13	70	70	N-S
20	603	5	H1	YUMA	3	10	70	70	N-S
21	604	5	H1	YUMA	3	7	70	70	N-S
22	605	5	H1	YUMA	3	6	70	70	S-N
23	606	5	H1	YUMA	3	11	70	70	S-N
24	608	5	H3	YUMA	3	8	60	70	S-N
25	609	5	H3	YUMA	3	12	60	70	S-N
26	610	5	H3	YUMA	3	14	60	70	N-S
27	611	5	H3	YUMA	3	11	60	70	N-S
28	612	5	H3	YUMA	3	-0	60	70	N-S
29	614	5	H3	YUMA	3	5	60	70	S-N
30	615	5	H3	YUMA	3	7	60	70	S-N
31	616	5	H3	YUMA	3	11	60	70	S-N
32	617	5	H3	YUMA	3	14	60	70	N-S
33	618	5	H3	YUMA	3	11	60	70	N-S
34	619	5	H3	YUMA	3	8	60	70	N-S
35	620	5	H1	YUMA	3	5	60	70	S-N
36	621	5	H1	YUMA	3	8	60	70	S-N
37	622	5	H1	YUMA	3	11	60	70	S-N
38	623	5	H1	YUMA	3	13	60	70	N-S
39	624	5	H1	YUMA	3	10	60	70	N-S
40	625	5	H3	YUMA	3	5	60	70	S-N
41	626	5	H3	YUMA	3	7	60	70	S-N
42	628	5	H3	YUMA	3	12	60	70	S-N
43	629	5	H3	YUMA	3	-0	60	70	N-S
44	630	5	H3	YUMA	3	13	60	70	N-S
45	631	5	H3	YUMA	3	11	60	70	N-S
46	632	5	H3	YUMA	3	7	60	70	N-S
47	633	5	H5	YUMA	3	15	60	70	S-N
48	634	5	H5	YUMA	3	12	60	70	S-N
49	635	5	H5	YUMA	3	10	60	70	S-N
50	637	5	H5	YUMA	3	14	60	70	N-S

Preceding page blank

NUM	MERDCID	CLASS	TYPE	SITE	SPEED	STAKE	A/S	GAIN	DIRECTION
51	638	5	H5	YUMA	3	12	60	70	N-S
52	639	5	H5	YUMA	3	9	60	70	N-S
53	669	4	UH-1	FT.BRAGG	80	200	40	70	
54	669	4	UH-1	FT.BRAGG	80	200	40	70	
55	670	4	UH-1	FT.BRAGG	80	200	40	70	
56	670	4	UH-1	FT.BRAGG	80	200	40	70	
57	670	4	UH-1	FT.BRAGG	80	200	40	70	
58	671	4	UH-1	FT.BRAGG	100	200	40	70	
59	671	4	UH-1	FT.BRAGG	100	200	40	70	
60	671	4	UH-1	FT.BRAGG	100	200	40	70	
61	672	4	UH-1	FT.BRAGG	100	200	40	70	
62	673	4	UH-1	FT.BRAGG	60	400	40	70	
63	673	4	UH-1	FT.BRAGG	60	400	40	70	
64	673	4	UH-1	FT.BRAGG	60	400	40	70	
65	674	4	UH-1	FT.BRAGG	60	400	40	70	
66	674	4	UH-1	FT.BRAGG	60	400	40	70	
67	675	4	UH-1	FT.BRAGG	80	400	40	70	
68	675	4	UH-1	FT.BRAGG	80	400	40	70	
69	676	4	UH-1	FT.BRAGG	80	400	40	70	
70	676	4	UH-1	FT.BRAGG	80	400	40	70	
71	677	4	UH-1	FT.BRAGG	100	400	40	70	
72	677	4	UH-1	FT.BRAGG	100	400	40	70	
73	678	4	UH-1	FT.BRAGG	100	400	40	70	
74	678	4	UH-1	FT.BRAGG	100	400	40	70	
75	679	4	UH-1	FT.BRAGG	60	600	40	70	
76	679	4	UH-1	FT.BRAGG	60	600	40	70	
77	680	4	UH-1	FT.BRAGG	60	600	40	70	
78	680	4	UH-1	FT.BRAGG	60	600	40	70	
79	680	4	UH-1	FT.BRAGG	60	600	40	70	
80	681	4	UH-1	FT.BRAGG	80	600	40	70	
81	681	4	UH-1	FT.BRAGG	80	600	40	70	
82	682	4	UH-1	FT.BRAGG	80	600	40	70	
83	682	4	UH-1	FT.BRAGG	80	600	40	70	
84	683	4	UH-1	FT.BRAGG	100	600	40	70	
85	683	4	UH-1	FT.BRAGG	100	600	40	70	
86	684	4	UH-1	FT.BRAGG	100	600	40	70	
87	684	4	UH-1	FT.BRAGG	100	600	40	70	
88	684	4	UH-1	FT.BRAGG	100	600	40	70	
89	640	3	TA-4	FT.BRAGG	250	200	40	70	
90	641	3	TA-4	FT.BRAGG	250	200	40	70	
91	642	3	TA-4	FT.BRAGG	300	200	23	70	
92	642	3	TA-4	FT.BRAGG	300	200	23	70	
93	642	3	TA-4	FT.BRAGG	300	200	23	70	
94	643	3	TA-4	FT.BRAGG	300	200	23	70	
95	644	3	TA-4	FT.BRAGG	450	200	23	70	
96	644	3	TA-4	FT.BRAGG	450	200	23	70	
97	645	3	TA-4	FT.BRAGG	450	200	23	70	
98	645	3	TA-4	FT.BRAGG	450	200	23	70	
99	646	3	TA-4	FT.BRAGG	250	400	23	70	
100	646	3	TA-4	FT.BRAGG	250	400	23	70	

NUM	MEROCID	CLASS	TYPE	SITE	SPEED	STAKE	A/S	GAIN	DIRECTION
101	647	3	TA-4	FT.BRAGG	250	400	23	70	
102	647	3	TA-4	FT.BRAGG	250	400	23	70	
103	648	3	TA-4	FT.BRAGG	300	400	23	70	
104	649	3	TA-4	FT.BRAGG	300	400	23	70	
105	649	3	TA-4	FT.BRAGG	300	400	23	70	
106	650	3	TA-4	FT.BRAGG	450	400	40	70	
107	650	3	TA-4	FT.BRAGG	450	400	40	70	
108	651	3	TA-4	FT.BRAGG	450	400	40	70	
109	651	3	TA-4	FT.BRAGG	450	400	40	70	
110	652	3	OV-10	FT.BRAGG	120	200	40	70	
111	652	3	OV-10	FT.BRAGG	120	200	40	70	
112	653	3	OV-10	FT.BRAGG	120	200	40	70	
113	653	3	OV-10	FT.BRAGG	120	200	40	70	
114	654	3	OV-10	FT.BRAGG	150	200	40	70	
115	654	3	OV-10	FT.BRAGG	150	200	40	70	
116	655	3	OV-10	FT.BRAGG	150	200	40	70	
117	655	3	OV-10	FT.BRAGG	150	200	40	70	
118	656	3	OV-10	FT.BRAGG	180	200	40	70	
119	657	3	OV-10	FT.BRAGG	180	200	40	70	
120	657	3	OV-10	FT.BRAGG	180	200	40	70	
121	658	3	OV-10	FT.BRAGG	120	400	40	70	
122	658	3	OV-10	FT.BRAGG	120	400	40	70	
123	659	3	OV-10	FT.BRAGG	120	400	40	70	
124	659	3	OV-10	FT.BRAGG	120	400	40	70	
125	660	3	OV-10	FT.BRAGG	150	400	40	70	
126	660	3	OV-10	FT.BRAGG	150	400	40	70	
127	661	3	OV-10	FT.BRAGG	150	400	40	70	
128	661	3	OV-10	FT.BRAGG	150	400	40	70	
129	662	3	OV-10	FT.BRAGG	180	400	40	70	
130	662	3	OV-10	FT.BRAGG	180	400	40	70	
131	663	3	OV-10	FT.BRAGG	180	400	40	70	
132	663	3	OV-10	FT.BRAGG	180	400	40	70	
133	664	3	OV-10	FT.BRAGG	120	600	40	70	
134	664	3	OV-10	FT.BRAGG	120	600	40	70	
135	665	3	OV-10	FT.BRAGG	120	600	40	70	
136	665	3	OV-10	FT.BRAGG	120	500	40	70	
137	666	3	OV-10	FT.BRAGG	150	600	40	70	
138	666	3	OV-10	FT.BRAGG	150	600	40	70	
139	667	3	OV-10	FT.BRAGG	150	600	40	70	
140	667	3	OV-10	FT.BRAGG	150	600	40	70	
141	668	3	OV-10	FT.BRAGG	180	600	40	70	
142	668	3	OV-10	FT.BRAGG	180	600	40	70	
143	382	2	M151	YUMA	6	9	50	70	E-W
144	383	2	M151	YUMA	6	10	50	70	E-W
145	384	2	M151	YUMA	6	11	50	70	W-E
146	385	2	M151	YUMA	6	10	50	70	W-E
147	386	2	M151	YUMA	16	-0	50	70	E-W
148	387	2	M151	YUMA	16	-0	50	70	E-W
149	388	2	M151	YUMA	16	11	50	70	W-E
150	389	2	M151	YUMA	16	10	50	70	W-E

NUM	MERCID	CLASS	TYPE	SITE	SPEED	STAKE	A/S	GAIN	DIRECTION
151	390	2	M151	YUMA	22	9	50	70	E-W
152	391	2	M151	YUMA	22	10	50	70	E-W
153	392	2	M151	YUMA	22	11	50	70	W-E
154	393	2	M151	YUMA	22	10	50	70	W-E
155	394	2	M151	YUMA	31	9	50	70	E-W
156	395	2	M151	YUMA	31	11	50	70	E-W
157	396	2	M151	YUMA	31	11	50	70	W-E
158	397	2	M151	YUMA	31	8	50	70	W-E
159	398	2	T2.5	YUMA	6	-0	46	70	W-E
160	399	2	T2.5	YUMA	6	-0	46	70	W-E
161	400	2	T2.5	YUMA	6	-0	46	70	W-E
162	401	2	T2.5	YUMA	6	12	46	70	W-E
163	402	2	T2.5	YUMA	6	11	46	70	W-E
164	403	2	T2.5	YUMA	6	10	46	70	W-E
165	404	2	T2.5	YUMA	16	-0	40	60	E-W
166	405	2	T2.5	YUMA	16	9	40	60	E-W
167	406	2	T2.5	YUMA	16	11	40	60	E-W
168	408	2	T2.5	YUMA	16	11	40	60	W-E
169	409	2	T2.5	YUMA	16	-0	40	60	W-E
170	411	2	T2.5	YUMA	22	9	40	70	E-W
171	412	2	T2.5	YUMA	22	12	40	70	E-W
172	413	2	T2.5	YUMA	22	-0	40	70	W-E
173	414	2	T2.5	YUMA	22	-0	40	70	W-E
174	415	2	T2.5	YUMA	22	-0	40	70	W-E
175	416	2	T2.5	YUMA	31	4	40	70	E-W
176	417	2	T2.5	YUMA	31	-0	40	70	E-W
177	418	2	T2.5	YUMA	31	15	40	70	W-E
178	419	2	T2.5	YUMA	31	12	40	70	W-E
179	420	2	T2.5	YUMA	31	8	40	70	W-E
180	422	2	M715	YUMA	6	10	50	70	E-W
181	423	2	M715	YUMA	6	-0	50	70	E-W
182	424	2	M715	YUMA	6	12	50	70	W-E
183	425	2	M715	YUMA	6	11	50	70	W-E
184	426	2	M715	YUMA	6	10	50	70	W-E
185	427	2	M715	YUMA	16	6	46	70	E-W
186	428	2	M715	YUMA	16	8	46	70	E-W
187	429	2	M715	YUMA	16	10	46	70	E-W
188	430	2	M715	YUMA	16	13	46	70	W-E
189	431	2	M715	YUMA	16	11	46	70	W-E
190	432	2	M715	YUMA	16	9	46	70	W-E
191	433	2	M715	YUMA	22	7	46	70	E-W
192	434	2	M715	YUMA	22	9	46	70	E-W
193	435	2	M715	YUMA	22	11	46	70	E-W
194	436	2	M715	YUMA	22	13	46	70	W-E
195	437	2	M715	YUMA	22	11	46	70	W-E
196	439	2	M715	YUMA	22	9	46	70	W-E
197	440	2	M792	YUMA	6	8	46	70	E-W
198	441	2	M792	YUMA	6	9	46	70	E-W
199	442	2	M792	YUMA	6	10	46	70	E-W
200	443	2	M792	YUMA	6	11	46	70	W-E

NUM	MERDCID	CLASS	TYPE	SITE	SPEED	STAKE	A/S	GAIN	DIRECTION
201	444	2	M792	YUMA	6	10	46	70	W-E
202	445	2	M792	YUMA	6	9	46	70	W-E
203	446	2	M792	YUMA	16	7	46	70	E-W
204	447	2	M792	YUMA	16	8	46	70	E-W
205	448	2	M792	YUMA	16	9	46	70	E-W
206	449	2	M792	YUMA	16	10	46	70	E-W
207	450	2	M792	YUMA	16	13	46	70	W-E
208	451	2	M792	YUMA	16	11	46	70	W-E
209	452	2	M792	YUMA	16	6	46	70	E-W
210	453	2	M792	YUMA	16	8	46	70	E-W
211	454	2	M792	YUMA	16	9	46	70	E-W
212	455	2	M792	YUMA	16	10	46	70	E-W
213	456	2	M792	YUMA	22	6	40	70	E-W
214	457	2	M792	YUMA	22	8	40	70	E-W
215	459	2	M792	YUMA	22	11	40	70	E-W
216	460	2	M792	YUMA	22	13	40	70	W-E
217	461	2	M792	YUMA	22	11	40	70	W-E
218	462	2	M792	YUMA	22	9	40	70	W-E
219	463	2	M792	YUMA	31	5	40	70	E-W
220	464	2	M792	YUMA	31	8	40	70	E-W
221	465	2	M792	YUMA	31	11	40	70	E-W
222	466	2	M792	YUMA	31	14	40	70	W-E
223	467	2	M792	YUMA	31	12	40	70	W-E
224	468	2	M792	YUMA	31	9	40	70	W-E
225	475	2	M151	GRAYLING	6	-0	50	70	S-N
226	476	2	M151	GRAYLING	6	-0	50	70	S-N
227	477	2	M151	GRAYLING	6	-0	50	70	S-N
228	478	2	M151	GRAYLING	6	-0	50	70	N-S
229	479	2	M151	GRAYLING	6	-0	50	70	N-S
230	480	2	M151	GRAYLING	16	-0	50	70	S-N
231	481	2	M151	GRAYLING	16	-0	50	70	N-S
232	482	2	M151	GRAYLING	16	-0	50	70	N-S
233	483	2	M151	GRAYLING	16	-0	50	70	N-S
234	484	2	M151	GRAYLING	22	-0	60	70	S-N
235	485	2	M151	GRAYLING	22	-0	60	70	S-N
236	486	2	M151	GRAYLING	22	-0	60	70	S-N
237	487	2	M151	GRAYLING	22	-0	60	70	N-S
238	488	2	M151	GRAYLING	22	-0	60	70	N-S
239	489	2	M151	GRAYLING	31	0	60	70	S-N
240	490	2	M151	GRAYLING	31	2	60	70	S-N
241	491	2	M151	GRAYLING	31	5	60	70	N-S
242	492	2	M151	GRAYLING	31	8	60	70	N-S
243	493	2	M151	GRAYLING	31	5	60	70	N-S
244	494	2	M151	GRAYLING	31	2	60	70	N-S
245	499	2	T2.5	GRAYLING	6	1	40	70	S-N
246	500	2	T2.5	GRAYLING	6	2	40	70	S-N
247	501	2	T2.5	GRAYLING	6	3	40	70	S-N
248	502	2	T2.5	GRAYLING	6	5	40	70	N-S
249	503	2	T2.5	GRAYLING	6	4	40	70	N-S
250	504	2	T2.5	GRAYLING	6	3	40	70	N-S

NUM	MERCID	CLASS	TYPE	SITE	SPEED	STAKE	A/S	GAIN	DIRECTION
251	505	2	T2.5	GRAYLING	16	1	40	70	S-N
252	506	2	T2.5	GRAYLING	16	2	40	70	S-N
253	507	2	T2.5	GRAYLING	16	4	40	70	S-N
254	508	2	T2.5	GRAYLING	16	7	40	70	N-S
255	509	2	T2.5	GRAYLING	16	6	40	70	N-S
256	510	2	T2.5	GRAYLING	16	4	40	70	N-S
257	511	2	T2.5	GRAYLING	16	2	40	70	N-S
258	512	2	T2.5	GRAYLING	22	1	40	70	S-N
259	513	2	T2.5	GRAYLING	22	3	40	70	S-N
260	514	2	T2.5	GRAYLING	22	5	40	70	S-N
261	515	2	T2.5	GRAYLING	22	7	40	70	N-S
262	516	2	T2.5	GRAYLING	22	4	40	70	N-S
263	517	2	T2.5	GRAYLING	22	2	40	70	N-S
264	518	2	T2.5	GRAYLING	31	0	40	70	S-N
265	519	2	T2.5	GRAYLING	31	1	40	70	S-N
266	520	2	T2.5	GRAYLING	31	4	40	70	S-N
267	521	2	T2.5	GRAYLING	31	8	40	70	N-S
268	522	2	T2.5	GRAYLING	31	5	40	70	N-S
269	523	2	T2.5	GRAYLING	31	2	40	70	N-S
270	526	2	T5.0	GRAYLING	6	1	30	70	S-N
271	527	2	T5.0	GRAYLING	6	2	30	70	S-N
272	528	2	T5.0	GRAYLING	6	3	30	70	S-N
273	529	2	T5.0	GRAYLING	6	6	30	70	N-S
274	530	2	T5.0	GRAYLING	6	4	30	70	N-S
275	531	2	T5.0	GRAYLING	6	3	30	70	N-S
276	532	2	T5.0	GRAYLING	16	1	30	70	S-N
277	534	2	T5.0	GRAYLING	16	4	30	70	S-N
278	535	2	T5.0	GRAYLING	16	8	30	70	N-S
279	536	2	T5.0	GRAYLING	16	6	30	70	N-S
280	537	2	T5.0	GRAYLING	16	5	30	70	N-S
281	538	2	T5.0	GRAYLING	16	3	30	70	N-S
282	539	2	T5.0	GRAYLING	22	1	30	70	S-N
283	540	2	T5.0	GRAYLING	22	3	30	70	S-N
284	541	2	T5.0	GRAYLING	22	5	30	70	S-N
285	542	2	T5.0	GRAYLING	22	8	30	70	N-S
286	543	2	T5.0	GRAYLING	22	5	30	70	N-S
287	544	2	T5.0	GRAYLING	22	3	30	70	N-S
288	545	2	T5.0	GRAYLING	31	0	30	70	S-N
289	546	2	T5.0	GRAYLING	31	2	30	70	S-N
290	547	2	T5.0	GRAYLING	31	5	30	70	S-N
291	548	2	T5.0	GRAYLING	31	8	30	70	S-N
292	549	2	T5.0	GRAYLING	31	-0	30	70	N-S
293	550	2	T5.0	GRAYLING	31	6	30	70	N-S
294	551	2	T5.0	GRAYLING	31	-0	30	70	N-S
295	555	2	M151	FT.BRAGG	6	11	50	70	S-N
296	556	2	M151	FT.BRAGG	6	10	50	70	S-N
297	557	2	M151	FT.BRAGG	6	9	50	70	S-N
298	558	2	M151	FT.BRAGG	16	-0	50	70	S-N
299	559	2	M151	FT.BRAGG	16	10	50	70	S-N
300	560	2	M151	FT.BRAGG	16	11	50	70	N-S

NUM	MERDCID	CLASS	TYPE	SITE	SPEED	STAKE	A/S	GAIN	DIRECTION
301	561	2	M151	FT.BRAGG	16	9	50	70	N-S
302	562	2	M151	FT.BRAGG	22	8	50	70	S-N
303	563	2	M151	FT.BRAGG	22	10	50	70	S-N
304	564	2	M151	FT.BRAGG	22	12	50	70	S-N
305	565	2	M151	FT.BRAGG	22	13	50	70	N-S
306	566	2	M151	FT.BRAGG	22	11	50	70	N-S
307	567	2	M151	FT.BRAGG	22	9	50	70	N-S
308	568	2	M151	FT.BRAGG	31	8	50	70	S-N
309	569	2	M151	FT.BRAGG	31	12	50	70	S-N
310	570	2	M151	FT.BRAGG	31	13	50	70	N-S
311	571	2	M151	FT.BRAGG	31	11	50	70	N-S
312	572	2	M151	FT.BRAGG	31	8	50	70	N-S
313	573	2	T2.5	FT.BRAGG	6	8	50	70	S-N
314	574	2	T2.5	FT.BRAGG	6	10	50	70	S-N
315	575	2	T2.5	FT.BRAGG	6	-0	50	70	S-N
316	576	2	T2.5	FT.BRAGG	6	12	50	70	N-S
317	577	2	T2.5	FT.BRAGG	6	11	50	70	N-S
318	578	2	T2.5	FT.BRAGG	6	9	50	70	N-S
319	579	2	T2.5	FT.BRAGG	16	8	50	70	S-N
320	580	2	T2.5	FT.BRAGG	16	9	50	70	S-N
321	581	2	T2.5	FT.BRAGG	16	11	50	70	S-N
322	583	2	T2.5	FT.BRAGG	16	11	50	70	N-S
323	584	2	T2.5	FT.BRAGG	16	9	50	70	N-S
324	591	2	T2.5	FT.BRAGG	22	8	50	70	S-N
325	592	2	T2.5	FT.BRAGG	22	10	50	70	S-N
326	593	2	T2.5	FT.BRAGG	22	11	50	70	S-N
327	594	2	T2.5	FT.BRAGG	22	13	50	70	N-S
328	595	2	T2.5	FT.BRAGG	22	11	50	70	N-S
329	596	2	T2.5	FT.BRAGG	22	9	50	70	N-S
330	597	2	T2.5	FT.BRAGG	31	9	50	70	S-N
331	598	2	T2.5	FT.BRAGG	31	12	50	70	S-N
332	600	2	T2.5	FT.BRAGG	31	11	50	70	N-S
333	601	2	T2.5	FT.BRAGG	31	9	50	70	N-S
334	3	1	M107	YUMA	16	1	30	70	E-W
335	4	1	M107	YUMA	16	5	30	70	E-W
336	5	1	M107	YUMA	16	8	30	70	E-W
337	6	1	M107	YUMA	16	12	30	70	E-W
338	7	1	M107	YUMA	16	19	30	70	E-W
339	8	1	M107	YUMA	16	15	30	70	W-E
340	9	1	M107	YUMA	16	13	30	70	W-E
341	10	1	M107	YUMA	16	11	30	70	W-E
342	11	1	M107	YUMA	16	7	30	70	W-E
343	13	1	M107	YUMA	16	5	30	70	E-W
344	14	1	M107	YUMA	16	8	30	70	E-W
345	15	1	M107	YUMA	16	10	30	70	E-W
346	16	1	M107	YUMA	16	12	30	70	E-W
347	17	1	M107	YUMA	16	14	30	70	E-W
348	19	1	M107	YUMA	16	13	30	70	W-E
349	20	1	M107	YUMA	16	11	30	70	W-E
350	21	1	M107	YUMA	16	9	30	70	W-E

NUM	MERDCIO	CLASS	TYPE	SITE	SPEED	STAKE	A/S	GAIN	DIRECTION
351	22	1	M107	YUMA	16	7	30	70	W-E
352	23	1	M107	YUMA	22	6	30	70	E-W
353	24	1	M107	YUMA	22	8	30	70	E-W
354	25	1	M107	YUMA	22	10	30	70	E-W
355	26	1	M107	YUMA	22	11	30	70	E-W
356	27	1	M107	YUMA	22	11	30	70	E-W
357	28	1	M107	YUMA	22	15	30	70	W-E
358	29	1	M107	YUMA	22	10	30	70	W-E
359	30	1	M107	YUMA	22	8	30	70	W-E
360	31	1	M107	YUMA	22	6	30	70	W-E
361	32	1	M107	YUMA	22	10	30	70	E-W
362	33	1	M107	YUMA	22	11	30	70	E-W
363	34	1	M107	YUMA	22	13	30	70	E-W
364	35	1	M107	YUMA	22	15	30	70	W-E
365	36	1	M107	YUMA	22	13	30	70	W-E
366	37	1	M107	YUMA	22	11	30	70	W-E
367	38	1	M107	YUMA	22	8	30	70	W-E
368	39	1	M107	YUMA	28	7	30	70	E-W
369	40	1	M107	YUMA	28	9	30	70	E-W
370	41	1	M107	YUMA	28	12	30	70	E-W
371	42	1	M107	YUMA	28	14	30	70	W-E
372	43	1	M107	YUMA	28	12	30	70	W-E
373	44	1	M107	YUMA	28	8	30	70	W-E
374	45	1	M107	YUMA	28	6	30	70	E-W
375	46	1	M107	YUMA	28	9	30	70	E-W
376	47	1	M107	YUMA	28	13	30	70	E-W
377	48	1	M107	YUMA	28	15	30	70	W-E
378	49	1	M107	YUMA	28	13	30	70	W-E
379	50	1	M107	YUMA	28	11	30	70	W-E
380	51	1	M107	YUMA	28	8	30	70	W-E
381	52	1	M60	YUMA	6	15	20	70	W-E
382	53	1	M60	YUMA	6	14	20	70	W-E
383	54	1	M60	YUMA	6	12	20	70	W-E
384	55	1	M60	YUMA	6	11	20	70	W-E
385	57	1	M60	YUMA	6	9	20	70	W-E
386	58	1	M60	YUMA	6	8	20	70	W-E
387	59	1	M60	YUMA	6	7	20	70	W-E
388	60	1	M60	YUMA	6	5	20	70	E-W
389	61	1	M60	YUMA	6	7	20	70	E-W
390	62	1	M60	YUMA	6	9	20	70	E-W
391	63	1	M60	YUMA	6	10	20	70	E-W
392	64	1	M60	YUMA	6	11	20	70	E-W
393	65	1	M60	YUMA	6	12	20	70	E-W
394	66	1	M60	YUMA	6	15	20	70	W-E
395	67	1	M60	YUMA	6	14	20	70	W-E
396	68	1	M60	YUMA	6	12	20	70	W-E
397	69	1	M60	YUMA	6	11	20	70	W-E
398	70	1	M60	YUMA	6	9	20	70	W-E
399	71	1	M60	YUMA	6	8	20	70	W-E
400	72	1	M60	YUMA	16	6	16	70	E-W

NUM	MERDCID	CLASS	TYPE	SITE	SPEED	STAKE	A/S GAIN	DIRECTION
401	73	1	M60	YUMA	16	7	16 70	E-W
402	74	1	M60	YUMA	16	9	16 70	E-W
403	75	1	M60	YUMA	16	11	16 70	E-W
404	76	1	M60	YUMA	16	14	16 70	E-W
405	77	1	M60	YUMA	16	14	16 70	N-E
406	78	1	M60	YUMA	16	11	16 70	N-E
407	79	1	M60	YUMA	16	9	16 70	N-E
408	80	1	M60	YUMA	16	6	16 70	N-E
409	81	1	M60	YUMA	16	3	16 70	N-E
410	82	1	M60	YUMA	16	4	16 70	E-W
411	83	1	M60	YUMA	16	7	16 70	E-W
412	84	1	M60	YUMA	16	8	16 70	E-W
413	85	1	M60	YUMA	16	11	16 70	E-W
414	86	1	M60	YUMA	16	14	16 70	E-W
415	87	1	M60	YUMA	16	15	16 70	N-E
416	88	1	M60	YUMA	16	12	16 70	N-E
417	89	1	M60	YUMA	16	9	16 70	N-E
418	90	1	M60	YUMA	16	6	16 70	N-E
419	91	1	M60	YUMA	22	5	16 70	E-W
420	92	1	M60	YUMA	22	7	16 70	E-W
421	93	1	M60	YUMA	22	9	16 70	E-W
422	94	1	M60	YUMA	22	12	16 70	E-W
423	95	1	M60	YUMA	22	15	16 70	E-W
424	96	1	M60	YUMA	22	18	16 70	N-E
425	97	1	M60	YUMA	22	14	16 70	N-E
426	98	1	M60	YUMA	22	11	16 70	N-E
427	99	1	M60	YUMA	22	8	16 70	N-E
428	100	1	M60	YUMA	31	4	16 70	E-W
429	101	1	M60	YUMA	31	8	16 70	E-W
430	102	1	M60	YUMA	31	13	16 70	E-W
431	103	1	M60	YUMA	31	16	16 70	E-W
432	104	1	M60	YUMA	31	17	16 70	N-E
433	105	1	M60	YUMA	31	12	16 70	N-E
434	106	1	M60	YUMA	31	11	16 70	N-E
435	107	1	M60	YUMA	31	8	16 70	N-E
436	108	1	M60	YUMA	31	4	16 70	N-E
437	109	1	M60	YUMA	31	4	16 70	E-W
438	110	1	M60	YUMA	31	8	16 70	E-W
439	111	1	M60	YUMA	31	9	16 70	E-W
440	112	1	M60	YUMA	31	13	16 70	E-W
441	113	1	M60	YUMA	31	16	16 70	E-W
442	114	1	M60	YUMA	31	16	16 70	N-E
443	115	1	M60	YUMA	31	12	16 70	N-E
444	116	1	M60	YUMA	31	10	16 70	N-E
445	117	1	M60	YUMA	31	7	16 70	N-E
446	118	1	M113	YUMA	6	4	30 70	E-W
447	119	1	M113	YUMA	6	-0	30 70	E-W
448	120	1	M113	YUMA	6	-0	30 70	E-W
449	121	1	M113	YUMA	6	8	30 70	E-W
450	124	1	M113	YUMA	6	-0	30 70	E-W

NUM	MERDCID	CLASS	TYPE	SITE	SPEED	STAKE	A/S	GAIN	DIRECTION
451	126	1	M113	YUMA	6	13	30	70	W-E
452	127	1	M113	YUMA	6	11	30	70	W-E
453	128	1	M113	YUMA	6	10	30	70	W-E
454	129	1	M113	YUMA	6	9	30	70	W-E
455	130	1	M113	YUMA	6	7	30	70	E-W
456	131	1	M113	YUMA	6	8	30	70	E-W
457	132	1	M113	YUMA	6	9	30	70	E-W
458	133	1	M113	YUMA	6	11	30	70	E-W
459	134	1	M113	YUMA	6	12	30	70	E-W
460	136	1	M113	YUMA	6	12	30	70	W-E
461	137	1	M113	YUMA	6	11	30	70	W-E
462	138	1	M113	YUMA	6	10	30	70	W-E
463	139	1	M113	YUMA	6	9	30	70	W-E
464	140	1	M113	YUMA	6	-0	30	70	W-E
465	142	1	M113	YUMA	16	8	26	70	E-W
466	143	1	M113	YUMA	16	9	26	70	E-W
467	144	1	M113	YUMA	16	11	26	70	E-W
468	145	1	M113	YUMA	16	13	26	70	W-E
469	146	1	M113	YUMA	16	11	26	70	W-E
470	147	1	M113	YUMA	16	9	26	70	W-E
471	148	1	M113	YUMA	16	8	26	70	W-E
472	149	1	M113	YUMA	16	7	26	70	E-W
473	150	1	M113	YUMA	16	8	26	70	E-W
474	151	1	M113	YUMA	16	10	26	70	E-W
475	152	1	M113	YUMA	16	12	26	70	E-W
476	153	1	M113	YUMA	16	13	26	70	E-W
477	154	1	M113	YUMA	16	14	26	70	W-E
478	155	1	M113	YUMA	16	12	26	70	W-E
479	156	1	M113	YUMA	16	11	26	70	W-E
480	157	1	M113	YUMA	16	9	26	70	W-E
481	158	1	M113	YUMA	16	7	26	70	W-E
482	159	1	M113	YUMA	22	6	26	70	E-W
483	160	1	M113	YUMA	22	8	26	70	E-W
484	162	1	M113	YUMA	22	12	26	70	E-W
485	164	1	M113	YUMA	22	15	26	70	W-E
486	165	1	M113	YUMA	22	13	26	70	W-E
487	166	1	M113	YUMA	22	11	26	70	W-E
488	167	1	M113	YUMA	22	9	26	70	W-E
489	168	1	M113	YUMA	22	6	26	70	W-E
490	169	1	M113	YUMA	22	4	26	70	E-W
491	170	1	M113	YUMA	22	7	26	70	E-W
492	171	1	M113	YUMA	22	9	26	70	E-W
493	172	1	M113	YUMA	22	11	26	70	E-W
494	173	1	M113	YUMA	22	14	26	70	E-W
495	174	1	M113	YUMA	22	15	26	70	W-E
496	175	1	M113	YUMA	22	13	26	70	W-E
497	176	1	M113	YUMA	22	11	26	70	W-E
498	177	1	M113	YUMA	22	8	26	70	W-E
499	178	1	M113	YUMA	22	5	26	70	W-E
500	179	1	M113	YUMA	31	5	20	70	E-W

NUM	MEROCID	CLASS	TYPE	SITE	SPEED	STAKE	A/S	GAIN	DIRECTION
501	180	1	M113	YUMA	31	8	20	70	E-W
502	181	1	M113	YUMA	31	12	20	70	E-W
503	182	1	M113	YUMA	31	16	20	70	W-E
504	183	1	M113	YUMA	31	12	20	70	W-E
505	184	1	M113	YUMA	31	11	20	70	W-E
506	185	1	M113	YUMA	31	9	20	70	W-E
507	186	1	M113	YUMA	31	6	20	70	E-W
508	187	1	M113	YUMA	31	9	20	70	E-W
509	188	1	M113	YUMA	31	12	20	70	E-W
510	189	1	M113	YUMA	31	15	20	70	E-W
511	190	1	M113	YUMA	31	18	20	70	W-E
512	191	1	M113	YUMA	31	15	20	70	W-E
513	192	1	M113	YUMA	31	12	20	70	W-E
514	193	1	M113	YUMA	31	8	20	70	W-E
515	194	1	M113	YUMA	31	5	20	70	W-E
516	195	1	M48	YUMA	6	5	26	70	E-W
517	196	1	M48	YUMA	6	6	26	70	E-W
518	197	1	M48	YUMA	6	8	26	70	E-W
519	198	1	M48	YUMA	6	9	26	70	E-W
520	199	1	M48	YUMA	6	11	26	70	E-W
521	200	1	M48	YUMA	6	13	26	70	E-W
522	201	1	M48	YUMA	6	14	26	70	W-E
523	202	1	M48	YUMA	6	13	26	70	W-E
524	203	1	M48	YUMA	6	11	26	70	W-E
525	204	1	M48	YUMA	6	9	26	70	W-E
526	205	1	M48	YUMA	6	8	26	70	W-E
527	206	1	M48	YUMA	6	8	26	70	E-W
528	207	1	M48	YUMA	6	9	26	70	E-W
529	208	1	M48	YUMA	6	10	26	70	E-W
530	209	1	M48	YUMA	6	11	26	70	E-W
531	210	1	M48	YUMA	6	12	26	70	E-W
532	211	1	M48	YUMA	6	13	26	70	W-E
533	212	1	M48	YUMA	6	12	26	70	W-E
534	213	1	M48	YUMA	6	11	26	70	W-E
535	214	1	M48	YUMA	6	10	26	70	W-E
536	215	1	M48	YUMA	6	8	26	70	W-E
537	216	1	M48	YUMA	16	8	20	70	E-W
538	217	1	M48	YUMA	16	9	20	70	E-W
539	218	1	M48	YUMA	16	11	20	70	E-W
540	219	1	M48	YUMA	16	13	20	70	E-W
541	220	1	M48	YUMA	16	15	20	70	W-E
542	221	1	M48	YUMA	16	13	20	70	W-E
543	222	1	M48	YUMA	16	11	20	70	W-E
544	223	1	M48	YUMA	16	8	20	70	W-E
545	224	1	M48	YUMA	16	6	20	70	W-E
546	225	1	M48	YUMA	16	6	20	70	E-W
547	226	1	M48	YUMA	16	8	20	70	E-W
548	227	1	M48	YUMA	16	9	20	70	E-W
549	228	1	M48	YUMA	16	11	20	70	E-W
550	229	1	M48	YUMA	16	13	20	70	E-W

NUM	MERDCID	CLASS	TYPE	SITE	SPEED	STAKE	A/S	GAIN	DIRECTION
551	230	1	M48	YUMA	16	15	20	70	H-E
552	231	1	M48	YUMA	16	14	20	70	H-E
553	232	1	M48	YUMA	16	11	20	70	H-E
554	233	1	M48	YUMA	16	9	20	70	H-E
555	234	1	M48	YUMA	16	6	20	70	H-E
556	235	1	M48	YUMA	22	5	20	70	E-W
557	236	1	M48	YUMA	22	7	20	70	E-W
558	237	1	M48	YUMA	22	9	20	70	E-W
559	238	1	M48	YUMA	22	11	20	70	E-W
560	239	1	M48	YUMA	22	13	20	70	E-W
561	240	1	M48	YUMA	22	15	20	70	H-E
562	241	1	M48	YUMA	22	13	20	70	H-E
563	242	1	M48	YUMA	22	11	20	70	H-E
564	243	1	M48	YUMA	22	8	20	70	H-E
565	245	1	M48	YUMA	22	8	20	70	E-W
566	246	1	M48	YUMA	22	9	20	70	E-W
567	247	1	M48	YUMA	22	6	20	70	E-W
568	248	1	M48	YUMA	22	8	20	70	E-W
569	249	1	M48	YUMA	22	9	20	70	E-W
570	250	1	M48	YUMA	22	12	20	70	E-W
571	251	1	M48	YUMA	22	14	20	70	E-W
572	252	1	M48	YUMA	31	6	16	70	E-W
573	253	1	M48	YUMA	31	12	16	70	E-W
574	254	1	M48	YUMA	31	17	16	70	H-E
575	255	1	M48	YUMA	31	12	16	70	H-E
576	257	1	M48	YUMA	31	8	16	70	H-E
577	271	1	M48	GRAYLING	6	-0	20	40	S-N
578	272	1	M48	GRAYLING	6	1	20	40	S-N
579	273	1	M48	GRAYLING	6	2	20	40	S-N
580	274	1	M48	GRAYLING	6	3	20	40	S-N
581	275	1	M48	GRAYLING	6	9	20	40	S-N
582	276	1	M48	GRAYLING	6	-0	20	40	N-S
583	277	1	M48	GRAYLING	6	6	20	40	N-S
584	278	1	M48	GRAYLING	6	5	20	40	N-S
585	279	1	M48	GRAYLING	6	1	20	40	N-S
586	280	1	M48	GRAYLING	6	1	20	40	N-S
587	281	1	M48	GRAYLING	16	2	20	40	S-N
588	282	1	M48	GRAYLING	16	5	20	40	S-N
589	283	1	M48	GRAYLING	16	7	20	40	S-N
590	284	1	M48	GRAYLING	16	8	20	40	N-S
591	285	1	M48	GRAYLING	16	7	20	40	N-S
592	286	1	M48	GRAYLING	16	5	20	40	N-S
593	287	1	M48	GRAYLING	16	2	20	40	N-S
594	288	1	M48	GRAYLING	20	1	20	40	S-N
595	289	1	M48	GRAYLING	20	3	20	40	S-N
596	290	1	M48	GRAYLING	20	5	20	40	S-N
597	291	1	M48	GRAYLING	20	8	20	40	S-N
598	292	1	M48	GRAYLING	20	8	20	40	N-S
599	293	1	M48	GRAYLING	20	6	20	40	N-S
600	294	1	M48	GRAYLING	20	4	20	40	N-S

NUM	HERDCIO	CLASS	TYPE	SITE	SPEED	STAKE	A/S	GAIN	DIRECTION
601	295	1	M48	GRAYLING	20	1	20	40	N-S
602	296	1	M113	GRAYLING	6	0	36	70	S-N
603	297	1	M113	GRAYLING	6	1	36	70	S-N
604	300	1	M113	GRAYLING	6	5	36	70	S-N
605	302	1	M113	GRAYLING	6	7	36	70	N-S
606	303	1	M113	GRAYLING	6	6	36	70	N-S
607	304	1	M113	GRAYLING	6	5	36	70	N-S
608	305	1	M113	GRAYLING	6	4	36	70	N-S
609	307	1	M113	GRAYLING	6	-0	36	70	N-S
610	309	1	M113	GRAYLING	16	7	36	70	N-S
611	310	1	M113	GRAYLING	16	5	36	70	N-S
612	311	1	M113	GRAYLING	16	2	36	70	N-S
613	312	1	M113	GRAYLING	16	J	36	70	S-N
614	313	1	M113	GRAYLING	16	2	36	70	S-N
615	314	1	M113	GRAYLING	16	4	36	70	S-N
616	315	1	M113	GRAYLING	16	8	36	70	N-S
617	316	1	M113	GRAYLING	16	6	36	70	N-S
618	317	1	M113	GRAYLING	16	4	36	70	N-S
619	318	1	M113	GRAYLING	16	2	36	70	N-S
620	319	1	M113	GRAYLING	22	8	36	70	N-S
621	320	1	M113	GRAYLING	22	5	36	70	N-S
622	321	1	M113	GRAYLING	22	1	36	70	N-S
623	322	1	M113	GRAYLING	22	J	36	70	S-N
624	324	1	M113	GRAYLING	22	6	36	70	S-N
625	325	1	M113	GRAYLING	28	J	36	70	S-N
626	326	1	M113	GRAYLING	28	2	36	70	S-N
627	327	1	M113	GRAYLING	28	5	36	70	S-N
628	328	1	M113	GRAYLING	28	9	36	70	S-N
629	329	1	M113	GRAYLING	28	8	36	70	N-S
630	330	1	M113	GRAYLING	28	6	36	70	N-S
631	331	1	M113	GRAYLING	28	2	36	70	N-S
632	332	1	M113	FT.BRAGG	6	12	40	70	N-S
633	334	1	M113	FT.BRAGG	6	10	40	70	N-S
634	335	1	M113	FT.BRAGG	6	8	40	70	N-S
635	337	1	M113	FT.BRAGG	16	11	40	70	S-N
636	338	1	M113	FT.BRAGG	16	13	40	70	S-N
637	339	1	M113	FT.BRAGG	16	14	40	70	N-S
638	340	1	M113	FT.BRAGG	16	12	40	70	N-S
639	341	1	M113	FT.BRAGG	16	8	40	70	N-S
640	342	1	M113	FT.BRAGG	16	6	40	70	N-S
641	343	1	M113	FT.BRAGG	22	6	40	70	S-N
642	344	1	M113	FT.BRAGG	22	8	40	70	S-N
643	345	1	M113	FT.BRAGG	22	10	40	70	S-N
644	346	1	M113	FT.BRAGG	22	11	40	70	S-N
645	347	1	M113	FT.BRAGG	22	-0	40	70	S-N
646	348	1	M113	FT.BRAGG	22	14	40	70	N-S
647	349	1	M113	FT.BRAGG	22	12	40	70	N-S
648	351	1	M113	FT.BRAGG	22	8	40	70	N-S
649	352	1	M113	FT.BRAGG	25	5	40	70	S-N
650	353	1	M113	FT.BRAGG	25	8	40	70	S-N

NUM	MERCID	CLASS	TYPE	SITE	SPEED	STAKE	A/S	GAIN	DIRECTION
651	354	1	M113	FT.BRAGG	25	11	40	70	S-N
652	355	1	M113	FT.BRAGG	25	14	40	70	S-N
653	356	1	M113	FT.BRAGG	25	14	40	70	N-S
654	357	1	M113	FT.BRAGG	25	13	40	70	N-S
655	358	1	M113	FT.BRAGG	25	11	40	70	N-S
656	359	1	M113	FT.BRAGG	25	9	40	70	N-S
657	360	1	M113	FT.BRAGG	25	7	40	70	N-S
658	364	1	M48	FT.BRAGG	6	14	30	70	N-S
659	366	1	M48	FT.BRAGG	6	11	30	70	N-S
660	368	1	M48	FT.BRAGG	16	-0	30	70	S-N
661	369	1	M48	FT.BRAGG	16	15	30	70	N-S
662	370	1	M48	FT.BRAGG	16	12	30	70	N-S
663	371	1	M48	FT.BRAGG	16	11	30	70	N-S
664	372	1	M48	FT.BRAGG	16	9	30	70	N-S
665	373	1	M48	FT.BRAGG	16	7	30	70	N-S
666	374	1	M48	FT.BRAGG	20	12	30	70	N-S
667	375	1	M48	FT.BRAGG	20	9	30	70	N-S
668	376	1	M48	FT.BRAGG	20	7	30	70	N-S
669	377	1	M48	FT.BRAGG	20	5	30	70	S-N
670	378	1	M48	FT.BRAGG	20	7	30	70	S-N
671	380	1	M48	FT.BRAGG	20	12	30	70	S-N

APPENDIX B

DIAGRAMS OF TEST SITES

(Provided by USAMERDC)

TEST SITE LAYOUT HQ1

PLACE
STAKES
(100M)

20

15

14

13

12

11

10

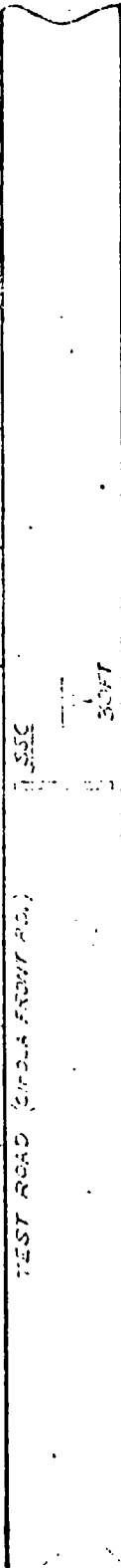
9

8

7

6

TEST ROAD (CIRCLA FRONT RD.)



100FT

35FT

255FT

500FT

GEOPHONE

MICROPHONE #2

10FT

7

11

12

13

14

15

16

17

18

19

20

21

22

23

24

25

26

27

28

29

30

31

32

33

34

35

36

37

38

39

40

41

42

43

44

45

46

47

48

49

50

51

52

53

54

55

56

57

58

59

60

61

62

63

64

65

66

67

68

69

70

71

72

73

74

75

76

77

78

79

80

81

82

83

84

85

86

87

88

89

90

91

92

93

94

95

96

97

98

99

100

101

102

103

104

105

106

107

108

109

110

111

112

113

114

115

116

117

118

119

120

121

122

123

124

125

126

127

128

129

130

131

132

133

134

135

136

137

138

139

140

141

142

143

144

145

146

147

148

149

150

151

152

153

154

155

156

157

158

159

160

161

162

163

164

165

166

167

168

169

170

171

172

173

174

175

176

177

178

179

180

181

182

183

184

185

186

187

188

189

190

191

192

193

194

195

196

197

198

199

200

201

202

203

204

205

206

207

208

209

210

211

212

213

214

215

216

217

218

219

220

221

222

223

224

225

226

227

228

229

230

231

232

233

234

235

236

237

238

239

240

241

242

243

244

245

246

247

248

249

250

251

252

253

254

255

256

257

258

259

260

261

262

263

264

265

266

267

268

269

270

271

272

273

274

275

276

277

278

279

280

281

Preceding page blank

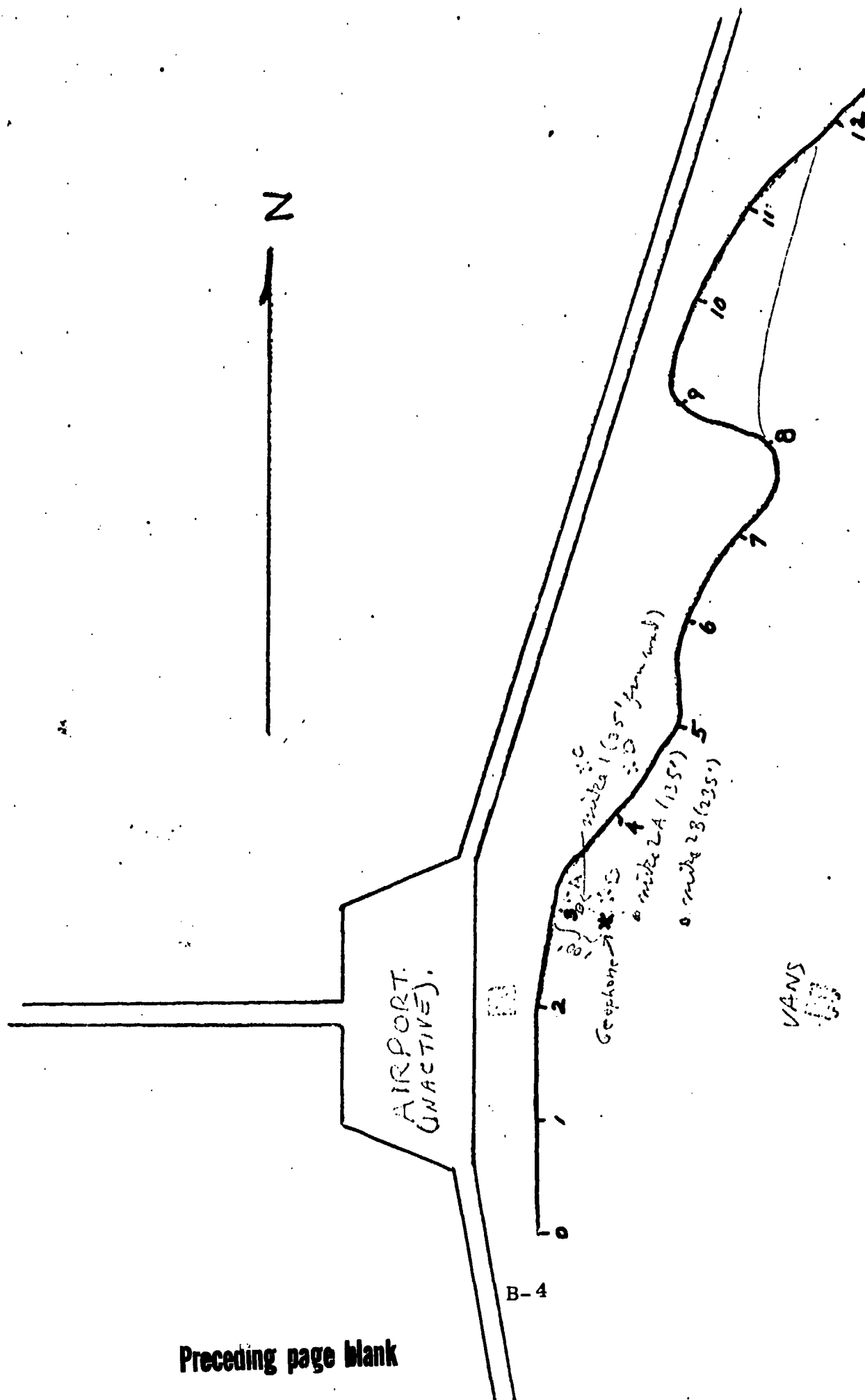
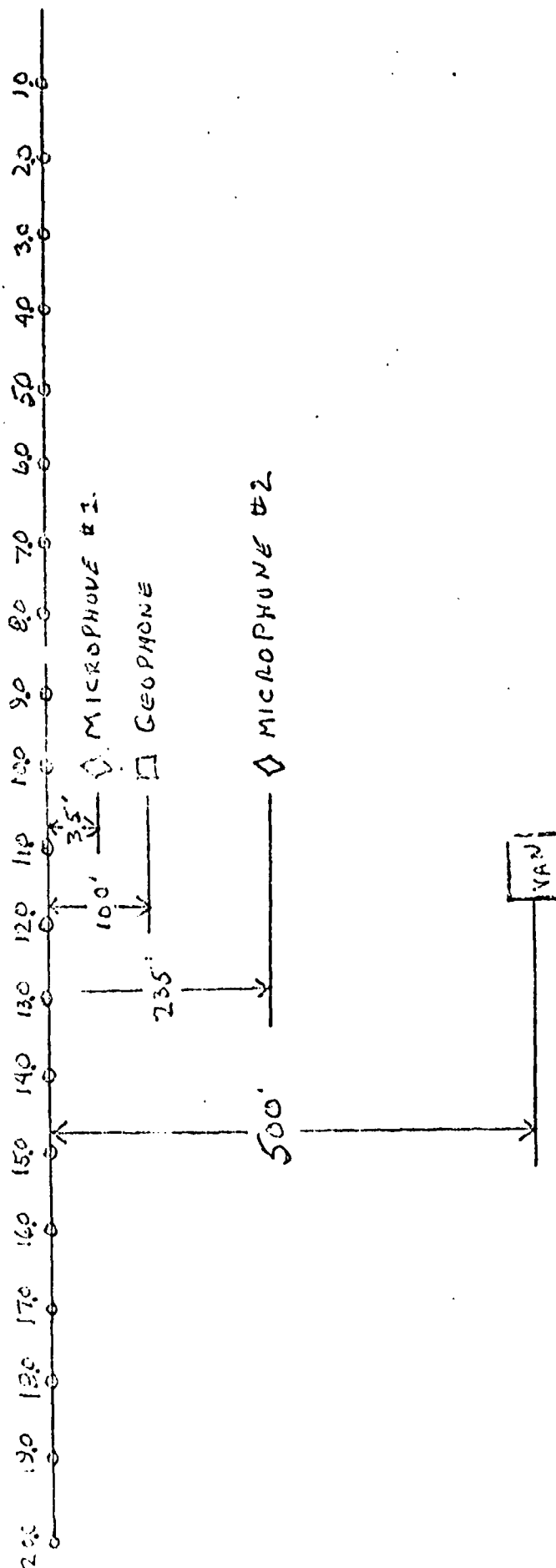


FIG. 2
GRAYLING SITE

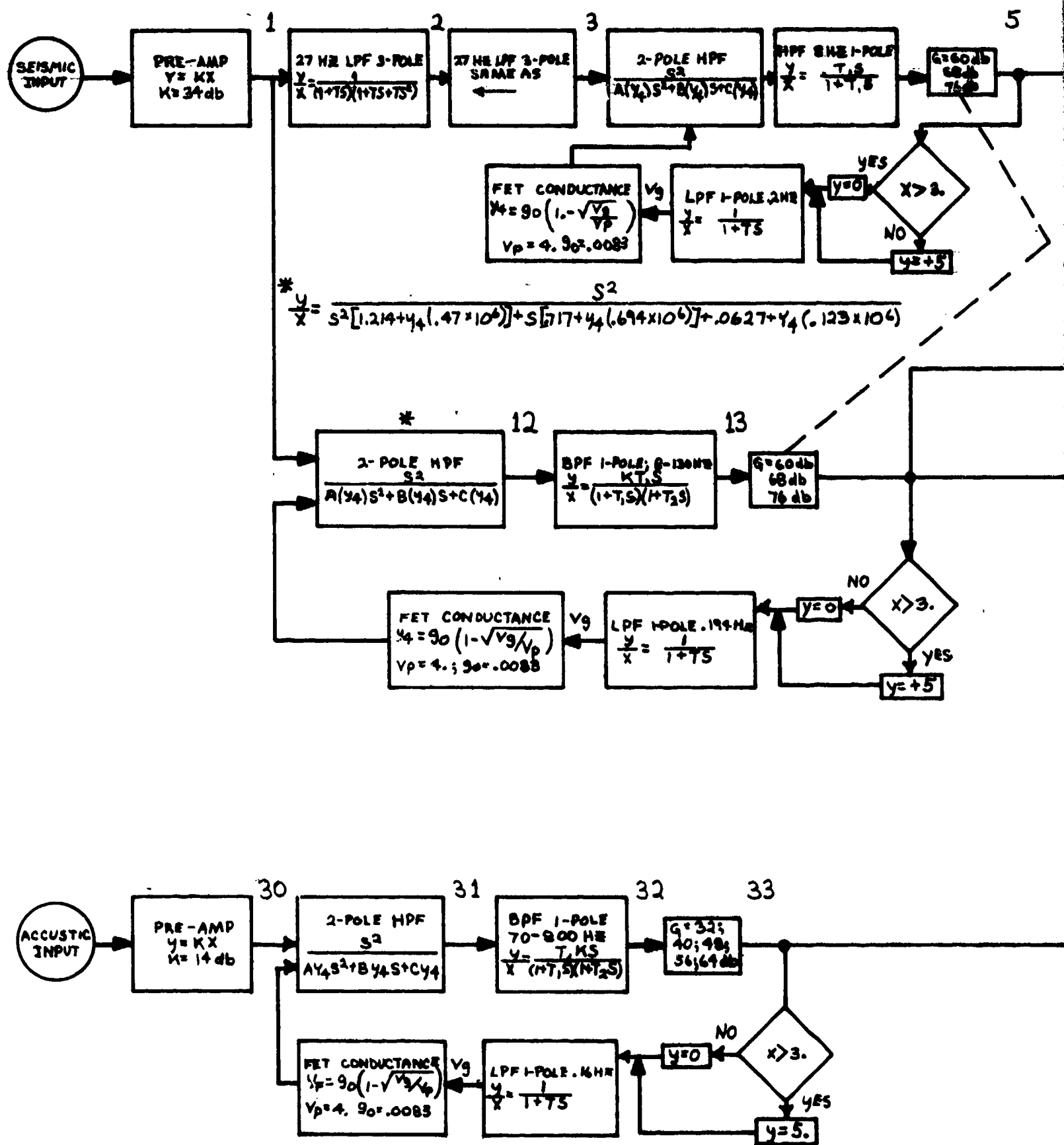
RANGE STAKES (X20)



FT. BRAGG SITE

APPENDIX C
SYLVANIA FEATURE EXTRACTOR DATA

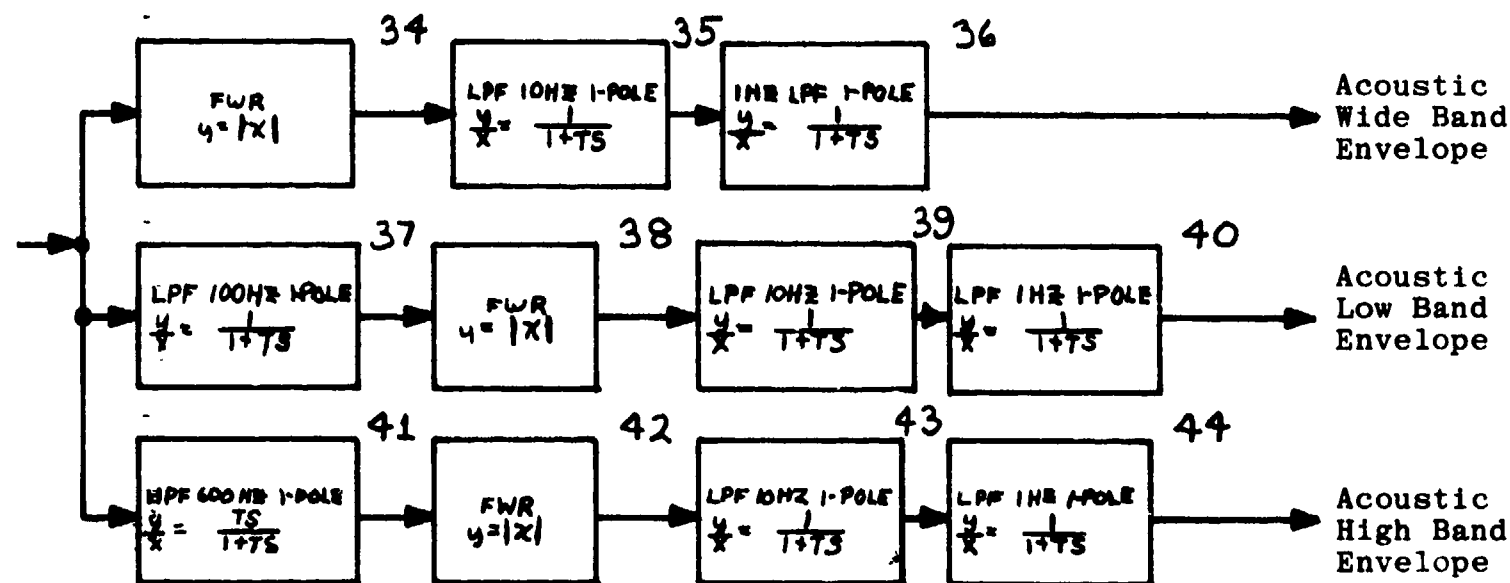
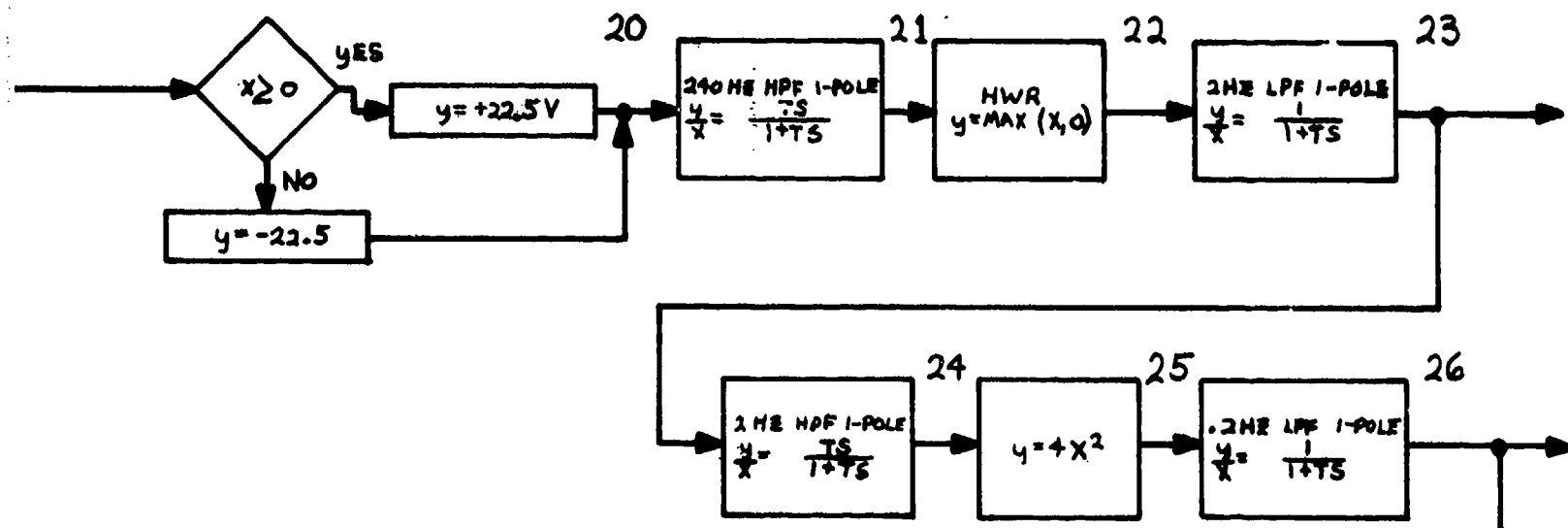
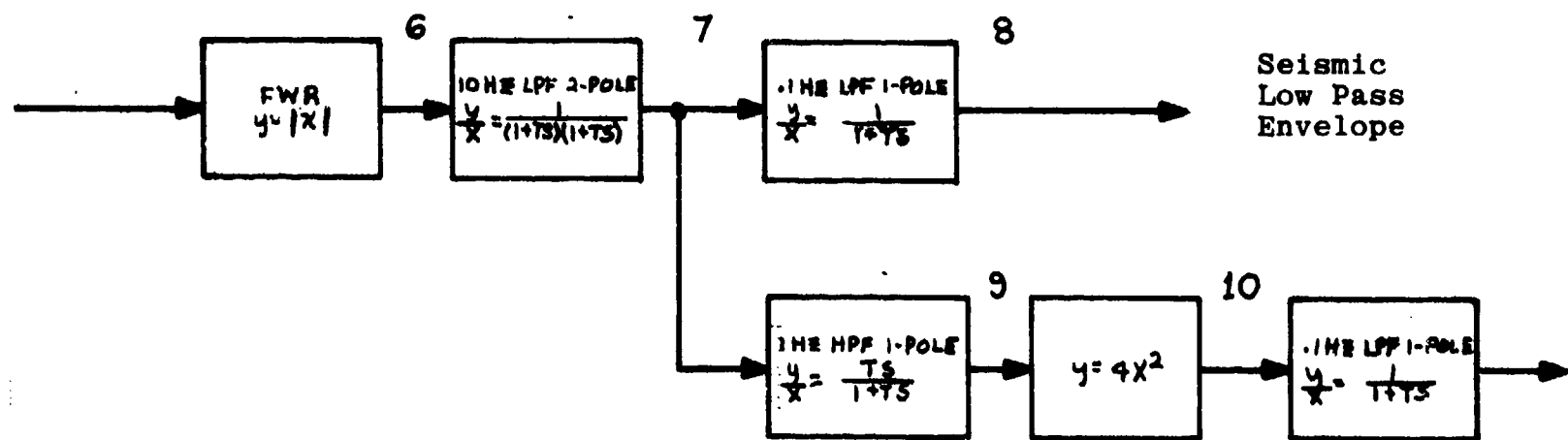
1. STC and SATC Flow Chart Showing Transfer Functions
2. Difference Equations Used in Sylvania Feature Extractors
3. FORTRAN Program Feature Extractor Samples



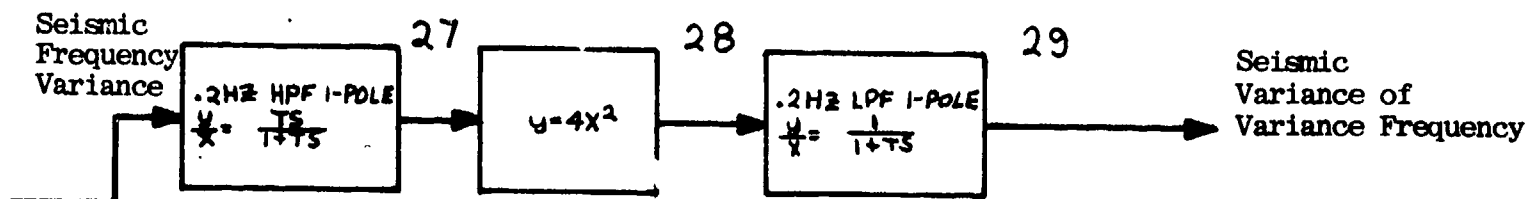
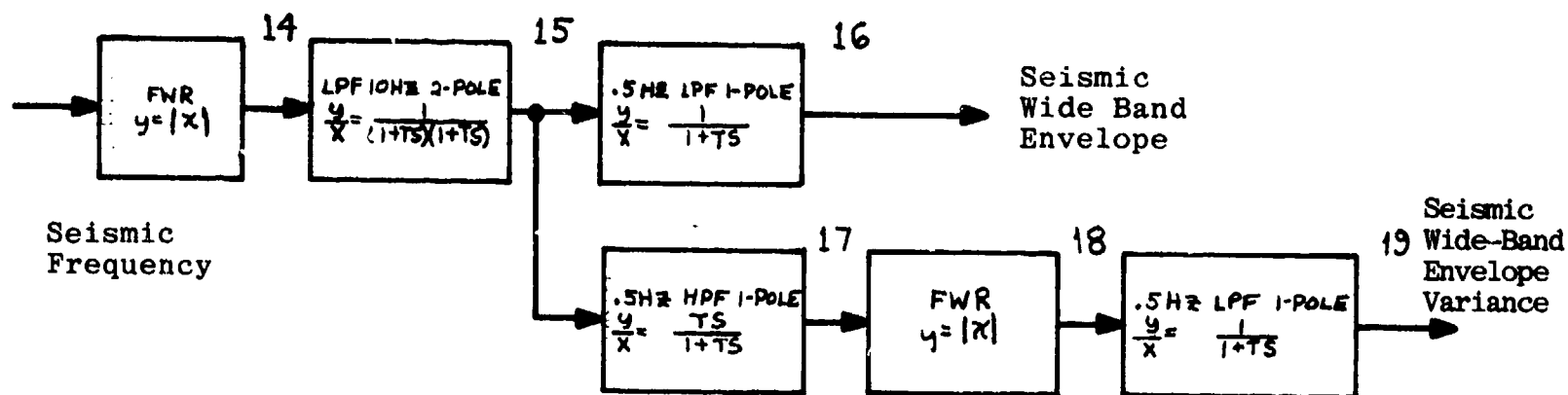
SYLVANIA SEISMIC AND SEISMIC ACOUSTIC FEATURE EXTRACTOR TRANSFER FUNCTIONS

Preceding page blank

C-3a



Seismic
Low Pass
Variance



DIFFERENCE EQUATIONS USED IN SYLVANIA FEATURE EXTRACTORS

(1) 1-Pole LPF

$$\frac{Y}{X} = 1/(1+Ts) \rightarrow y_i = Ax_i + By_{i-1}$$

where

$$A = 2\pi f\Delta t / (1 + 2\pi f\Delta t)$$

$$B = 1 / (1 + 2\pi f\Delta t)$$

$$x_i = \text{Present Input Value}$$

$$y_i = \text{Present Output Value}$$

$$y_{i-1} = \text{Past Output Value}$$

$$f = \text{Cutoff Frequency}$$

$$\Delta t = \text{Sampling Interval}$$

(2) 2-Pole LPF

$$\frac{Y}{X} = 1/(1+Ts)^2 \rightarrow y_i = Ax_i + By_{i-1} - Cy_{i-2}$$

where

$$A = (2\pi f\Delta t)^2 / [(2\pi f\Delta t)^2 + 2(2\pi f\Delta t) + 1]$$

$$B = [2(2\pi f\Delta t) + 2] / [(2\pi f\Delta t)^2 + 2(2\pi f\Delta t) + 1]$$

$$C = 1 / [(2\pi f\Delta t)^2 + 2(2\pi f\Delta t) + 1]$$

(3) 3-Pole LPF

$$y/x = 1/(1+Ts)(1+Ts+Ts^2)$$

$$\rightarrow y_i = Ax_i + By_{i-1} - Cy_{i-2} + Dy_{i-3}$$

where

$$A = 2(2\pi f\Delta t)^3 / \text{DEN}$$

$$B = [2(2\pi f\Delta t)^2 + 4(2\pi f\Delta t) + 3] / \text{DEN}$$

$$C = [2(2\pi f\Delta t) + 3] / \text{DEN}$$

$$D = 1 / \text{DEN}$$

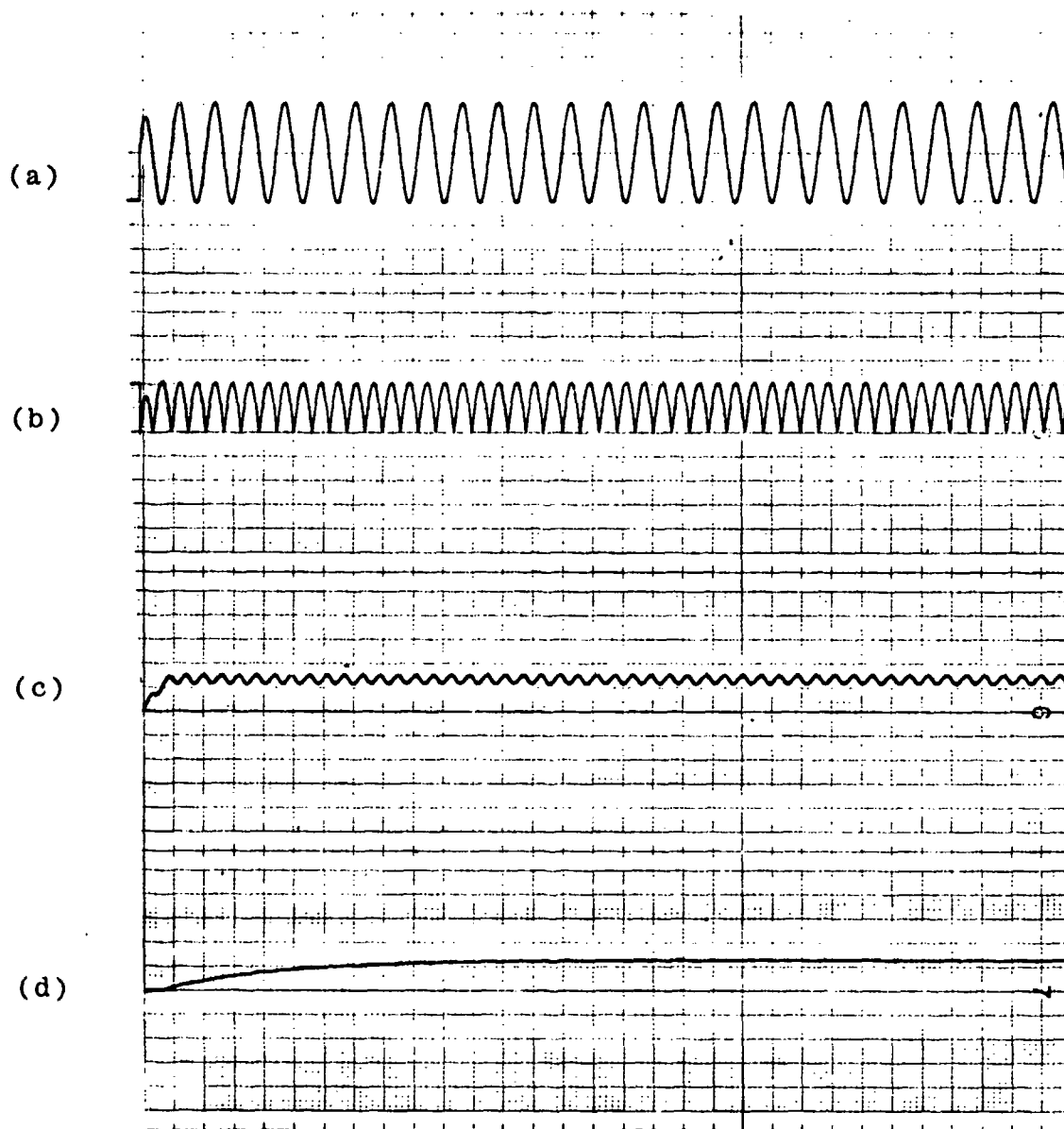
$$\text{DEN} = (2\pi f\Delta t)^3 + 2(2\pi f\Delta t)^2 + 2(2\pi f\Delta t) + 1$$

(4) 1-Pole HPF

$$y/x = Ts/(1+Ts) \rightarrow y_i = A(x_i - x_{i-1} + y_{i-1})$$

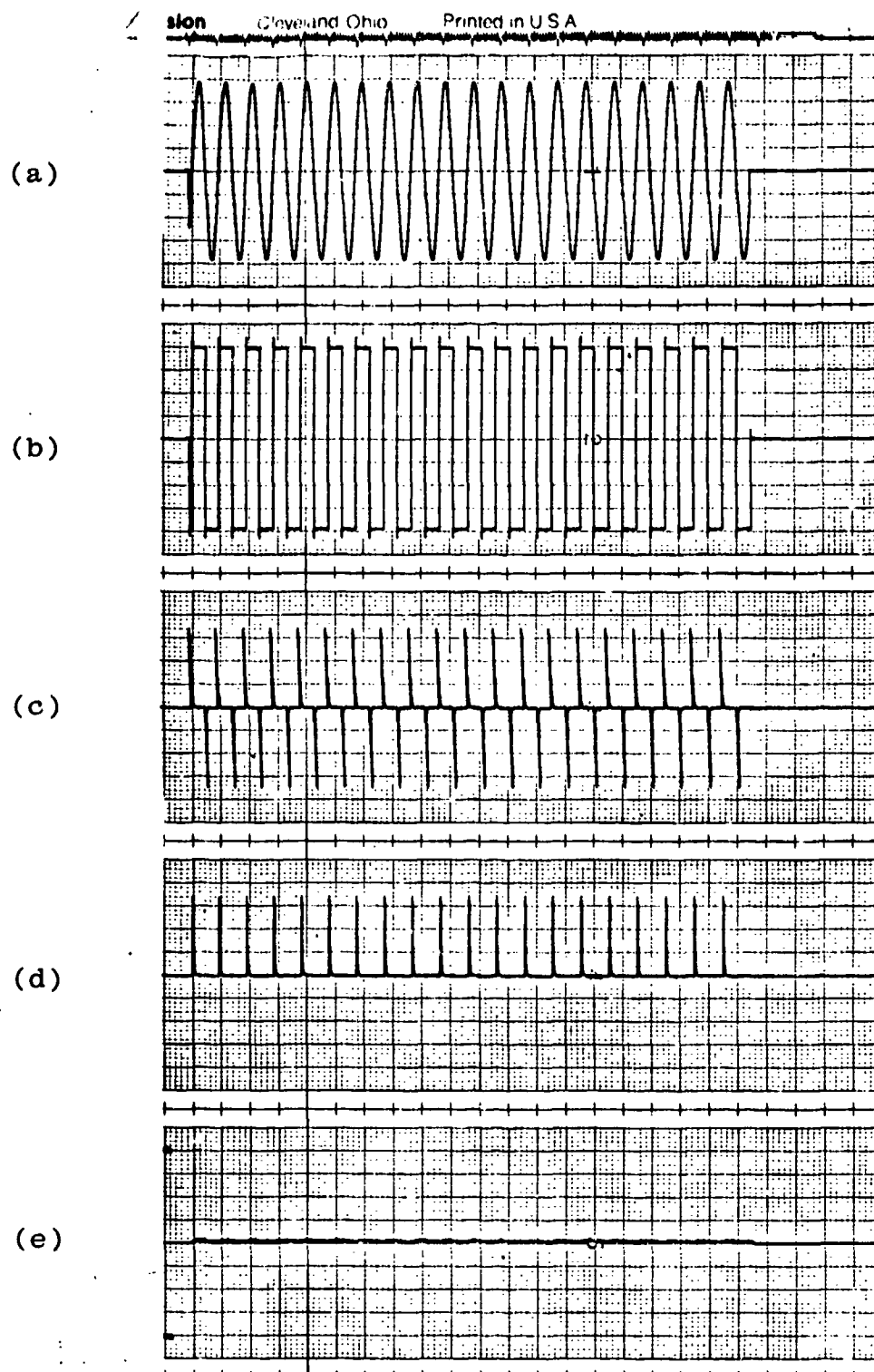
where

$$A = 1 / (2\pi f\Delta t + 1)$$



Sample Output From the Sylvania Feature Extractor FORTRAN program:

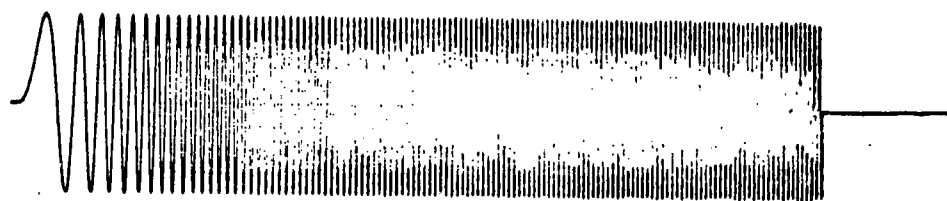
- (a) 20 Hz sinusoidal input
- (b) Full wave rectifier output
- (c) 10 Hz LPF output
- (d) Wide band envelope feature



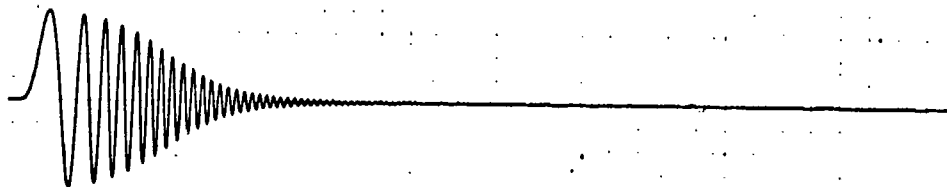
Sample Output From the Sylvania Feature Extractor FORTRAN program:

- (a) 30 Hz sinusoidal input
- (b) Limiter Output
- (c) 240 Hz HPF output
- (d) Half wave rectifier output
- (e) Seismic frequency feature

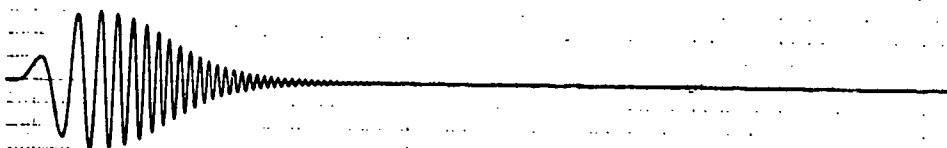
(a)



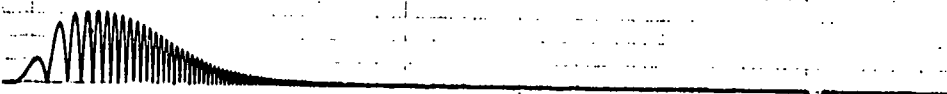
(b)



(c)



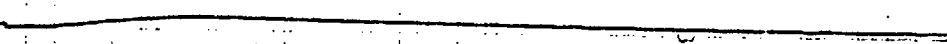
(d)



(e)



(f)

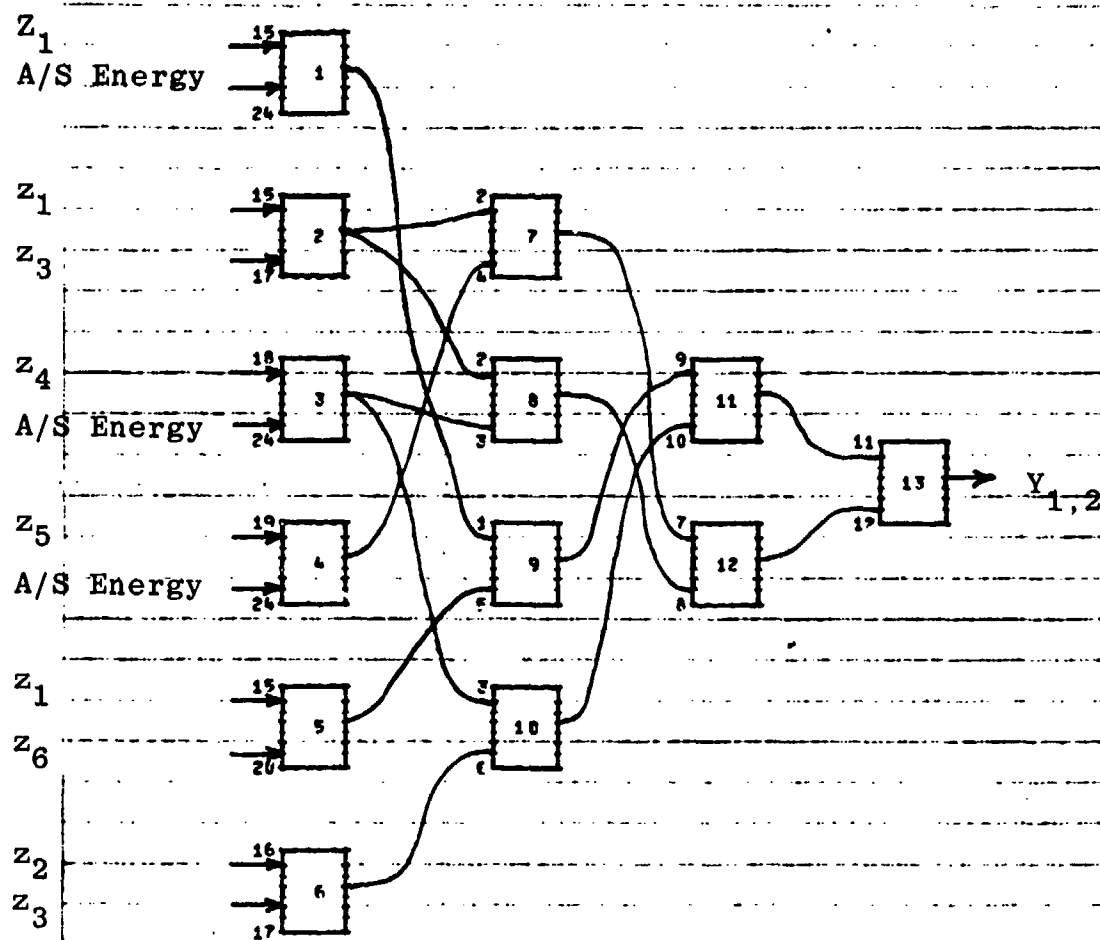


Sample Output From the Sylvania Feature Extractor FORTRAN Program

- (a) Sinusoidal test function with increasing frequency
- (b) Low pass filter output
- (c) Low band amplifier output
- (d) Full wave rectifier output
- (e) 10 Hz LPF output
- (f) Low band envelope feature

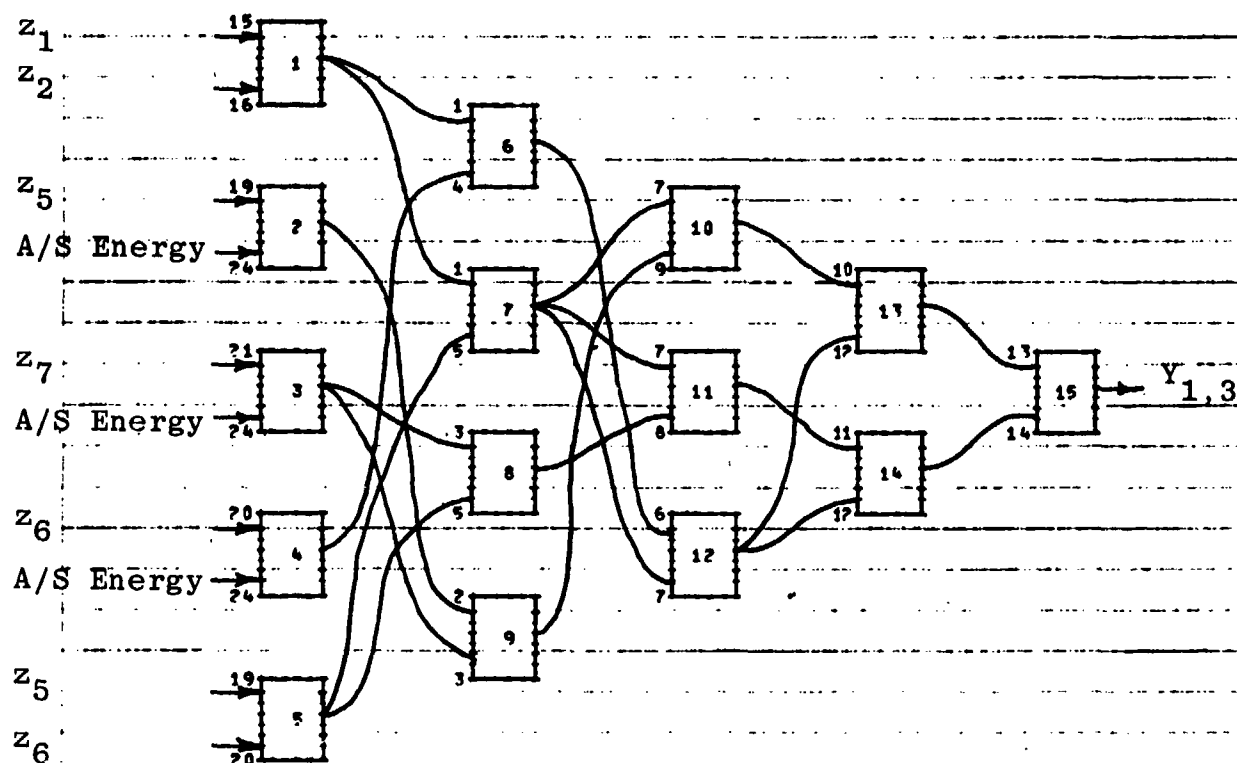
APPENDIX D

ADAPTIVE LEARNING NETWORK NONLINEAR DISCRIMINANT FUNCTION
STRUCTURES, EIGENVECTOR WEIGHTS, AND TABLE OF ERRORS AND
CLASS 1 AND CLASS 2 ERROR HISTOGRAMS WITH RESPECT TO RANGE
FOR NONLINEAR CLASSIFIER G



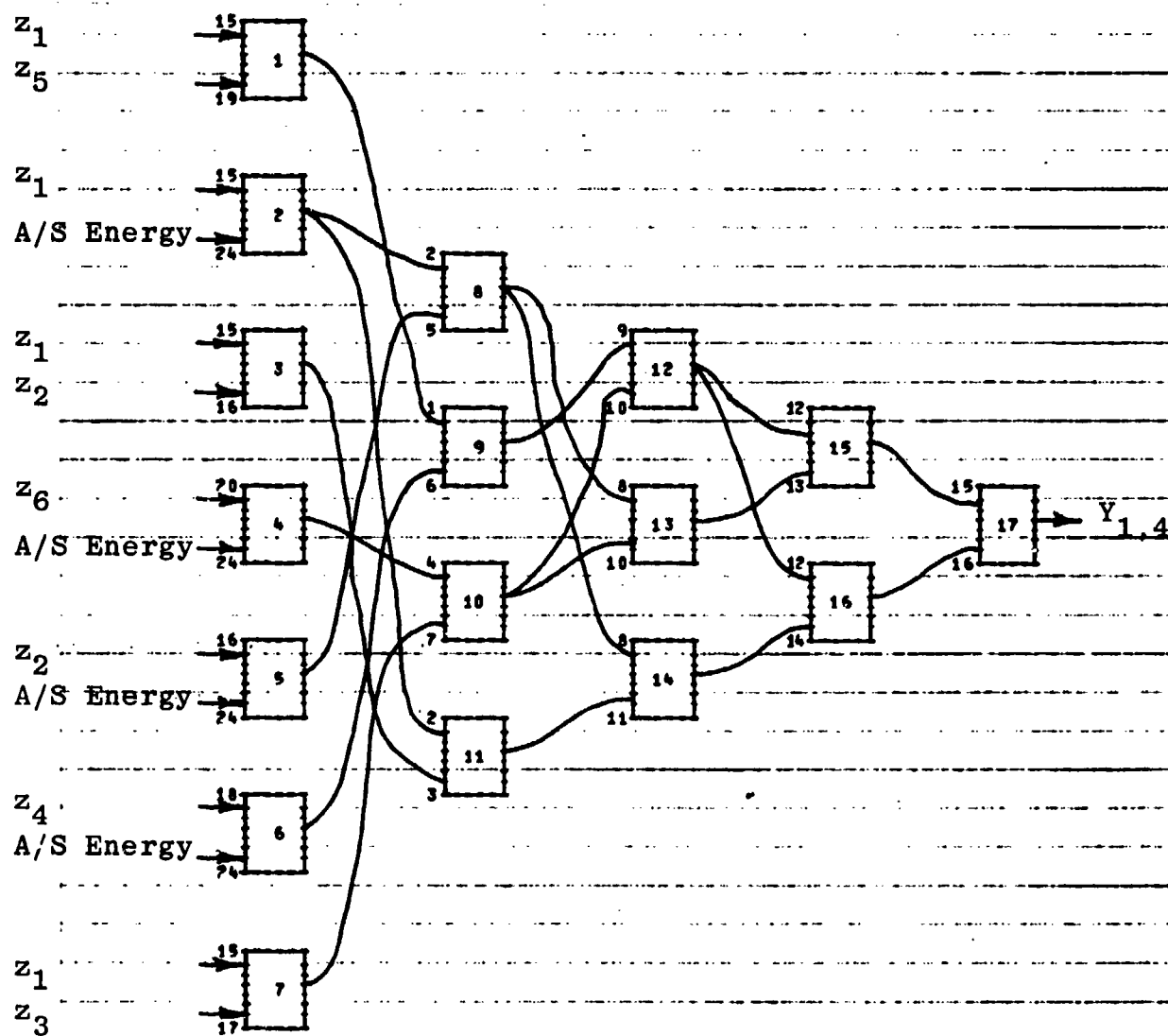
ELFN	NETWORK WEIGHTING COEFFICIENTS					
	W0	W1	W2	W3	W4	W5
1	.11471F+C1	.43004E+00	-.47134E+00	-.32116E+00	.12729F+00	.16553E-01
2	-.45669F+00	-.36510F+00	.14293F+01	.26896E+00	.22248F+00	.18751E+C1
3	.80371F+C0	-.52596E-C1	-.61622E-01	-.44591F+00	.97571E+00	-.42843F-C1
4	.96077F+C0	-.15864E+01	-.66711F-01	.27263F+00	-.20549E+01	-.43318E-C1
5	.76370F+00	-.10772E+01	.20196F+C1	-.12247E+01	-.12126E+01	-.19083E+C1
6	-.17442F+C0	-.19240E+00	.11364F+C1	-.11081E+01	-.68139F-01	.11599F+C1
7	.24656F+C0	.75154E+00	.51933E+00	.16666E+00	-.35766E+00	-.26992F+C0
8	.11823F+C0	.68831E+00	.58946F+C1	.46572E+00	-.42720F+00	-.16696F+C0
9	.23774F-C1	.80151E+00	.22942F+00	.12031E+01	-.13815F+00	-.83197F+C0
10	-.32879E-C1	.81641E+00	.53381F+C1	.18657E+00	.28484E+00	-.53856E+C0
11	.30370F-C1	.51066E+00	.62987E+00	-.47474E-01		
12	-.95797E-C1	.54927F+00	.45664E+00	.15696E+00		
13	.21945E-C1	.24999E+00	.89384F+00	-.24825E-01		

FIGURE D.1: NONLINEAR PAIRWISE DISCRIMINANT FUNCTION: CLASS 1 VERSUS CLASS 2



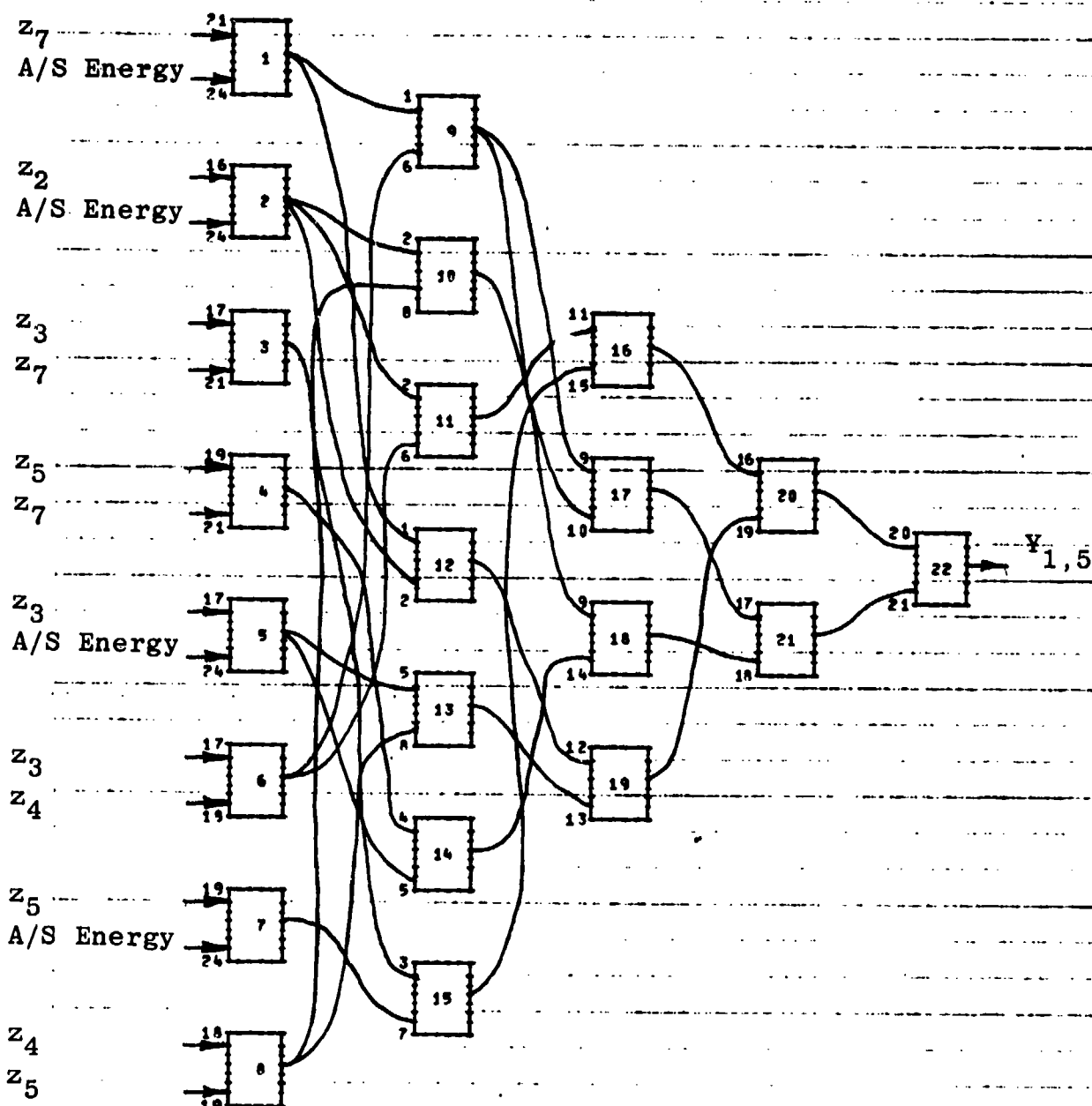
NETWORK WEIGHTING COEFFICIENTS							
ELF4	W0	W1	W2	W3	W4	W5	
1	.91078E+00	-.81804E+00	-.40225E+00	.77297E+00	-.17185E+01	-.12443E+01	
2	.52849E+00	.24767E+01	.14056E+00	-.19601E+00	-.32731E+01	-.69229E+01	
3	.17612E+01	.17066E+01	-.49766E+00	-.78102E+00	-.41809E+01	.47680E+02	
4	.15474E+01	.22847E+01	-.43770E+00	-.46077E+00	.19613E+00	-.61202E+02	
5	.71260E+01	.27059E+01	-.89509E+00	-.91401E+00	-.34765E+01	-.33689E+01	
6	-.25357E+00	.81279E+00	.59889E+00	.30504E+00	.26081E+00	.14502E+00	
7	-.17459E+00	.91152E+00	.72919E+00	.36352E+00	.17790E+00	.11886E+00	
8	.12494E+01	.81217E+00	.53129E+00	.44785E+00	-.10771E+00	-.62295E+01	
9	-.13814E+00	.86309E+00	.25747E+00	.97913E+00	-.37447E+01	-.67859E+00	
10	-.76697E+02	.61636E+00	.49844E+00	.16947E+01			
11	.48663E+01	.69970E+00	.41215E+00	-.70520E+01			
12	.11885E+00	.85086E+00	.16804E+00	-.16413E+00			
13	-.20098E+01	.27321E+00	.73870E+00	.26738E+01			
14	-.46180E+01	.12274E+00	.89284E+00	.58908E+01			
15	.51854E+02	.13861E+01	-.38701E+00	-.61725E+02			

FIGURE D.2: NONLINEAR PAIRWISE DISCRIMINANT FUNCTION: CLASS 1 VERSUS CLASS 3



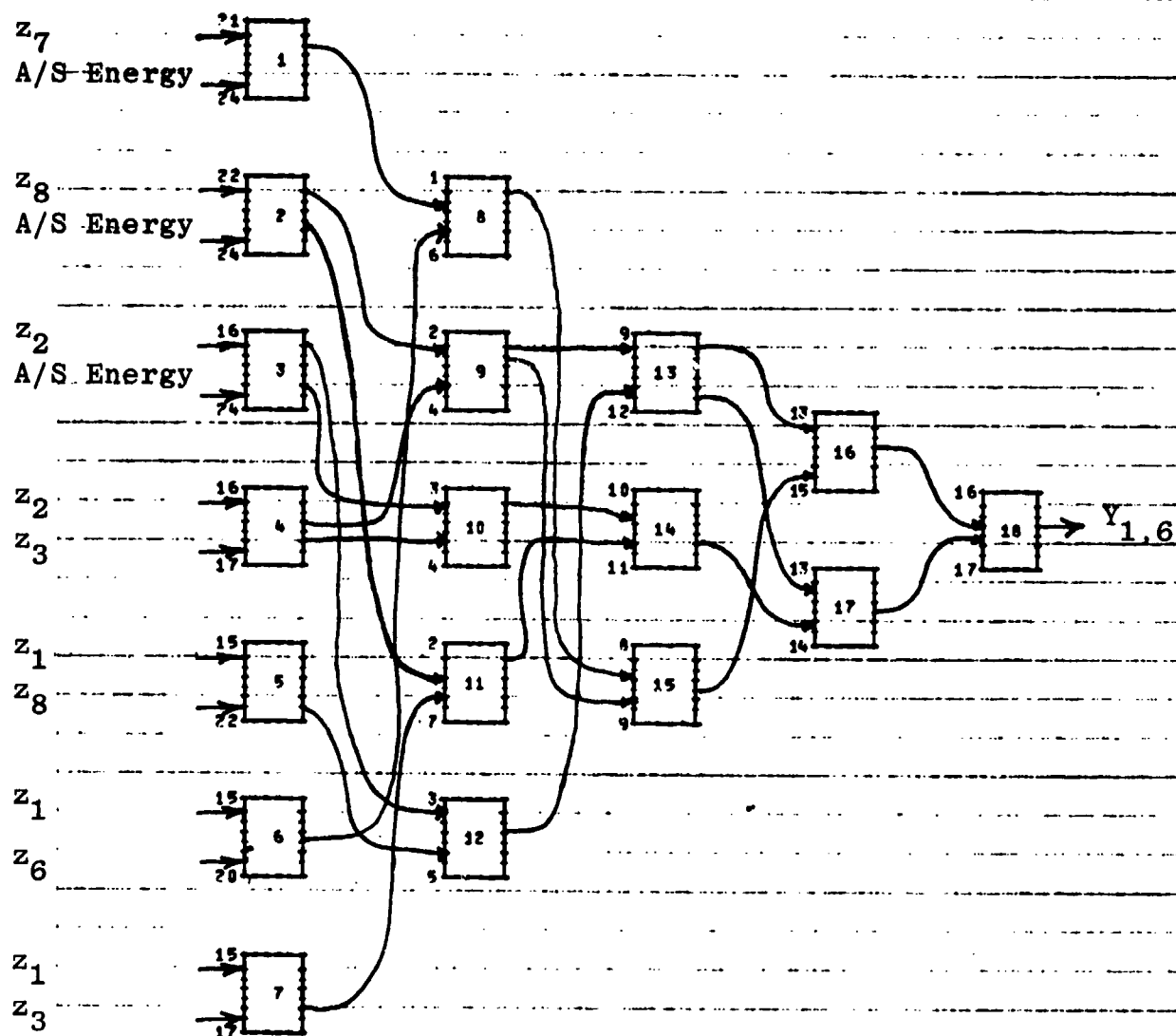
NETWORK WEIGHTING COEFFICIENTS						
ELFM	W0	W1	W2	W3	W4	W5
1	-.42950E+00	-.84019E+00	-.62763E+00	.97272E+00	.45723E-01	-.47591E+00
2	-.38515E+01	-.43243E+01	.19793E+01	.87452E+00	-.59782E+00	-.26439E+00
3	-.24886E+00	-.93492E+00	.47885E+00	-.69082E+00	.16887E+00	-.76556E+00
4	.27081E+01	.74518E+01	-.91615E+00	-.61537E+00	-.26208E+01	.56685E-01
5	.13716E+01	.13339E+01	-.23987E+00	-.10997E+00	-.13776E+01	-.30260E-01
6	.12055E+01	.40892E+01	-.41759E+00	-.92314E+00	-.14793E+01	-.26287E-03
7	-.47776E+00	-.11918E+01	.43513E+00	-.60505E+00	.47430E+00	.14646E+00
8	-.32167E+00	.31119E+00	.86788E+00	.12884E+01	-.54768E+00	-.25077E+00
9	.32179E+00	.81528E+00	.19394E+00	.15107E+01	-.90860E+00	-.83374E+00
10	.45726E+00	.33676E+00	.65541E+00	.12966E+01	-.67133E+00	-.10237E+01
11	-.12887E+00	.75045E+00	.36923E+00	.97497E+00	-.19764E+00	-.95407E+00
12	-.32570E+00	.54959E+00	.53261E+00	.36788E+00		
13	-.16072E+00	.82078E+00	.19712E+00	.17911E+00		
14	-.23762E-01	.98791E+00	.12852E-01	.25931E-01		
15	.20448E+00	.36272E+00	.65075E+00	-.21459E+00		
16	.10455E+00	.43143E+00	.58008E+00	-.11024E+00		
17	-.21515E+00	.26585E+01	-.14575E+01	.22804E+00		

FIGURE D.3: NONLINEAR PAIRWISE DISCRIMINANT FUNCTION CLASS 1 VERSUS CLASS 4



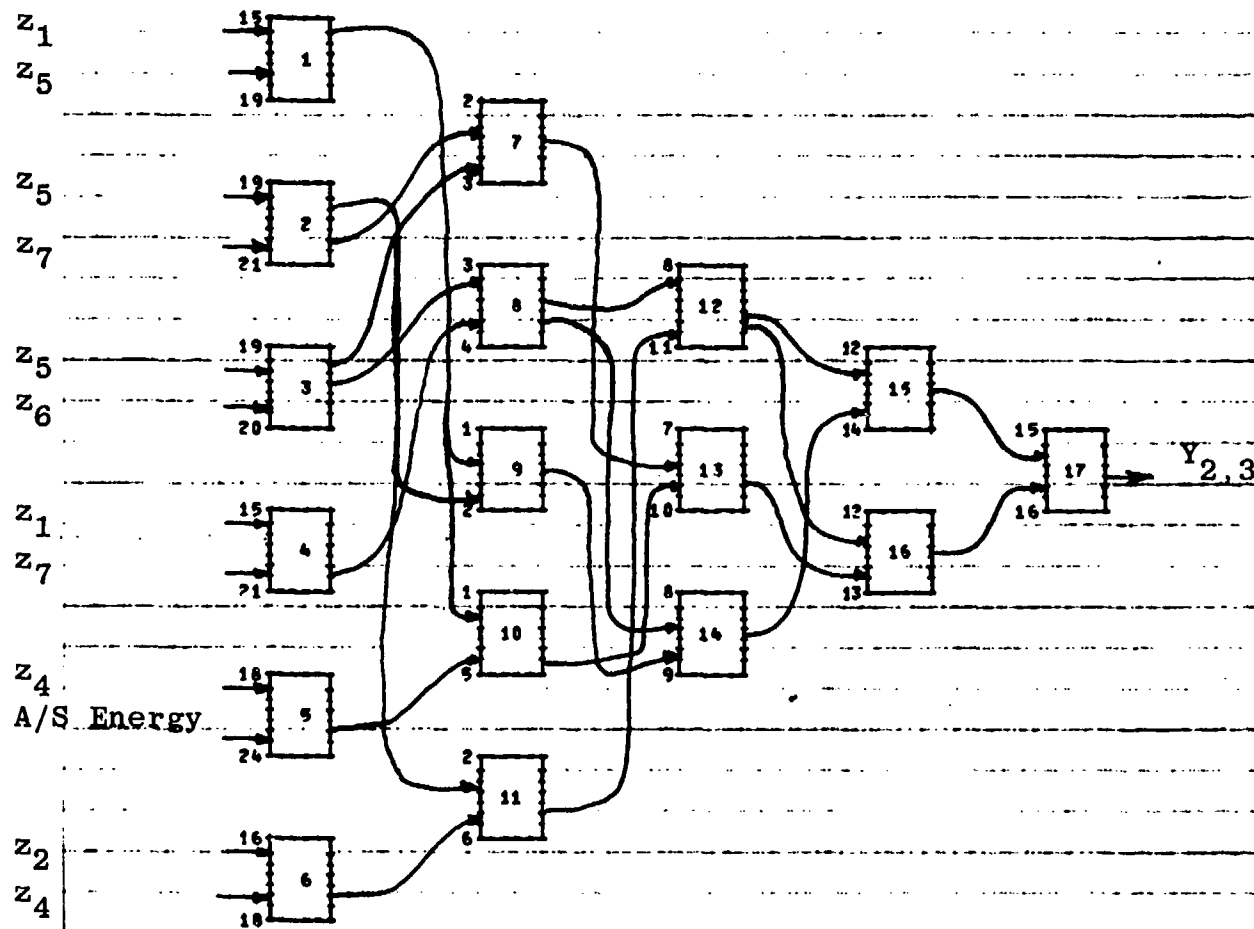
FLM	NETWORK WEIGHTING COEFFICIENTS					
	W0	W1	W2	W3	W4	W5
1	-.19392E-01	.48771E+01	-.14441E+00	-.75740E+00	.35429E+01	-.74861E-02
2	.63479E+00	-.75553E+00	.39471E+00	.37171E+00	-.20739E+01	-.12685E+00
3	-.69779E+00	-.31012E+00	.32139E+01	.49440E+01	-.11449E+01	.22749E+01
4	-.90121E+00	-.12563E+01	.26553E+01	-.51441E+01	.11191E+01	.12568E+01
5	.17130E+01	.70809E+01	-.39950E+00	-.13162E+01	-.14768E+01	-.95134E-02
6	-.74715E+00	.69443E+00	-.71267E+01	-.27468E+01	.35950E+00	.21613E+01
7	.61792E+00	-.43271E+01	-.16927E+00	.62017E+00	.10180E+01	-.75520E-01
8	-.75049E+00	-.17543E+01	-.11543E+01	.72575E+01	.10442E+01	.99083E+00
9	.42040E+00	.80742E+00	.30446E+00	.26544E+00	-.29325E+00	-.51719E+00
10	-.25154E+00	.12149E+01	.11609E+00	.10202E+01	.19017E+00	-.62271E+00
11	-.31112E+00	.11214E+01	.27477E+00	.51045E+00	.30184E+00	-.24187E+00
12	-.17790E+00	.47510E+00	.76137E+00	.55544E+00	-.35950E+00	.13269E+00
13	.64814E-01	.73811E+00	.39270E+00	.67060E+00	-.71091E-01	-.54455E+00
14	-.16210E+00	.71122E+00	.45786E+00	.18427E+00	.25160E-01	.44648E-01
15	-.14797E+00	.68367E+00	.64944E+00	.73124E+00	-.93726E-01	-.12681E-01
16	.24045E+00	.71955E+00	.81913E+00	-.28764E+00		
17	-.59814E-02	.49411E+00	.54560E+00	.76476E-02		
18	-.14540E-01	.45739E+00	.59151E+00	.18770E-01		
19	.78679E-01	.70937E+00	.35357E+00	-.10294E+00		
20	-.10812E+00	.80224E+00	.77899E+00	.11933E+00		
21	-.58465E-01	.39167E+00	.40647E+00	.65592E-01		
22	.79944E-01	.61995E+00	.37443E+00	-.84505E-01		

FIGURE D.4: NONLINEAR PAIRWISE DISCRIMINANT FUNCTION CLASS 1 VERSUS CLASS 5



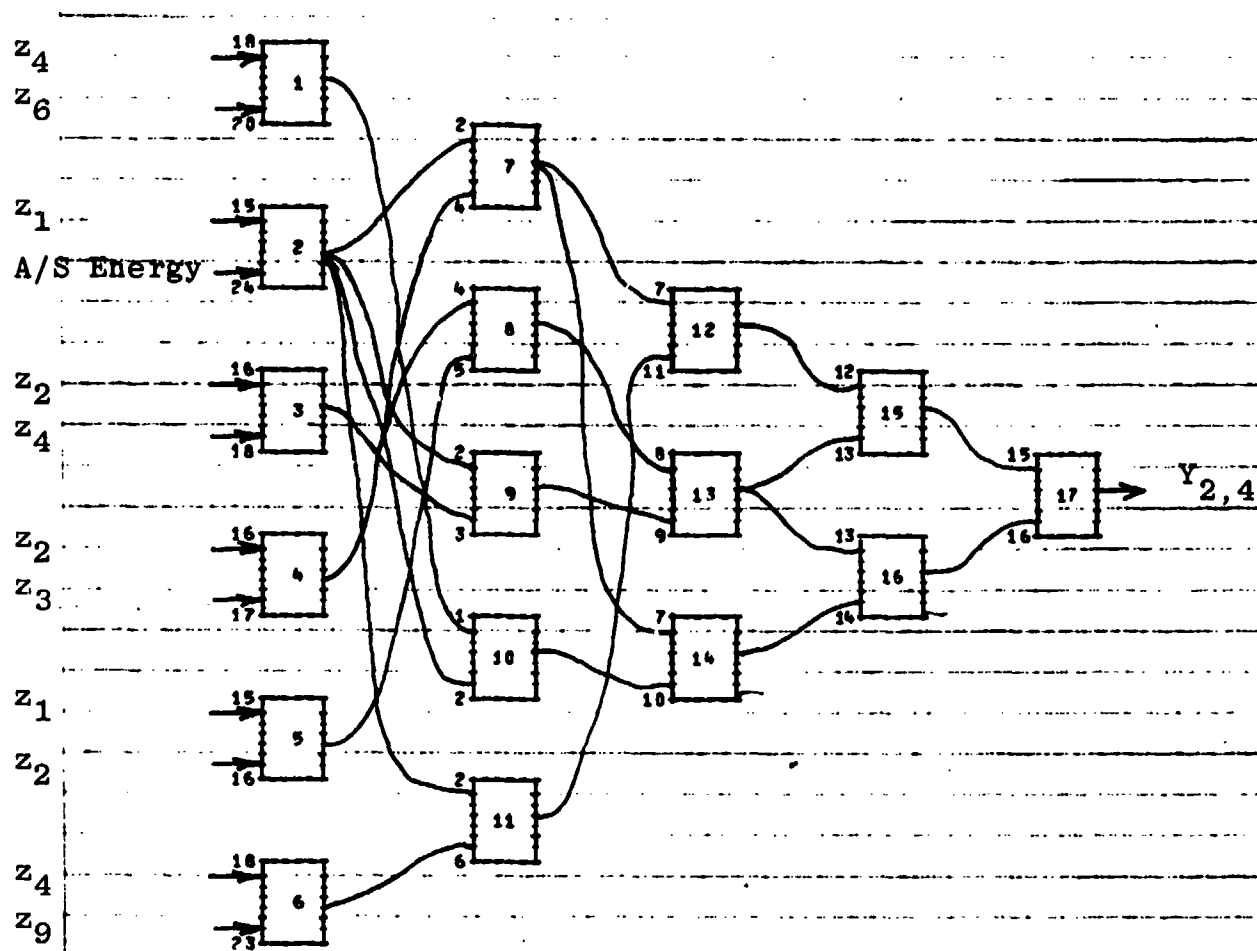
ELEM	NETWORK WEIGHTING COEFFICIENTS					
	W0	W1	W2	W3	W4	W5
1	.10971F+01	.28527E+01	-.85918E+00	-.61903E+00	.49084E+01	.81027E-01
2	.17997F+00	-.13497E+01	-.67991E+00	.27877E+00	.28481E+01	.56174E-01
3	.12704F+00	-.15920E+01	-.40671E+00	.73150F+00	.16899E+00	.30497E-01
4	-.25772F+00	-.11052E+01	.13042F+01	-.24011F+01	.57916E-01	.71679E+00
5	-.17907F+00	-.94097E+00	-.39557E+00	-.16116E+01	-.24111E+00	.36178E+01
6	.74955F+00	-.15955E+01	.24065E+01	.92099E-01	-.80660E+00	-.55314E+01
7	.68217E-01	-.69497E+00	.94999E+00	-.19957E+01	-.16695F+00	-.17022F+01
8	-.20452F+00	.81236E+00	.77041F+00	.47984E+00	-.14451F-01	-.14756E+00
9	.61671E-01	.77806E+00	.11264F+00	.10057E+01	-.37748E+00	-.53701E+00
10	.62131F-01	.77535F+00	.24047F+00	.75089E+00	-.29214F+00	-.41842E+00
11	.15259F+00	.10246F+01	-.18448E-02	.62059E+00	-.28757F+00	-.44166E+00
12	.88631F-01	.72067E+00	.36172F+00	.55053E+00	-.25013E+00	-.30815E+00
13	-.19475F+00	.51745E+00	.53943E+00	.44764E+00		
14	-.27106F+00	.72797E+00	.32017F+00	.31422E+00		
15	-.73578F-01	.72023F+00	.29376F+00	.80070E-01		
16	.24181F+00	.13455E+01	-.34321F+00	-.29264E+00		
17	.19519F+00	.13901F+01	-.38950E+00	-.20502E+00		
18	-.25549F+00	.65256E+00	.35536F+00	.26307E+00		

FIGURE D.5: NONLINEAR PAIRWISE DISCRIMINANT FUNCTION CLASS 1 VERSUS CLASS 6



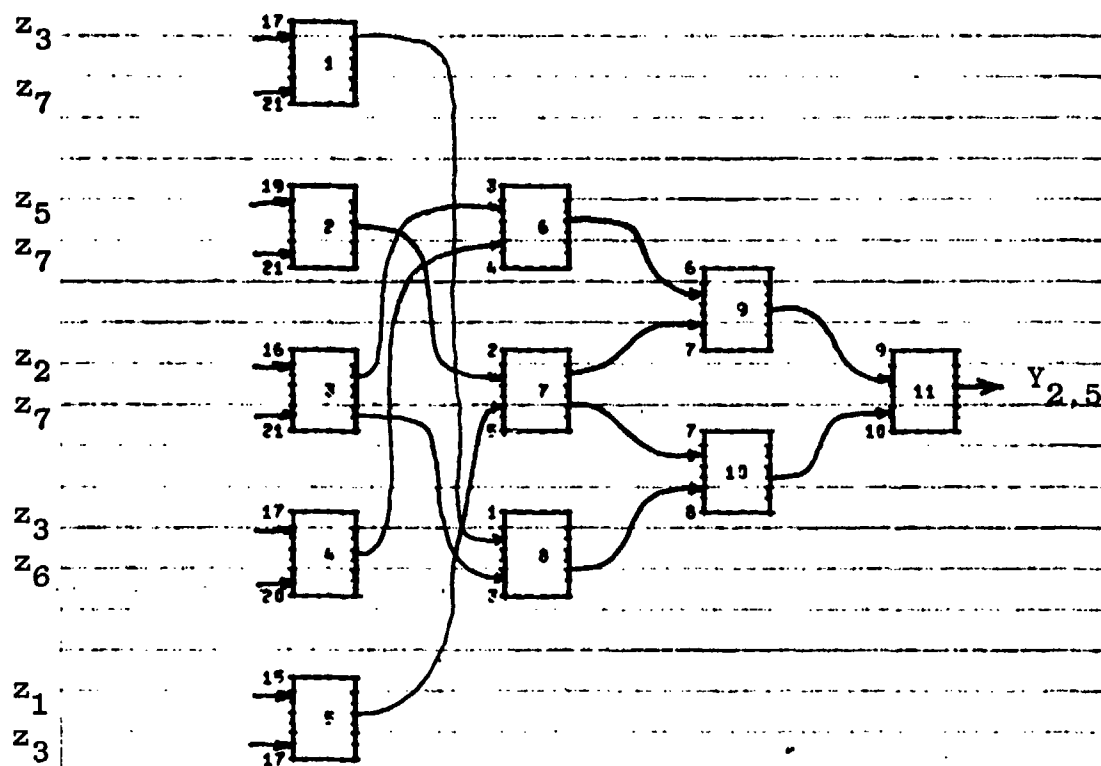
ELFM	NETWORK WEIGHTING COEFFICIENTS					
	W0	W1	W2	W3	W4	W5
1	.11923E+00	-.45497E+00	.30510E+01	.15057E+01	-.68855E+00	-.10135E+01
2	-.21776E-01	.26146E+01	-.40861E+00	-.49631E+01	.11561E+01	-.91219E+01
3	.76742E-01	.30399E+01	-.12750E+01	.16175E+01	.48840E+00	-.64161E+01
4	.72179E+00	-.56211E+00	-.90229E-01	-.39480E+00	-.82805E+00	-.47429E+01
5	-.40744E+00	.12016E+01	.31730E+00	.73295E+00	-.93725E+00	-.71349E-01
6	-.35237E+00	-.12229E+01	.24240E+01	-.41234E+01	.19646E+00	.68773E+00
7	-.12054E-01	.30525E+00	.74824E+00	.48967E+00	-.30562E+00	-.62889E-01
8	-.49814E-01	.10467E+01	.13070E+01	.62951E+00	.20864E-01	.46121E+00
9	-.35561E-01	.10154E+01	.74135E-01	.52246E+00	.19401E+00	-.65760E+00
10	-.15672E+00	.81621E+00	.57096E+00	.48342E+00	-.18805E-01	.32119E-01
11	-.61824E-02	.75255E+00	.74455E+00	.67145E+00	-.12928E+00	-.94912E-01
12	.11874E+00	.39834E+00	.69081E+00	-.17787E+00		
13	.73543E-01	.28227E+00	.83776E+00	-.14371E+00		
14	.97847E-01	.74886E+00	.12567E+00	-.15433E+00		
15	-.86199E-01	.10184E+01	.10810E-02	.12143E+00		
16	-.66946E-01	.10527E+01	-.45749E-01	.92992E-01		
17	.14185E+00	.34974E+01	-.24903E+01	-.17578E+00		

FIGURE D.2: NONLINEAR PAIRWISE DISCRIMINANT FUNCTION: CLASS 2 VERSUS CLASS 3



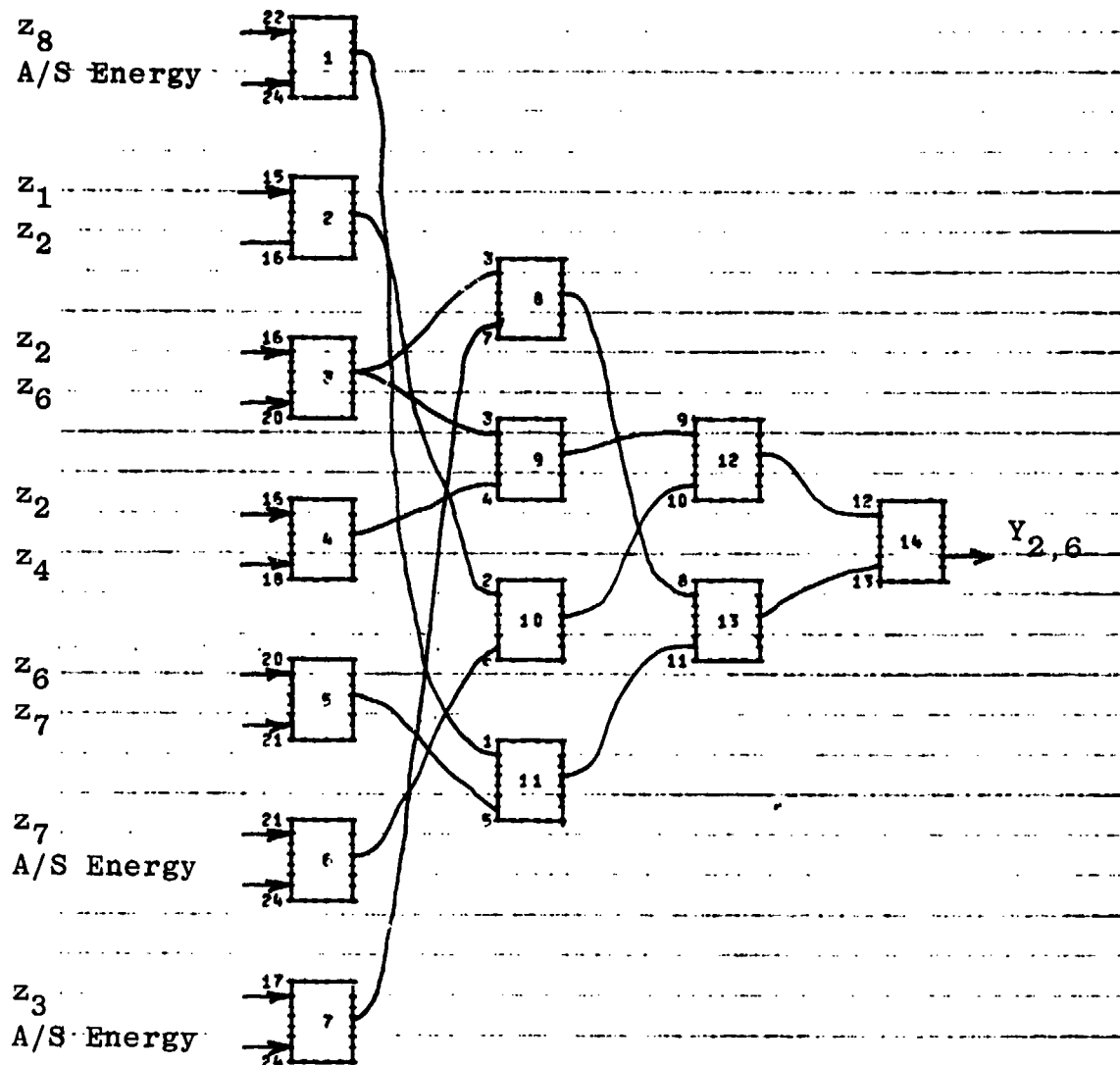
NETWORK WEIGHTING COEFFICIENTS						
FLEN	W0	W1	W2	W3	W4	W5
1	-.33725E-01	.1A062E+01	.24827E+00	.1A408E+01	-.78274E+00	-.35300E+01
2	-.13094E+01	-.19075E+01	.10A95E+01	.18052E+00	-.A6772E+00	-.22174E+00
3	-.42199E-01	.36657E+00	.18542E+01	-.122A6E+01	-.12761E+01	-.45919E+00
4	.57091E+00	.10105E+01	-.96006E+00	-.15174E+01	-.25762E+01	-.22547E+01
5	.202A8E-01	-.14940E+01	.44851E+00	-.40362E+00	-.10759E+01	-.14761E+01
6	-.67522E-01	.20336E+01	.14076E+01	.167A2E+01	-.58397E+00	-.85248E+01
7	-.46917E+00	.95905E+00	.60277E+00	.666A8E+00	.25523E+00	.73503E-02
8	-.47373E+00	.65494E+00	.9729A E+00	.75494E+00	.1C732E-01	.21759E+00
9	-.54563E+00	.14967E+01	.10949E+00	.56917E+00	.71421E+00	-.30455E+00
10	-.54676E+00	.11407E-02	.15500E+01	.61258E+00	-.25733E+00	.68621E+00
11	-.54066E+00	.15043E+01	.35605E-01	.65475E+00	.61718E+00	-.23A52E+00
12	-.42738E+00	.65334E+00	.44813E+00	.51832E+00		
13	-.42277E+00	.54605E+00	.561A4E+00	.51571E+00		
14	-.42694E+00	.65119E+00	.45007E+00	.52171E+00		
15	.2A242E+00	.77220E+00	.24614E+00	-.293A9E+00		
16	.2A156E+00	.35899E+00	.66004E+00	-.29326E+00		
17	-.30049E+00	.13344E+01	-.72374E+00	.30816E+00		

FIGURE D.7: NONLINEAR PAIRWISE DISCRIMINANT FUNCTION CLASS 2 VERSUS CLASS 4



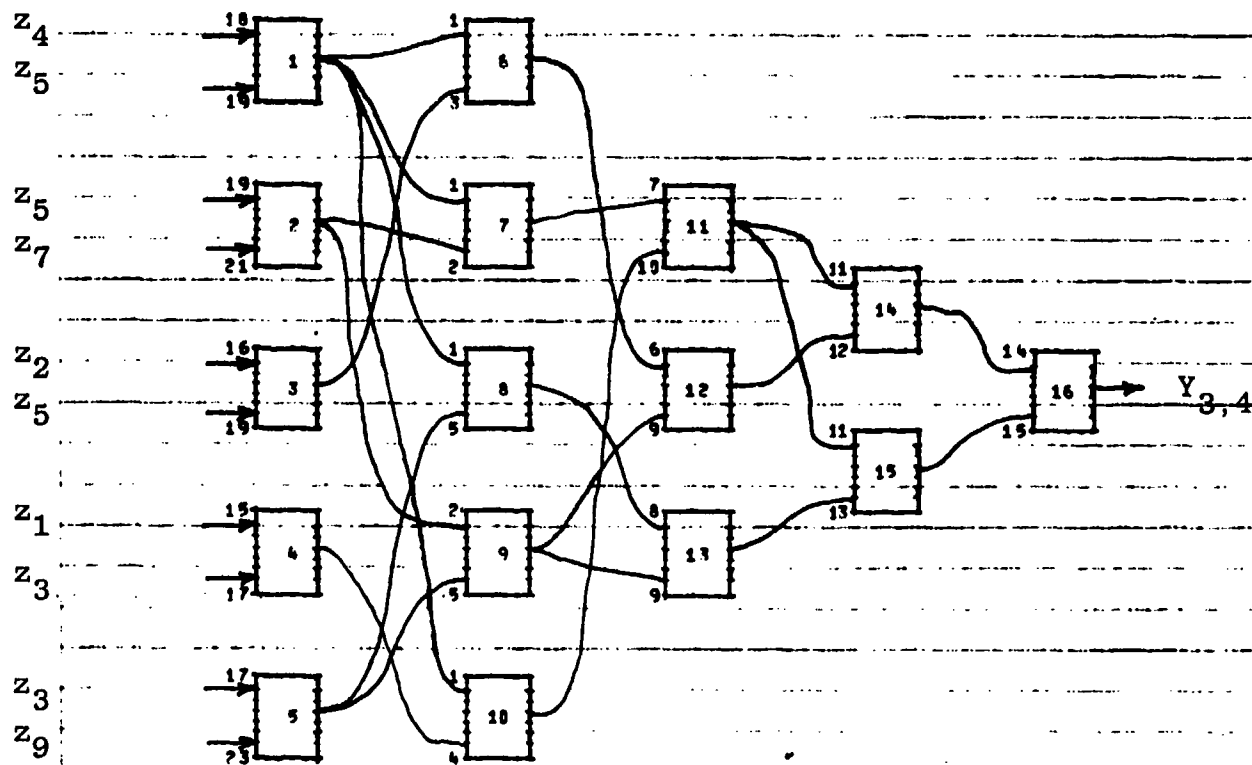
NETWORK WEIGHTING COEFFICIENTS						
FLFM	W0	W1	W2	W3	W4	W5
1	-.39103E+00	-.45476E-01	.27022E+01	-.45064E+00	-.13746E+01	.23016E+01
2	-.97429E+00	-.93211E+00	.11996E+01	-.97248E+01	.24773E+01	.27028E+01
3	-.65794E+00	-.12505E+00	.26914E+01	-.63909E+00	-.19556E+00	.32315E+01
4	.54039E+00	-.76491E+00	-.78973E+00	.17450E+01	-.25846E+01	-.23247E+01
5	.61939E+00	-.50156E+00	-.62254E+00	-.10927E+00	-.42401E+00	-.29377E+01
6	.27549E+00	.85232E+00	.31591E+00	.44886E+00	-.37188E+00	-.32521E+00
7	.22051E+00	.93609E+00	.93705E-01	.24895E+00	-.18229E+00	-.35750E+00
8	.15751E+00	.10513E+01	-.54136E-01	.27880E+01	-.89456E+00	-.21506E+01
9	-.12552E+00	.30839E+00	.73974E+00	.16265E+00		
10	-.10140E+00	.76773E+00	.27999E+00	.13453E+00		
11	.16096E+00	.23693E+01	-.13600E+01	-.18502E+00		

FIGURE D.8: NONLINEAR PAIRWISE DISCRIMINANT FUNCTION: CLASS 2 VERSUS CLASS 5



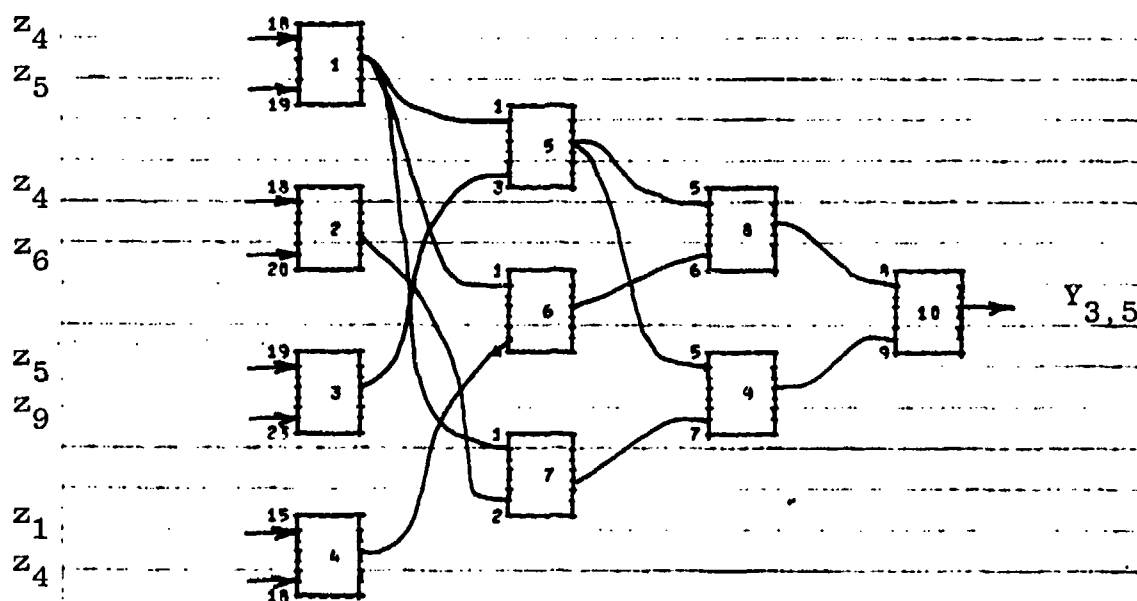
ELEM	NETWORK WEIGHTING COEFFICIENTS					
	W0	W1	W2	W3	W4	W5
1	.25059E+00	.36444E+00	-.47697E+00	-.11846E+01	.66222E+01	.14157E+00
2	-.11114E+01	-.30731E+00	-.92670E+00	.75145E+00	.67434E-01	.13645E+01
3	-.13201E+01	-.14475E+01	-.39880E+00	.25909E+01	.10112E+01	.10515E+02
4	-.53546E+00	-.10394E+01	-.43211E+00	.11606E+01	.66714E+00	-.18593E+01
5	-.45960E+00	-.90015E+00	-.24449E+01	-.17411E+01	.69794E+01	-.18970E+00
6	-.16444E+01	-.31353E+01	-.74303E+00	.12450E+01	.21498E+01	.12208E+00
7	.56778E+00	.20095E+01	-.17051E+00	-.96749E+00	-.48536E+01	.19155E-02
8	-.55122E+00	.66039E+00	.99446E+00	.53643E+00	.14976E+00	.35751E+00
9	-.74277E-02	.19922E+01	-.10436E+01	.71980E+01	-.58991E+00	-.24550E+01
10	.34619E+00	.73263E+00	.19476E+00	.13640E+01	-.93747E+00	-.88349E+00
11	.19946E+00	.10813E+01	.50103E-01	.12727E+01	-.31143E+00	-.85443E+00
12	-.34511E+00	.67000E+00	.47045E+00	.52114E+00		
13	-.22010E+00	.74904E+00	.35295E+00	.72216E+00		
14	.17908E+00	.60829E+00	.40418E+00	-.18834E+00		

FIGURE D.9: NONLINEAR PAIRWISE DISCRIMINANT FUNCTION: CLASS 2 VERSUS CLASS 6



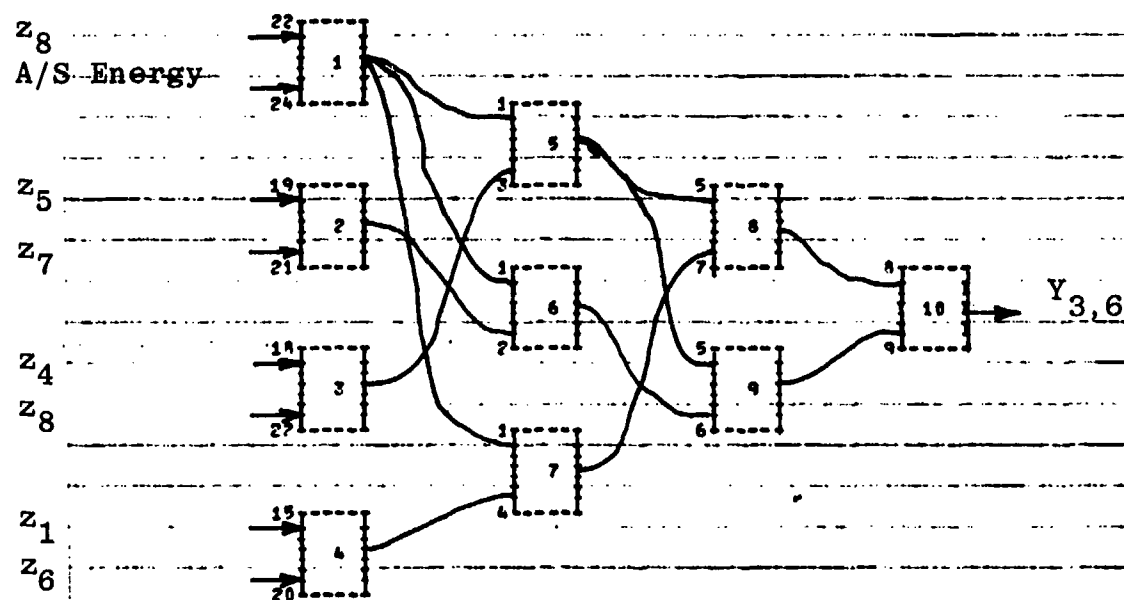
FLFM	NETWORK WEIGHTING COEFFICIENTS					
	W0	W1	W2	W3	W4	W5
1	-.2A090F+00	-.25093E+01	-.31795F+01	.1340AE+01	.25207E+01	.33474E+C1
2	-.64A07F+00	-.26513E+01	.14097F+01	-.67773E+01	.330A5F+01	.38723E+C1
3	-.64179F+00	.15996E+01	-.15119F+01	-.62860E+01	-.10040F+01	.25570F+C1
4	-.30314F+00	-.22717E+01	.93205E+00	.75203E+01	-.13693F+01	-.28868F+C1
5	.54691E+00	-.24826E+01	.233A8F+01	.52066E+01	-.20114E+01	-.58058F+C1
6	.17A17F+00	.66671E+00	.35A23E+00	-.A8746E+00	.2F136E+00	.39963E+C0
7	.4A804F+00	.11934E+01	-.15791E+00	.23702E+01	-.11621F+01	-.16933E+C1
8	.19034E-C1	.73927E+00	.32997E+00	-.17169E+00	-.11713E+00	.27948F+C0
9	.2AF38F+00	.59799E+00	.49919E+00	.21017E+00	-.36A13E+00	-.12341F+C0
10	-.39F20F-C1	.66127E+00	.39942F+00	-.55247E+00	.73A53E-01	.50325E+C0
11	-.14422F+00	.54769E+00	.47069E+00	.15910E+00		
12	-.16042F+00	.5A451E+00	.43484F+00	.1A745E+00		
13	-.27543F-C1	.5A289E+00	.42399E+00	.31124E-01		
14	.14C33E+00	.AA564E+00	.11917E+00	-.14684E+00		
15	.A2358F-C1	.99179E+00	.94301E-02	-.A6A95E-01		
16	-.4A206F+00	.88456E+01	-.78421F+01	.50270E+00		

FIGURE D.10: NONLINEAR PAIRWISE DISCRIMINANT FUNCTION: CLASS 3 VERSUS CLASS 4



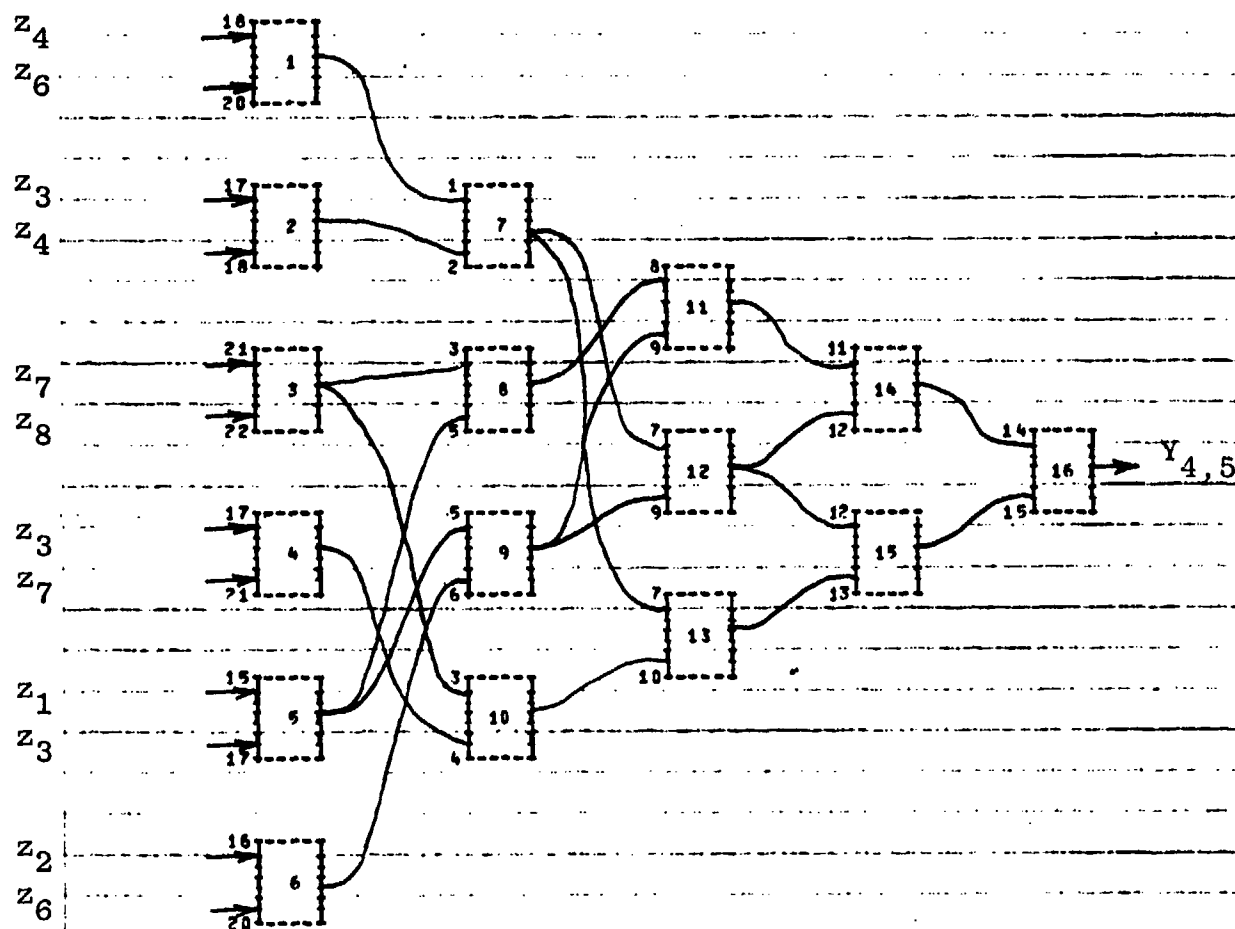
FLM	NETWORK WEIGHTING COEFFICIENTS					
	M0	M1	M2	M3	M4	M5
1	-.51316E+00	-.10351E+01	-.25A05E+01	.15462E+01	.64791F+00	.26362E+C1
2	-.56109F+00	-.25461E+01	.A5205E+00	-.31576E+01	.30621E+01	-.21411E+C1
3	-.32175F+00	-.32908E+01	-.15414F+01	.40414E+01	.34779E+C1	-.42799F+C1
4	-.15675E+00	-.95992E+00	-.30920E+01	-.73045E+01	-.77298E-01	.73107E-C2
5	.37510F+C0	.12711E+01	-.19643E+00	.A3612E+00	-.92E95F+00	-.23226E+C0
6	.27342F+C0	.95170E+00	.10011F+00	-.39186E+00	-.16190E+00	.24861E+CC
7	.337A5F+C0	.A8907E+00	.1676AF+00	-.6177E-01	-.2A144E+00	-.16430F-C1
8	-.30671F+00	.75037E+00	.2540AF+00	.32053E+00		
9	-.30719F+00	.79140E+00	.21216E+00	.31654E+00		
10	.30274E+00	.A5624E+00	.14924E+00	-.30466E+00		

FIGURE D.11: NONLINEAR PAIRWISE DISCRIMINANT FUNCTION: CLASS 3 VERSUS CLASS 5



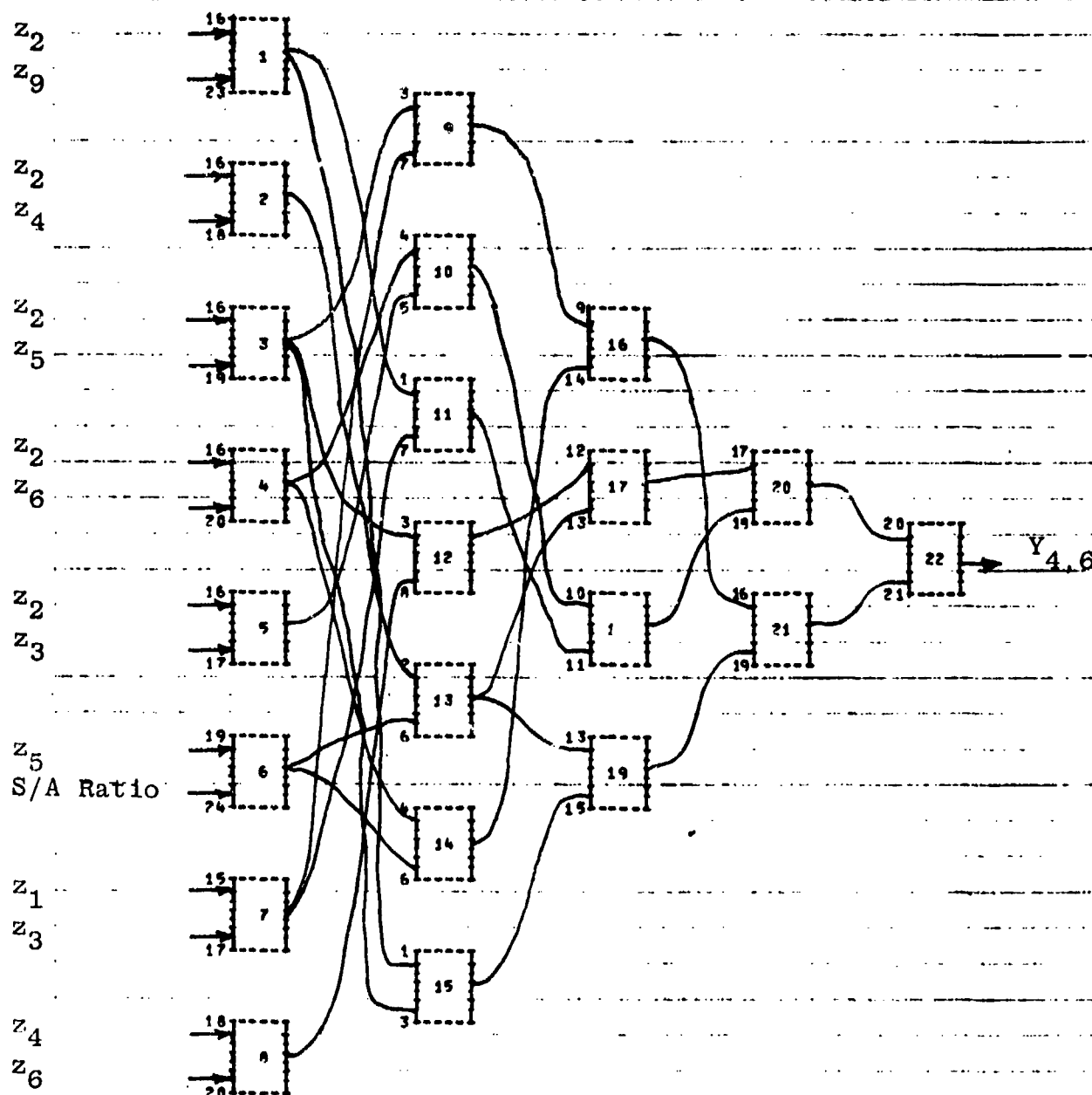
ELFN	NETWORK WEIGHTING COEFFICIENTS					
	W0	W1	W2	W3	W4	W5
1	.02705E+00	-.15662E+01	-.15143E+01	-.51716E+00	.60316E+01	.30040E+00
2	-.71245E+00	.37462E+01	-.61424E+01	.10601E+02	-.67442E+01	-.37993E+01
3	-.25096E+00	-.41915E+01	-.20741E+01	-.10243E+02	.94593E+01	.31908E+01
4	-.12825E+01	.11120E+01	.43865E+01	.77914E+01	.14475E+01	.12006E+02
5	-.43275E+00	.10561E+01	-.40107E+01	.34094E+00	.30749E+00	-.19113E+00
6	-.46382E+00	.10091E+01	.33349E-01	.77567E-01	.45499E+00	-.34960E-01
7	-.44541E+00	.10637E+01	-.47863E-01	-.11913E+00	.57924E+00	.37327E-01
8	.42494E+00	.47225E+00	.52976E+00	-.42580E+00		
9	.39846E+00	.57392E+00	.42756E+00	-.40328E+00		
10	-.40352E+00	.72419E+00	.27631E+00	.40376E+00		

FIGURE D.12: NONLINEAR PAIRWISE DISCRIMINANT FUNCTION: CLASS 3 VERSUS CLASS 6



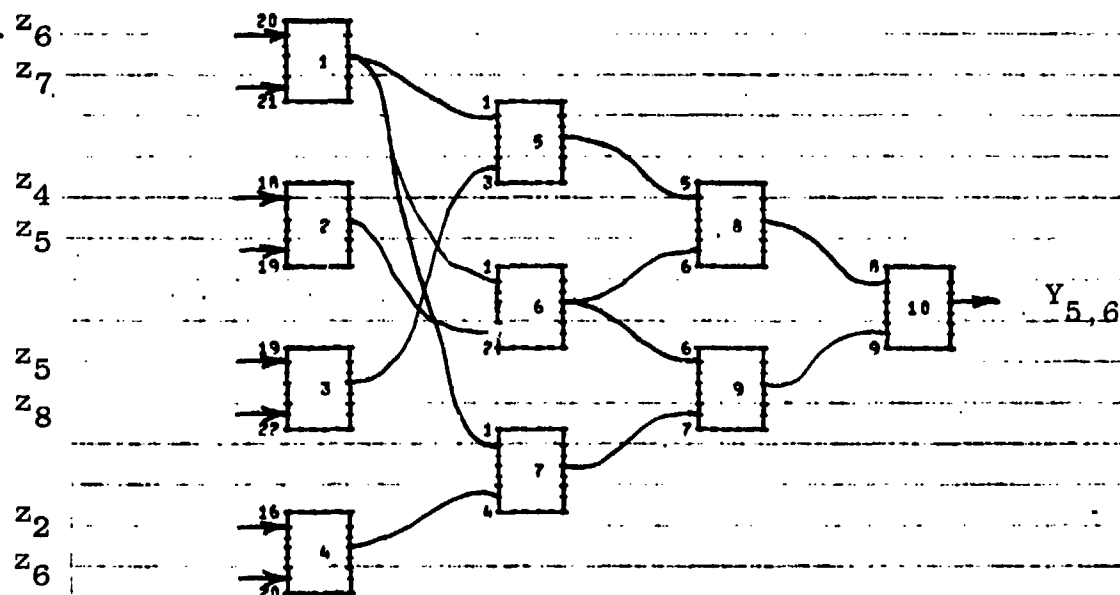
ELPH	NETWORK WEIGHTING COEFFICIENTS					
	W0	W1	W2	W3	W4	W5
1	-.26014E+00	-.27495E+01	.22707E+01	.13490E+01	.10A85E+01	-.3A777E+01
2	-.345A7E+00	.92133E-01	-.20985E+01	.15581E+01	.36543E+01	.11684E+01
3	-.23042E+00	.53590E+01	.17604E+01	-.35108E+01	-.50249E+01	-.10100E+01
4	-.A5753E+00	-.23121E+01	.49161E+01	.12102E+02	-.3A708E+01	-.10867E+02
5	.6A421E+00	.30675E+01	-.31751E+01	-.95150E+01	.27611E+01	.93506E+01
6	.17905E+00	-.65841E+01	.67336E+00	.18870E+01	-.78902E+01	-.23A61E+01
7	-.12665E+00	.12042E+01	-.13282E+02	-.57415E+01	.27342E+01	.33351E+01
8	-.17A17E+00	.10957E+01	-.A9514E-01	.2A917E+00	.59012E-01	-.98264E-01
9	-.21516E+00	.21866E+00	.A7044E+00	-.71510E+00	.4A588E+00	.37084E+00
10	-.24065E+00	.65278E+00	.39511E+00	-.11431E+01	.75188E+00	.64721E+00
11	.86376E-01	.A0A64E+00	.21634E+00	-.786A6E-01		
12	-.29714E-01	.69196E+00	.34157E+02	.35984E-01		
13	.30076E-01	.20139E+00	.40A10E+00	-.73222E-01		
14	-.22422E-01	.A3659E+00	.16A15E+00	.24294E-01		
15	-.17251E-01	.27437E+00	.73445E+00	.18769E-01		
16	.34252E-01	.42964E+00	.57310E+00	-.36132E-01		

FIGURE D.13: NONLINEAR PAIRWISE DISCRIMINANT FUNCTION: CLASS 4 VERSUS CLASS 5



ELFM	NETWORK WEIGHTING COEFFICIENTS					
	W0	W1	W2	W3	W4	W5
1	-.29748E+00	-.43944E+01	-.18471E+01	-.16638E+11	-.31616E+01	.39675E+01
2	-.53176E+00	-.77720E+01	-.13205E+01	.22574E+01	-.10502E+01	.13539E+01
3	-.28741E+00	-.47902E+01	-.20478E+01	-.74618E+01	-.41344E+01	-.68436E+01
4	-.40623E+00	-.43449E+01	.57535E+00	.71075E+00	-.29708E+01	-.49354E+00
5	-.38123E+00	-.45571E+01	-.11745E+01	-.17485E+01	-.31474E+01	-.24162E+01
6	.12121E+01	-.38455E+01	-.10927E+01	.50469E+01	.12179E+02	.21516E+00
7	.34088E+00	.26095E+01	-.79614E+01	-.12436E+02	.15720E+01	.88010E+01
8	.32510E+00	-.33561E+01	.22802E+01	.65536E+01	-.25523E+01	-.14292E+01
9	-.51557E+00	.72607E+00	.31517E+00	.15200E+00	.31653E+00	.69446E+01
10	-.49912E+00	.93521E+00	.11405E+00	-.1145E+00	.61110E+01	.56347E+01
11	-.54073E+00	.64935E+00	.37191E+00	.961E+01	.33862E+00	.13577E+00
12	-.33404E+00	.83607E+00	.22627E+00	.25873E+00	.19253E+00	-.52370E+01
13	-.74545E+00	.15825E+01	.99454E+00	.12940E+01	-.89699E+00	-.22600E+00
14	-.48725E+00	.52259E+00	.50481E+00	.20775E+00	.15291E+00	.14515E+00
15	-.25288E+00	-.15314E+00	.25158E+01	-.12674E+01	-.17262E+00	.16704E+01
16	.28060E+00	.60730E+00	.39293E+00	-.28079E+00		
17	.39688E+00	.54429E+00	.45789E+00	-.15724E+00		
18	.29725E+00	.24165E+00	.75972E+00	-.29910E+00		
19	.37697E+00	.72496E+00	.27710E+00	-.33447E+00		
20	-.49174E+00	.51549E+00	.49544E+00	.48199E+00		
21	-.31279E+00	.66524E+00	.13411E+00	.33315E+00		
22	.29260E+00	.81649E+00	.18357E+00	-.29261E+00		

FIGURE D.14: NONLINEAR PAIRWISE DISCRIMINANT FUNCTION: CLASS 4 VERSUS CLASS 6



ELN	NETWORK WEIGHTING COEFFICIENTS					
	W0	W1	W2	W3	W4	W5
1	.10672E+00	-.16996E+01	-.32149E+01	.65620E+00	.66139E+01	-.23628E+01
2	.19160E+00	-.61017E+00	.55510E+01	.87179E+01	-.46401E+01	-.51627E+00
3	-.72811E+02	.44794E+01	-.24803E+00	.50687E+00	.13251E+01	.37773E+00
4	-.14483E+01	-.33221E+01	.24592E+01	.87699E+01	.24974E+00	.11175E+02
5	-.44470E+00	.82309E+00	.22980E+00	.76070E+00	.25234E+00	-.12276E+00
6	-.35635E+00	.79997E+00	.23747E+00	.77394E+00	.18349E+00	-.17235E+00
7	-.87029E+00	.14527E+01	-.38673E+00	-.11576E+01	.14268E+01	.36164E+00
8	.31070E+00	.10616E+01	-.59723E-01	-.32063E+00		
9	.41571E+00	.55130E+00	.45401E+00	-.41873E+00		
10	-.42569E+00	.41264E+00	.58829E+00	.42627E+00		

FIGURE D.15: NONLINEAR PAIRWISE DISCRIMINANT FUNCTION: CLASS 5 VERSUS CLASS 6

TABLE D.1
EIGENVECTOR WEIGHTS*

Feature	z ₁	z ₂	z ₃	z ₄	z ₅	z ₆	z ₇	z ₈	z ₉
1	.26186	.09304	.15424	.20260	.17713	-.05579	-.03942	.17947	-.03049
2	-.10233	-.07159	-.04976	.11193	-.14732	.02496	-.02012	-.31040	.10182
3	-.19969	-.04620	-.09955	-.11009	-.15139	-.02621	.00624	-.19279	.13253
4	-.25069	-.23278	-.12931	-.29816	.15790	.10583	-.10659	.10698	-.06333
5	.15434	.32831	.54845	-.38601	.13980	.10346	.05731	-.02090	.07510
6	-.26877	-.04313	-.00054	.19443	-.17529	.29810	-.03520	-.43755	-.11547
7	-.00113	-.10838	-.19162	.05318	-.07612	.01435	.03729	-.03641	.08762
8	.15951	-.21511	-.32444	.14835	-.06540	-.23526	.09414	.44134	.14478
9	-.21827	.11414	-.04816	-.28173	.13900	.03353	.08777	.22098	-.00814
10	.11515	.07188	.08779	.12112	.06346	-.04608	-.02588	.15584	-.05235
11	.25888	.04400	.13654	.33191	-.14699	-.05309	.00235	-.13798	.06230
12	-.28427	-.17733	-.23205	-.22414	.07168	-.18393	.05808	-.15747	.13365
13	-.06344	-.20004	.05056	.07244	.28241	-.11292	-.45942	.00636	-.19388
14	.13876	-.11398	.05238	.15367	.28673	.23674	.48570	-.05574	.45537
15	-.21045	-.05037	.00566	-.09715	-.29913	.04297	.40254	.11303	-.64238
16	.04351	.45434	-.14241	-.16727	-.30682	.17115	-.37428	-.04536	.21350
17	-.03087	-.17953	.03946	.07650	.33928	-.12524	-.30015	.00351	-.10101
18	-.04376	-.16055	-.02162	.07261	.22499	.26983	-.14406	-.27178	-.14271
19	-.38078	.13409	.03500	.22198	.03326	-.03148	-.03851	.16655	-.08163
20	-.47810	.18361	.23665	.32800	.03209	-.47967	.23162	-.18016	-.11360
21	-.26266	.16934	.10106	.15556	-.51759	.38164	-.17490	.16886	-.00409
22	-.31627	.11056	-.06248	.26598	-.11386	.42117	-.10873	.37434	.08304
23	.19520	.06829	.05940	.05263	.11097	-.08826	.00234	.04276	-.18973
24	-.04332	.03151	.02987	.14756	.04601	-.21440	-.02051	.04192	.26189
25	-.01103	.02733	.03920	.06573	.04753	-.06013	.00066	.06581	.03775
26	.05619	.25192	-.23522	.05443	.20408	.01558	.05669	-.04440	-.07389
27	.00096	.38267	-.36353	.08924	.32935	.01654	.08568	-.07813	-.11873
28	.77747	.36833	-.33196	.04624	.24133	.00465	.05441	-.06759	-.09575

* Eigenvector weights used to transform the 28 Honeywell and Sylvania features to nine z variables.

TABLE D.2

ERRORS MADE IN NONLINEAR CLASSIFIER G FOR THE SIX TARGET CLASSES

NUM	MERDCID	CLASS	TYPE	SITE	SPEED	RANGE	A/S	GAIN	DIRECTION	SET ^{1/}
1	498	6	N	GRAYLING	-0	-0	60	70		E
2	553	6	N	FT.BFAGG	-0	-0	30	70	N-S	E
3	554	6	N	FT.BRAGG	-0	-0	30	70	N-S	E
4	586	6	N	YUMA	-0	-0	50	70		E
5	603	5	H1	YUMA	3	20	70	70	N-S	E
6	620	5	H1	YUMA	3	-500	60	70	S-N	E
7	679	4	UH-1	FT.BPAGG	60	600	40	70		E
8	679	4	UH-1	FT.BFAGG	60	600	40	70		E
9	640	3	TA-4	FT.BPAGG	250	200	40	70		E
10	642	3	TA-4	FT.BFAGG	300	200	23	70		E
11	642	3	TA-4	FT.BFAGG	300	200	23	70		E
12	644	3	TA-4	FT.BFAGG	450	200	23	70		E
13	645	3	TA-4	FT.BPAGG	450	200	23	70		E
14	650	3	TA-4	FT.BFAGG	450	400	40	70		E
15	655	3	OV-10	FT.BFAGG	150	200	40	70		E
16	387	2	M151	YUMA	16	-0	50	70	E-W	E
17	389	2	M151	YUMA	16	20	50	70	W-E	E
18	392	2	M151	YUMA	22	100	50	70	W-E	E
19	403	2	T2.5	YUMA	6	20	46	70	W-E	E
20	411	2	T2.5	YUMA	22	100	40	70	E-W	E
21	412	2	T2.5	YUMA	22	-200	40	70	F-W	E
22	415	2	T2.5	YUMA	22	-0	40	70	W-E	E
23	420	2	T2.5	YUMA	31	-200	40	70	W-E	E
24	430	2	M715	YUMA	16	300	46	70	W-E	E
25	436	2	M715	YUMA	22	300	46	70	W-E	E
26	437	2	M715	YUMA	22	100	46	70	W-E	O
27	439	2	M715	YUMA	22	-100	46	70	W-E	O
28	450	2	M792	YUMA	16	300	46	70	W-E	E
29	456	2	M792	YUMA	22	400	40	70	E-W	E
30	465	2	M792	YUMA	31	-100	40	70	E-W	E
31	505	2	T2.5	GRAYLING	16	200	40	70	S-N	O
32	516	2	T2.5	GRAYLING	22	100	40	70	N-S	E
33	521	2	T2.5	GRAYLING	31	500	40	70	N-S	E
34	522	2	T2.5	GRAYLING	31	200	40	70	N-S	E
35	556	2	M151	FT.BPAGG	6	-20	50	70	S-N	E
36	569	2	M151	FT.BFAGG	31	-200	50	70	S-N	O
37	571	2	M151	FT.BFAGG	31	100	50	70	N-S	O
38	576	2	T2.5	FT.BRAGG	6	200	50	70	N-S	O
39	581	2	T2.5	FT.BPAGG	16	-100	50	70	S-N	E
40	593	2	T2.5	FT.BPAGG	22	-100	50	70	S-N	E
41	598	2	T2.5	FT.BPAGG	31	-200	50	70	S-N	E
42	26	1	M107	YUMA	22	-100	30	70	E-W	E
43	28	1	M107	YUMA	22	500	30	70	W-E	E
44	39	1	M107	YUMA	28	300	30	70	E-W	E
45	41	1	M107	YUMA	28	-200	30	70	E-W	E
46	47	1	M107	YUMA	28	-300	30	70	E-W	E
47	90	1	M60	YUMA	16	-400	16	70	W-E	E
48	236	1	M48	YUMA	22	300	20	70	E-W	E
49	245	1	M48	YUMA	22	200	20	70	E-W	E
50	272	1	M48	GRAYLING	6	200	20	48	S-N	E

TABLE D.2
(Continued)

NUM	MERDCID	CLASS	TYPE	SITE	SPEED	RANGE	A/S	GAIN	DIRECTION	SET ^{1/}
51	274	1	M48	GRAYLING	6	-20	20	40	S-N	E
52	275	1	M48	GRAYLING	6	-600	20	40	S-N	E
53	277	1	M48	GRAYLING	6	300	20	40	N-S	E
54	279	1	M48	GRAYLING	6	-200	20	40	N-S	E
55	280	1	M48	GRAYLING	6	-200	20	40	N-S	E
56	281	1	M48	GRAYLING	16	100	20	40	S-N	E
57	286	1	M48	GRAYLING	16	200	20	40	N-S	E
58	287	1	M48	GRAYLING	16	-100	20	40	N-S	E
59	288	1	M48	GRAYLING	20	200	20	40	S-N	E
60	294	1	M48	GRAYLING	20	100	20	40	N-S	E
61	295	1	M48	GRAYLING	20	-200	20	40	N-S	E
62	302	1	M113	GRAYLING	6	400	36	70	N-S	E
63	332	1	M113	FT.BFAGG	6	200	40	70	N-S	E
64	337	1	M113	FT.BFAGG	16	-100	40	70	S-N	E
65	338	1	M113	FT.BFAGG	16	-300	40	70	S-N	E
66	339	1	M113	FT.BFAGG	16	400	40	70	N-S	E
67	340	1	M113	FT.BFAGG	16	200	40	70	N-S	E
68	346	1	M113	FT.BFAGG	22	-100	40	70	S-N	E
69	349	1	M113	FT.BFAGG	22	200	40	70	N-S	E
70	352	1	M113	FT.BFAGG	25	500	40	70	S-N	E
71	354	1	M113	FT.BFAGG	25	-100	40	70	S-N	E
72	355	1	M113	FT.BFAGG	25	-400	40	70	S-N	E
73	356	1	M113	FT.BFAGG	25	400	40	70	N-S	E
74	357	1	M113	FT.BFAGG	25	300	40	70	N-S	E
75	360	1	M113	FT.BFAGG	25	-300	40	70	N-S	E
76	370	1	M48	FT.BFAGG	16	200	30	70	N-S	E
77	377	1	M48	FT.BFAGG	20	500	30	70	S-N	E

^{1/}
"D" stands for design and "E" for evaluation under title
descriptor "SET."

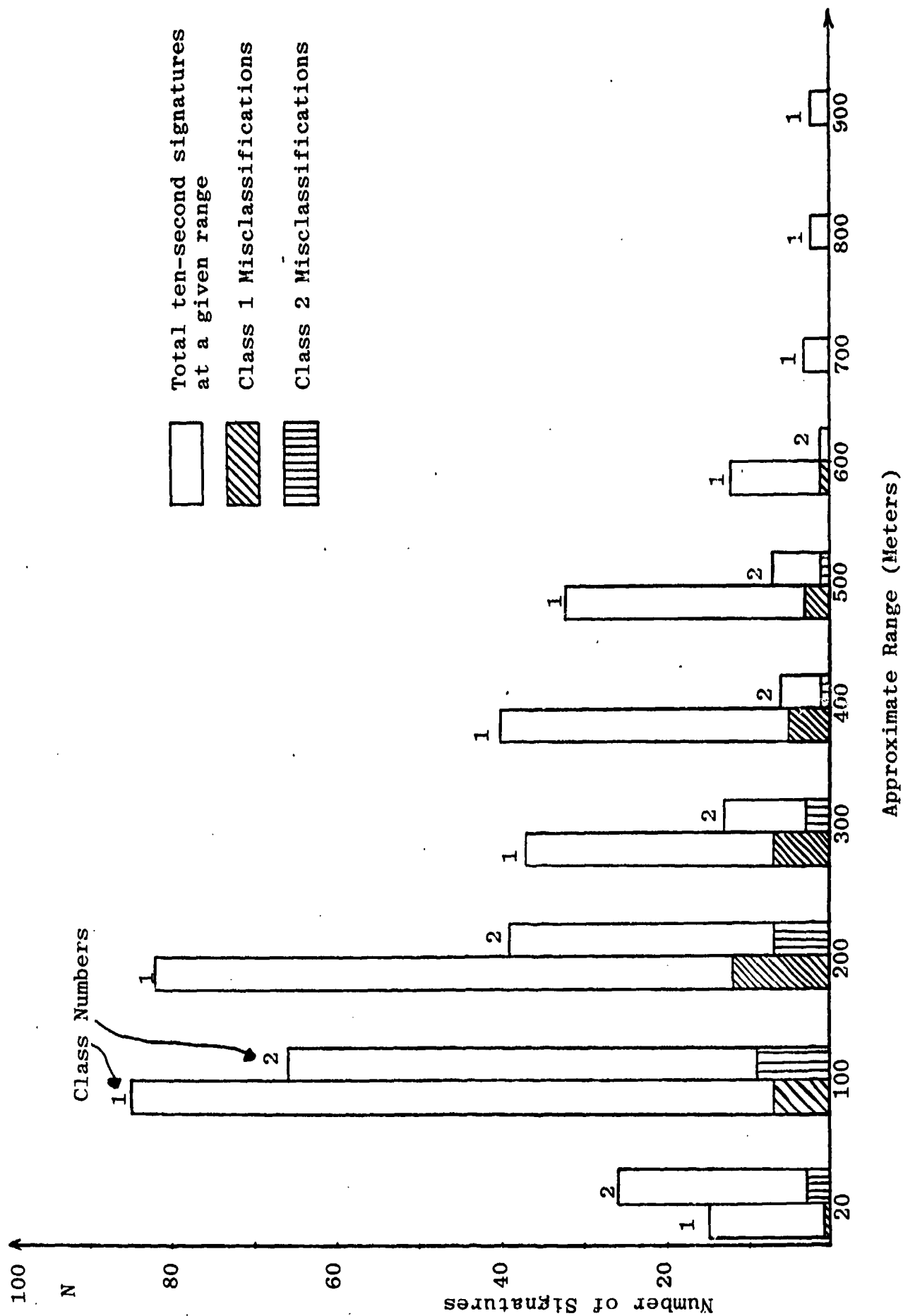


FIGURE D.16: DISTRIBUTION OF CLASS 1 AND CLASS 2 TEN-SECOND SIGNATURES WITH RESPECT TO APPROXIMATE RANGE, SHOWING MISCLASSIFICATIONS MADE BY NONLINEAR CLASSIFIER (G) AT GIVEN RANGE